Coordination Chemistry Reviews 254 (2010) 1918–1947

Contents lists available at ScienceDirect

Coordination Chemistry Reviews

journal homepage: www.elsevier.com/locate/ccr

Review

Advances in the coordination chemistry of nitrogen ligand complexes of coinage metals

Ahmed A. Mohamed*

Department of Chemistry, Texas A&M University, College Station, TX 77842-3012, USA

Contents

* Tel.: +1 979 845 3762; fax: +1 979 845 2373.
E-mail address: amohamed@mail.chem.tamu.edu.

0010-8545/$ – see front matter. Published by Elsevier B.V.
doi:10.1016/j.ccr.2010.02.003

ARTICLE INFO

Article history:
Received 19 October 2009
Accepted 4 February 2010
Available online 12 February 2010

This article is dedicated to my mentor Professor John P. Fackler, Jr. on the occasion of his 75th birthday. His guidance has enlightened my life and will continue to do so.

Keywords:
Coinage metals
Metal–metal bonding
Multinuclear
Anionic nitrogen ligands
Applications

ABSTRACT

Coinage metals nitrogen chemistry has not been studied extensively until recently. The focus of this review is the base- and halide-free complexes of the monoanionic nitrogen ligands. This review describes how minor ligand modifications can result in a drastic change in the metal–metal interactions in multinuclear compounds. Crystal structures of these complexes show individual complexes, dimers, supramolecular columnar packing or more complex supramolecular aggregates. Bulky substituents on the ligands can prevent intermolecular metal–metal interactions or the formation of supramolecular architectures. The nuclearity and metal–metal interactions in these complexes are controlled by ligand steric and electronic factors and solvent of crystallization. Many classes of nitrogen ligand coordination compounds have given rise to advances in several fundamental and applied research aspects. Recent potential applications of nitrogen ligand complexes are highlighted particularly for those complexes included in this review.

Published by Elsevier B.V.

1. Introduction

Studies involving coinage metal complexes of nitrogen donor ligands range from classical coordination chemistry to the developing field of bioinorganic chemistry. Many classes of these coordination compounds that exhibit various structures have been reported, which has given rise to advances in several fundamental and applied research aspects. There are wide applications for these materials in medicine [1], light emitting diodes fabrication [2], lubricant additives [3], catalysis [4], chemical vapor deposition [5], liquid crystals [6] and ionic liquids [7]. The applications of coinage metal nitrogen complexes represent a major step forward in this area of research.

The interest in metal amide complexes, particularly those of copper, is due to their potential applications in electrophosphorescence devices (EL) [8] and homogenous catalysis [9]. Amide chemistry, specifically the dialkylamides and disilylamides, was reviewed in 1976 by Bradley and Chisholm [10]. An overview of the current state of the tripodal amide complexes in main group and transition metal chemistry has been presented by Gade [11]. Bailey highlighted the synthesis of useful metal amides and imides with applications in organic synthesis in *Science of Synthesis* [12]. Another book *Metal Amide Chemistry*, which appeared recently by Lappert et al., describes the synthesis, structure, reactions and applications of metal amides and related compounds which are stable at ambient temperatures and particularly those which are mono-, di-, or oligonuclear [13].

Pyrazole ligands have been utilized in various applications ranging from anion-recognizing materials to liquid crystals. Copper pyrazolates, for example, form a multinuclear copper cavity with centered anions [14]. Triangular copper(II) pyrazolate complexes can accommodate μ^3-bridging halides; the controlled interchange of these anions brings about an orderly transition from antiferromagnetic to ferromagnetic exchange among the copper centers [15]. In addition, trinuclear copper complexes with trigonal symmetry are of pursuit in terms of both industrial applications and in understanding the mechanism of action of copper-containing enzymes [16]. Metallomesogens, liquid crystals containing metal ions, from substituted gold pyrazolates with long alkyl chains have attracted much attention in expectation of their unique properties [17,18].

Several aspects of the structural chemistry of metal pyrazolates have been investigated such as the use of *ab-initio* X-ray powder diffraction (XRPD) methods to determine the structure of polymeric metal pyrazolate complexes [19], the polydentate ligands containing pyrazole as main donor groups and of their metal complexes [20], the interesting coordination modes from pyrazolate ligands [21], the role of the pyrazolate ligands in building polynuclear transition metal systems [22], various bonding modes for pyrazole-based ligands and the resulting coordination complexes [23], and the structural diversity and the metal coordination modes adopted by pyrazoles and pyrazolides-flexible synthons [24].

Triazoles have been investigated for pharmaceutical purposes. Triazole metal interactions play a major role in the biological actions of triazole containing drugs. The industrial applications of metal-triazole compounds include anti-corrosion coatings, photographic materials, dyes and additives for oils and greases [25]. Specifically azole complexes with silver are of special interest due to their potential applications in photography and silver plating. The first silver azole complex was reported in 1893 [26]. A comprehensive review of metal complexes with triazolates and polyazolates was published by More and Robinson [27]. Haasnoot reviewed the mononuclear, oligonuclear and polynuclear metal coordination compounds with triazole derivatives [28].

The interest in amidinate and guanidinate complexes stems from their diverse applications in many areas of chemistry including organocatalysis [29]. The utilization of bulky guanidinates for the stabilization of low oxidation state metallacycles was reviewed recently by Jones [30]. Edelmann reviewed the nitrogen-silated benzamidines as versatile building blocks in main group and coordination chemistry [31], and the coordination chemistry of amidinate and guanidinate ligands [32]. Amidine ligands coordination chemistry [33] and the neutral guanidines and monoanionic and dianionic guanidinates coordination chemistry have been reviewed by Bailey and Pace [34]. Bicyclic-guanidines were reviewed by Coles in light of the recent advances in the synthesis of new derivatives and the potential for cross-stimulation of different areas [35].

Tris(pyrazolyl)hydroborates (TpRR′) containing alkyl or aryl substituents at the pyrazolate positions are of special interest because of their coordination chemistry and are ideal for bioinorganic model building [36]. The methylated pyrazolylborate complex is of significance since it forms a carbonyl complex with stretching frequency even closer to that of carboxyhemocyanin than the unmethylated analogue. Dinuclear copper complexes of tris(pyrazolyl)borate ligands have been studied as models for the enzyme oxyhaemocyanin [37]. The coordination chemistry of scorpionate has also made an incredible increase in the number of potentially useful ligand derivatives through deliberate syntheses of water-soluble coordinated ligands. Such derivatives

are expected to be highly useful in the synthesis of enzyme model complexes, which are soluble and stable under physiological conditions [38]. Dias and Lovely highlighted the important role of poly(pyrazolyl)borates and alkanes in the stabilization of Group 11 metal complexes of small carbon-based ligands. Poly(pyrazolyl)borates in particular have led to significant discoveries in the chemistry of carbon monoxide and ethylene. The coinage metal complexes of CO and olefins have been implicated in several catalytic processes [39].

The interest in the synthesis and structure of related scorpionates has expanded to ligands with thioimidazolyl, selenoimidazolyl, phosphine and N-heterocyclic carbene donors [40], the coordination chemistry of bis- and tris(mercaptoimidazolyl)borate ligands with both main group and transition metals [41], the heteroscorpionate $[RR'C(pz)_2]$ ligand derived from bis(pyrazol-1-yl)methane [42], statistical analyses of structural features of copper and silver complexes of scorpionate ligand as a function of the steric and electronic properties and the nature of the counterion [43], preparation of poly(imidazoyl)borates, poly(pyrazoyl)silanes, poly(azolyl)-phosphine, -phosphinate, -phosphazene and -phosphine oxides ligands [44], and electronic effects and novel coordination modes of new pyrazolylborate ligands [45].

Other reviews emerged on the less studied nitrogen ligands such as the coordination chemistry of pentaazadienide ligand by Beck [46]. The chemistry of the heavy metal azides, especially silver azide, has been the subject of several previous studies [47] and the reactions of transition metal azide complexes and their reaction products by Strähle [48]. The chemistry of β-diketiminate complexes has been reviewed by Lappert [49].

The chemistry of silver and gold elements differs greatly although they possess similar electronic structures and ionization potentials. The differences between silver and gold are consequences of the relativistic effects, which are especially important for gold. There is a contraction of 6s orbitals, and this stabilization minimizes the energy gap between 6s and 5d orbitals, which also undergo an expansion. Both of these effects are much less pronounced in silver, resulting in that the energetic separation of the valence d and s shells of gold is significantly smaller than that in silver [50].

Silver nitrogen complexes are abundant and were developed before those of gold. The structure of $[Ag(NH_3)_2]Br$ was reported sixty years before that of the analogous gold complex [51]. The simplest silver(I) complex is dicoordinate and compounds of this type $[AgL_2]$ occur for a variety of ligands such as NH_3, melamine, succinimide and pyridine. Pyridine and related ligands, for example, form silver(I) aggregates with different structural motifs [52].

Gold(I) is often described as a soft metal ion and therefore can be expected to have a preference for soft donor ligands such as sulfur and carbon, over hard donor ligands such as those which bond through nitrogen or oxygen [53]. The affinity of gold for nitrogen can be increased if a phosphine ligand is present on the gold because of the efficient π-acceptor nature of the phosphine. Therefore, the majority of the gold(I) complexes with anionic N-donor ligands are complexes of the type R_3PAuL [54]. Early gold(I) chemistry with nitrogen ligands started as amine complexes which exist as dinuclear and tetranuclear units and stabilized by halide or phosphine. The amine complexes are further aggregated by gold–gold interaction and hydrogen bonding. Known examples in this category are the dinuclear complex $[AuCl(cy_2NH)]_2$ and the tetranuclear complex $[AuCl(piperidine)]_4$ [55].

Specific reviews on gold nitrogen chemistry appeared recently. In 2003, Fackler and Burini reviewed the synthesis and structure of trinuclear gold cyclic complexes. The work highlights the structural chemistry and properties of gold complexes of carbeniates (N,C) and benzylimidazolates (N,C) [56]. A recent gold chemistry book, *Gold Chemistry: Highlights and Future Directions*, edited by Fabian Mohr, included a chapter on gold(III) chemistry of nitrogen and oxygen ligands [57]. The book also included a comprehensive chapter on gold amidinate chemistry. The chapter highlights the new research accomplishments in the Fackler laboratory on the nitrogen ligand complexes of gold [58]. Strähle briefly reviewed the nitrogen ligand complexes of gold in chapter 11 published in *Gold: Progress in Chemistry, Biochemistry and Technology*, edited by Schmidbaur. The chapter described the early base-stabilized gold nitrogen complexes of the type $AuXL_n$ and AuX_3L_n [59]. In 2008, Steinhauser and his coworkers reviewed the early history of the fascinating chemistry of fulminating gold [60].

Table 1
List of the monoanionic nitrogen ligands mentioned in this review.

	Ligand	Name	Nuclearity
1	$[N_3]^-$	Azide	1,2,polymer
2	$[NR_2]^-$	Amide	3,4
3	$[CH(NR)_2]^-$	Amidinate	2,3,4
4	$[R_2N(RN)_2C]^-$	Guanidinate	2,4,6
5	$[RN_3R]^-$	Triazenide	2,3,4,polymer
6	$[RN_5R]^-$	Pentaazadienide	2,3
7	$[HC\{(H)C(R)N\}_2]^-$	β-Diketiminate	2,4
8	$[Pz]^-$	Pyrazolate	3,4,6,polymer
9	$[Tz]^-$	Triazolate	3,polymer
10	$[Tp]^-$	Hydrotris(azolyl)borate	2,3,polymer

The chemistry of nitrogen ligands in this review is arranged by the ligand type, and within each category the metals discussed are arranged in the following order: copper, silver then gold. The present review covers the last three decades along with a few earlier references. This review is not intended to tabulate the crystallographic data but to provide a comparative discussion of the monoanionic nitrogen ligands. For details of the versatile coordination chemistry of nitrogen ligands and the properties of complexes, the reader should refer to the works cited before in this section.

This review describes the recent progress in the nitrogen ligands of coinage metals, highlighting much of the most recent work. The ligands depicted in Table 1 and shown in Fig. 1 are a representative group of the multitude of nitrogen ligand varieties discussed in this review article. Addressed first are minor ligand modifications and how they can often result in drastic changes in the intramolecular and intermolecular metal–metal attractions in multinuclear compounds. The potential applications pertained to the various types of ligand complexes are mentioned briefly. The purpose of this part of the review is to highlight the more recent applications of coinage metals nitrogen ligand complexes. The growing interest in nitrogen ligand applications originates from their coordination flexibility. The applications of gold nitrogen complexes in particular represent a major step forward in this area of research since the well-known correlation between the ligand and nuclearity in this class of compounds was just being fully realized.

This paper provides a narrative of the progress in this chemistry, identifies potential applications of nitrogen ligand complexes of coinage metals, and highlights the needs in this field. There are opportunities in synthesis, structure, photophysics and computation to make valuable contributions. Experimentally and intellectually, the concept of the excited state in these complexes is challenging. For these reasons, it is hoped that this review paper serves as motivation for others to enter this developing field.

2. Azide complexes

Azide is a linear anion that is isoelectronic with CO_2 and N_2O. According to the valence bond theory (VBT), azide can be represented by several resonance structures, an important one being $N^- = N^+ = N^-$ [61]. The chemistry of metal azide complexes received

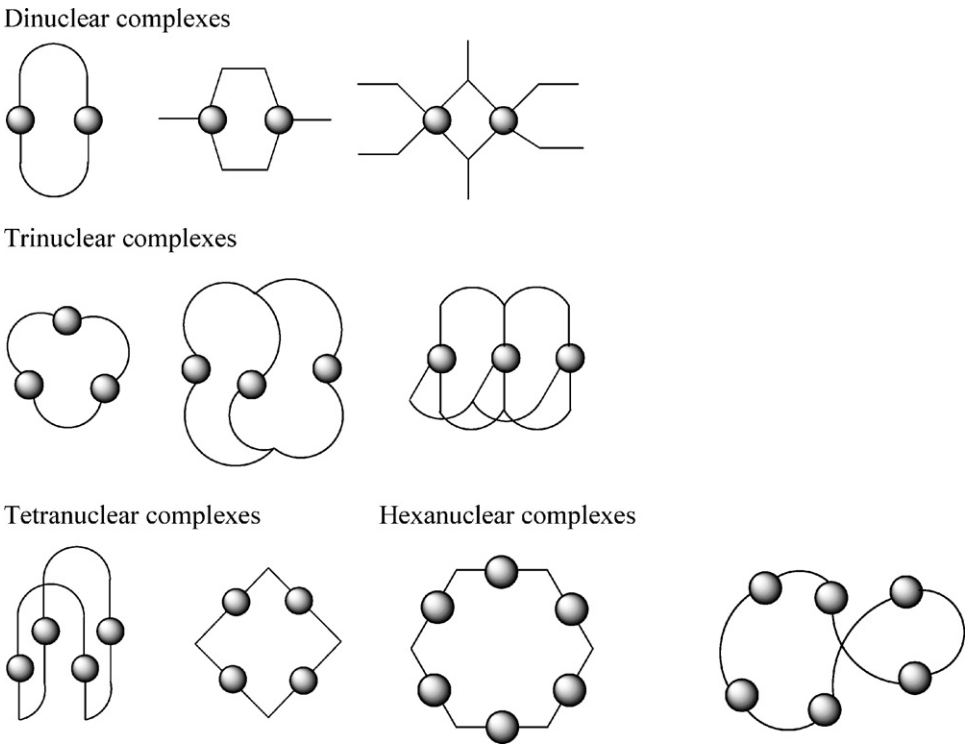

Fig. 1. Structure of the metallacycle in the complexes cited in this review.

little attention due to their explosive nature. Azide complexes characterized so far contain an azide group bound to one metal atom (square-planar arrangement), an azide group bridging two metal atoms through the same nitrogen (four-membered ring), and an azide group bridging two metal atoms from an azide group bridging two metal atoms by the two end nitrogen centers (eight-membered ring). In linear and unsymmetrical azides, the N–N bond distances average is 1.154 Å. The long N–N distance always occurs between nitrogen in the middle and the nitrogen coordinated to the metal [62].

In 1948, Wilsdorf published a report regarding the structure of a neutral copper(I) azide complex, CuN_3. From this crystallography paper, it is clear that CuN_3 crystallizes in the tetragonal system with a unit cell similar to that of potassium, rubidium and cesium azides [63]. The structure consists of copper ions and azide groups arranged in chains in the direction of the body diagonal of the cell [63]. The work on copper(I) azide was subsequently expanded by Soderquist to synthesize a neutral copper(II) azide polymer $[Cu(N_3)_2]_n$ [64]. This complex is a primary explosive as it is extremely reactive to friction and electric fields. This indicates that the compound has small activation energies for thermal and electrical breakdown. Crystals of $[Cu(N_3)_2]_n$ were prepared for X-ray crystallography by mixing $CuSO_4{\cdot}5H_2O$ and NaN_3 by diffusion in a solution of 1% acetic acid to yield long, prismatic, green-black needles [64]. In the crystal structure of the orthorhombic copper(II) azide complex there are four $Cu(N_3)_2$ molecules in the unit cell (Fig. 2). The structure consists of infinite planar $[Cu(N_3)_2]_n$ chains packed laterally with long Cu–N distances within the chains and distorted octahedral coordination around each copper atom. There is a copper–copper distance of 3.08 Å between the chains [64].

$$2[Ph_4P][CuCl_3] + 6AgN_3 \rightarrow [Ph_4P]_2[Cu_2(N_3)_6] + 6AgCl \quad (1)$$

The dinuclear copper(II) azide complex $[Ph_4P]_2[Cu_2(N_3)_6]$ is prepared from the reaction of chlorocuprate $[Ph_4P][CuCl_3]$ with silver azide AgN_3 (2:6 stoichiometry) in CH_2Cl_2 suspension, Eq. (1) [65]. The azidocuprates form nonexplosive brown crystals that have a low sensitivity to moisture. The compound meets D_2h symmetry (Fig. 3). In the anions, the square-planar copper atoms are linked to a planar Cu_2N_2 four-membered ring by the N∞ atoms of two azide ligands. The other azide ligands, bonded terminally, complete coordination number four at the copper atoms [65]. A square-planar copper(II) azide complex $[Et_4N]_2[Cu(N_3)_4]$ is turned into brown prisms by mixing an ethanol solution of $Cu(NO_3)_2$ salt with aqueous solution of $[Et_4N]N_3$ and NaN_3 [66]. Four nitrogen atoms from the terminal azide ligands coordinate each copper atom in the anion. In the black crystals of $[Ph_3PNPPh_3]_2[Cu(N_3)_4]$, the non-planar $[Cu(N_3)_4]^{2-}$ anions have reduced site symmetry with deviations of their non-coordinated γ-N atoms from the CuN_4 plane [67].

In view of the prominent bridging character from the outer nitrogen donors in the azide ligands, azide complexes are versatile precursors for the construction of bridged arrangements. The "honeycomb-like" structure of $[Me_4N][Cu(N_3)_3]$ consists of chains

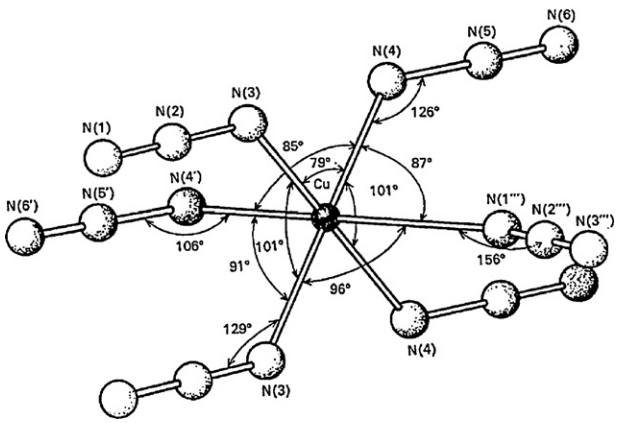

Fig. 2. Perspective view of the octahedral environment of a copper atom in $[Cu(N_3)_2]$; from Ref. [64].

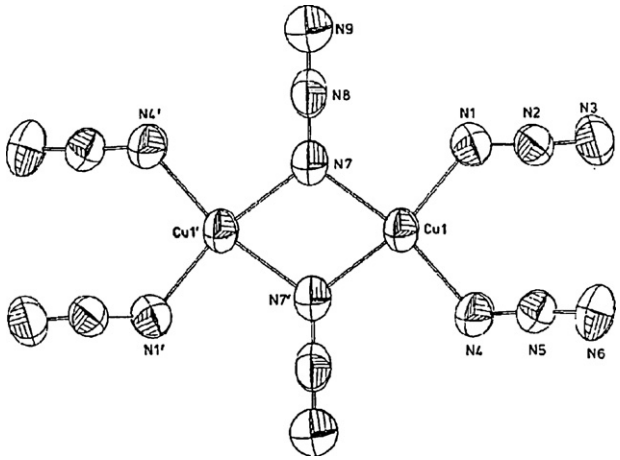

Fig. 3. Structure of $[Ph_4P]_2[Cu_2(N_3)_6]$ (Cu–Cu = 3.128 Å); from Ref. [65].

of copper(II) atoms that are simultaneously bridged by one EO (end-on) and two EE (end-to-end) azide bridges (Fig. 4). There are two nonequivalent copper atoms in the structure, which are located on inversion centers. Each copper atom is bonded to six nitrogen atoms belonging to six azide ligands, four acting as EE bridging ligands and two as EO bridging ligands. The bridging angle corresponding to the EO azide bridge is Cu–N–Cu 132.5(3)° [68].

Klapötke et al. [69] recently reported a breakthrough study that highlighted the role of cation size in the structural complexity and versatility of silver azide complexes. Two rather unusual silver azide complexes were isolated after reacting $[Ph_4P][N_3]$ or $[Ph_3S][N_3]$ with one equivalent of silver azide complex AgN_3 in acetonitrile. The colorless silver azide compounds $[Ph_4P][Ag(N_3)_2]$ or $[Ph_3S][Ag(N_3)_2]$ were characterized (Figs. 5 and 6). Trials to synthesize the silver azide complexes using various counter cations such as $[Me_4N]^+$ and $[Ph_3PNPPh_3]^+$ under the same conditions were unsuccessful. Clearly, the reaction progress and stability depend on the cation size. The $[Me_4N]^+$ cation is too small to stabilize the polymeric structure. The $[Ph_3PNPPh_3]^+$ cation is the wrong size as well: it is too large to form the unstable monomeric structure [69].

The crystal structure of silver azide AgN_3 in its high-temperature modification was determined from X-ray powder diffraction data at 170 °C. The structure consists of two-dimensional layers containing silver and nitrogen in which the silver atoms are coordinated by four nitrogen atoms exhibiting a distorted square coordination environment. These sheets are linked together by weaker perpendicular Ag–N contacts [70].

Azide ligands have the potential to be encapsulated inside rectangles and trigonal prisms of silver atoms. The reaction co-crystallization of AgN_3 with $AgNO_3$ in water (1:1 stoichiometry) produces AgN_3 as a white powder, and crystallizes from aqueous

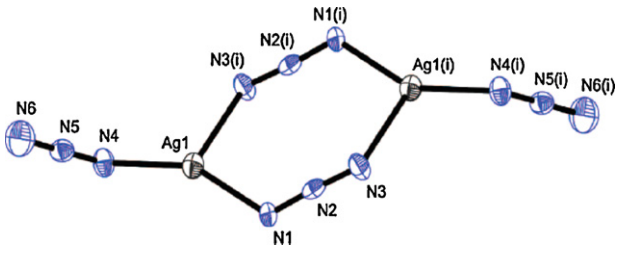

Fig. 5. Structure of $[Ag(N_3)_2]^-$ as $[Ph_4P]^+$; from Ref. [69].

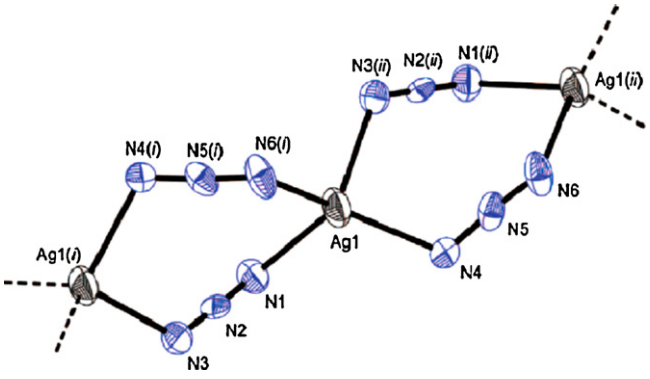

Fig. 6. Structure of $[Ag(N_3)_2]^-$ as $[Ph_3S]^+$; from Ref. [69].

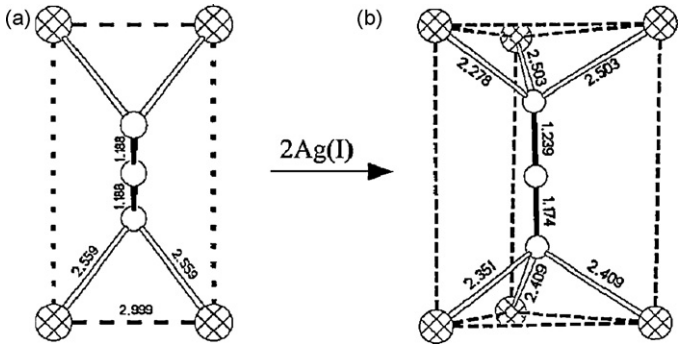

Fig. 7. Coordination in (a) AgN_3 and (b) $AgN_3{\cdot}2AgNO_3$; from Ref. [71].

NH_3 to yield X-ray quality crystals. The layer-type crystal structure stacks together with the azide ligands in bridging tetradentate (μ-1,1,3,3) coordination (Fig. 7a). The structure is constructed from edge-sharing regular rectangles, each composed of silver atoms at the vertices and accommodating an out-of-plane azide anion [71]. The reaction co-crystallization of AgN_3 with $AgNO_3$ (1:2 stoichiometry) produces $AgN_3{\cdot}2AgNO_3$, which shows the azide ligand in a

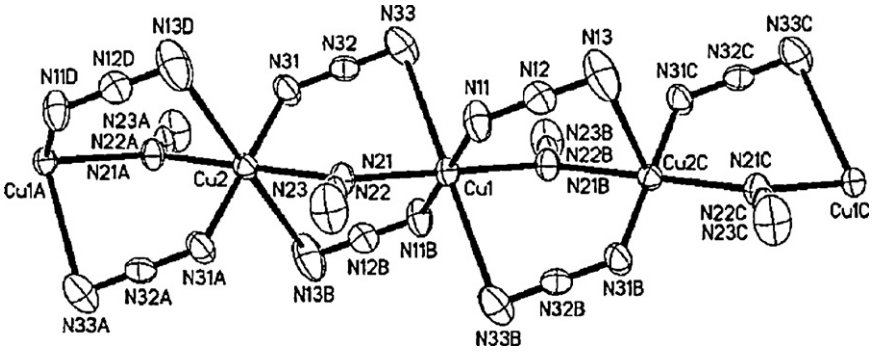

Fig. 4. Structure of $[Me_4N][Cu(N_3)_3]$ (Cu–Cu = 3.737(1) Å); from Ref. [68].

Table 2
Some properties of the two polymorphs of $[Ph_4As][Au(N_3)_4]$ [74,76].

	Polymorph 1	Polymorph 2
Synthesis	$KAuCl_4/NaN_3/[Ph_4As]Cl$	$KAuCl_4/NaN_3/[Ph_4As]Cl$
Solvent of crystallization	CH_2Cl_2/petroleum ether	Dried CH_2Cl_2 (traces of pentane)
Configuration	Whirlwind	Windmill
Space group	Tetragonal *P4/n*	Monoclinic *C2/c*
N–N–N bond angle (°)	171.9(23)	175.8(3) and 174.4(3)
N–Au–N bond angle (°)	89.3(7)	89.6(1)

bridging hexadentate (μ-1,1,1,3,3,3) coordination as an encapsulated species inside a trigonal prism. The azide ligand is linear and symmetrical (Fig. 7b). With the incorporation of additional silver atoms, the short edges (Ag···Ag 2.999(2) Å) of each Ag_4 rectangle are lengthened in conversion to Ag_6 trigonal prism with Ag···Ag distance exceeding 3.4 Å [72].

Very little work has been done during the last few years on azide complexes of gold. Although not a major area of study, the aim in this particular research is to develop synthetic methods to stabilize gold azide complexes for X-ray characterization. In 1898, the first gold(III) azide complex AuN_3 was prepared from the reaction of NaN_3 and $AuCl_3$ [73]. Later, several reports claimed the synthesis of the highly unstable neutral gold(I) azide complex AuN_3, neutral gold(III) azide complex $Au(N_3)_3$, and the charged gold(I) azide complex $[Au(N_3)_2]^-$, but no further information on their X-ray structures was reported. The stability of gold(III) azide complexes is largely influenced by the counter cation size. The gold(III) tetraazide anion $[Au(N_3)_4]^-$ can be stabilized using relatively large counter cations such as $[Ph_4As]^+$, $[Et_4N]^+$, $[n\text{-}Bu_4N]^+$ and $[Me_3(cetyl)N]^+$ [74]. In contrast, alkali metal gold(III) tetraazide complexes are described as extremely explosive materials [75].

Two orange-red polymorphs are isolated from a $[Ph_4As][Au(N_3)_4]$ complex in aqueous solution from the reaction of $KAuCl_4$ with an excess of sodium azide in the presence of $[Ph_4As]Cl$ [74b,d]. The tendency of bulky ammonium or arsonium salts of gold(III) to explode is very low; their stability is high because of the bulky cations. $[Ph_4As][Au(N_3)_4]$ complex crystallizes from CH_2Cl_2/petroleum ether in the tetragonal space group P4/n (Table 2). The $[Au(N_3)_4]^-$ anion adopts a "whirlwind" configuration [74c]. Another polymorph crystallizes from dried CH_2Cl_2, which contained traces of pentane. The anion is in a "windmill" shape and crystallizes in the monoclinic space group C2/c [76].

The highly explosive gold(III) azide complexes are prepared as $[NH_4]^+$, $[Me_4N]^+$, or alkali metal salts. The orange-red crystals of $[NH_4][Au(N_3)_4]$ explode violently upon contact with a flame. Complex $[Me_4N][Au(N_3)_4]$ exists as polymeric stacking of the anion $[Au(N_3)_4]^-$, consisting of weak gold–gold interactions of 3.507(3) and 3.584(3) Å (Fig. 8). Full geometry optimization at gold–gold distance of 2.0 Å resulted in the dissociation of the dimer. It is likely that the gold–gold interactions are the result of packing effects [77]. The reaction of binary azides with $HAuCl_4$ in aqueous solution at room temperature resulted in orange-red compounds with alkali metal counter cations, $A[Au(N_3)_4]$ (A = K, Rb, Cs). The gold(III) center is located in a distorted tetragonal planar coordination built by the inner nitrogen centers of the azide. Generally, compounds with large cations such as $[Ph_4As]^+$ ions show C_4h symmetry, whereas in all alkali metal gold azide complexes the anion shows C_2 symmetry [78].

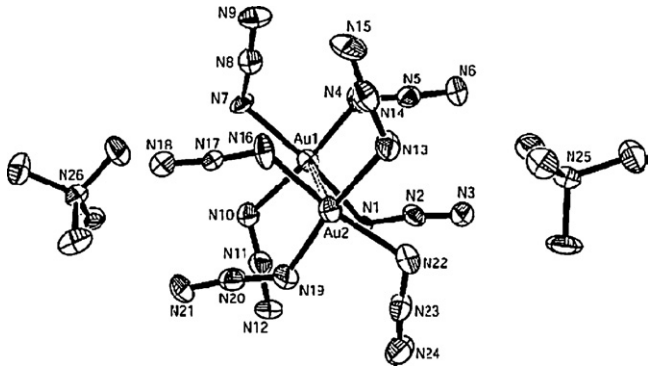

Fig. 8. Structure of the dimer of $[Me_4N][Au(N_3)_4]$; from Ref. [77].

The coordination chemistry of azide has produced several clusters from the phosphine-stabilized gold azides [79]. Homo- and heterometallic gold clusters were synthesized by Strähle in attempts to synthesize gold(III) nitrido complexes by the controlled decomposition of the gold(I) azide complexes R_3PAuN_3 at lower temperatures under the influence of UV radiation to yield complete reductive-elimination of the azide group. The resulting gold(0) fragments $R_3PAu(0)$ combine to form gold clusters. The decomposition reactions of phosphine gold azide complexes formed clusters such as $[(Ph_3PAu)_8]^{2+}$, $[Au(Ph_3PAu)_8(AuCl)_2]^+$ and $[Au(Me_2PhPAu)_{10}(AuCl)_2]^{3+}$. If the photolysis of R_3PAuN_3 is carried out in the presence of a metal carbonyl complex, the $R_3PAu(0)$ fragments can substitute CO ligands to afford heterometallic clusters [79].

3. Amide complexes

Amido ligands $[NR_2]^-$ may act as both two-electron σ- and two-electron π-donors. Amides are expected to form stronger bonds with vacant d-orbitals or p-acceptor early transition metals, which is on contrary to their expected weak bonding with late π-donor electron-rich transition metals [10]. A close similarity in terms of stability and structural features is present among the alkoxide and amide copper complexes, Cu–OR and Cu–NR_2: a possible consequence of the similar thermodynamic stability in the Cu–O and Cu–N bonds. Despite the preparation of a growing number of amide complexes, the details of bonding remain hidden. An important question presently overlooked involves the donor bonds vs. d^{10}–d^{10} interaction in holding the metal and amido ligands together [13]. Structures for various neutral base-free metal amides of the formula $M_4(\mu\text{-}L)_4$, L = NR_2, $N(SiR_xR'_y)_2$ and $N(SnR_3)_2$ have been described. The metal centers and the nitrogen atoms are nearly coplanar (Table 3).

3.1. Synthesis of amide complexes

$$MX + LiNRR'(\text{in ether}) \rightarrow 1/n[M(NRR')]_n (n = 3 \text{or} 4) + LiX \quad (2)$$

$$M(NR_2)_2 (M = Sn, Pb) + 2AgNCO(\text{in ether}) \rightarrow 1/4[Ag(R_2N)_2]_4 \quad (3)$$

$$\text{Copper(I) mesitylene} + R_2NH \rightarrow [R_2NCu]_n + \text{mesitylene} \quad (4)$$

Table 3
The M···M distances (Å) for the amide complexes.

Complex	M···M	Ref.
$[CuN(SiMe_3)_2]_4$	2.6770(7)–2.6937(2)	[83]
$[AgN(SiMe_3)_2]_4$	2.973(2)–3.024(2)	[81]
$[AuN(SiMe_3)_2]_4$	3.0100(3), 3.0355(3)	[84]
$[CuN(SiMePh_2)_2]_3$	2.481(8)	[85]
$[CuN(SiMe_2Ph)_2]_4$	2.687(29)	[85]
$[Cu(Me_2N)]_4$	2.702(2)	[86]
$[Cu(Et_2N)]_4$	2.664(3)	[87]
[Ag(2,2′,6,6′-tetramethylpiperidine)]$_4$	2.973(2), 3.016(2)	[81]
$[Cu(cyclo\text{-}N(CH_2)_4)]_4$	2.717(2)	[86]
$[Cu(MeNCH_2CH_2NMe_2)]_4$	2.618(2)	[86]
$[CuN(SnMe_3)_2]_4$	2.703(1), 2.712(1)	[88]
$[Cu(NHBu^t)]_4$	2.943(1)[a], 2.720(2)[b], 2.742(1)[b]	[88]

[a] Intermolecular distance.
[b] Intramolecular distance.

(R = *n*-Bu, *n* = 4 based on molecular weight determination by cryoscopy in benzene)

Coinage metal amide complexes can be synthesized using three methods (Eqs. (2)–(4)), the first involves the preparation of amides by the metathesis of metal halide with lithium amide, a procedure is widely used in the synthesis of the three coinage metal amide complexes [80]. The second involves the metathetical exchange reaction between metal amides such as $M(NR_2)_2$, M = Sn, Pb, and silver cyanate AgNCO in ether to produce thermally robust silver amides in 50% yield [81]. The third was reported by Saegusa and involves the synthesis of copper dialkylamides via amine exchange with copper mesitylene in THF at ambient temperature. The reaction requires adding amine in excess quantities. Copper(I) amides were easily isolated by evaporating the reaction mixture or by filtering the precipitate. This method is useful for the preparation of copper(I) amides free of coordinating ligands or salts. None of the amide complexes from this procedure were structurally characterized. However, the molecular weight determination of copper complex with $[n\text{-}Bu_2N]^-$ ligand shows that the complex exists as tetranuclear units in benzene [82].

3.2. Trinuclear and tetranuclear amide complexes

The colorless tetranuclear copper(I) complex $[CuN(SiMe_3)_2]_4$ is prepared by the reaction of CuCl or $CuCl_2$ with $LiN(SiMe_3)_2$ [83]. The square-planar tetranuclear complex contains a nearly square Cu_4 core, with copper atoms at the center of the sides and nitrogen atoms at the corners (Fig. 9). The symmetry of the $Cu_4N_4Si_8$ portion of the complex is approximately D_{4h}; the Cu_4N_4 core of the complex is planar within 0.007 Å. The $[CuN(SiMe_3)_2]_4$ complex has only 2-fold symmetry which allows the $SiMe_3$ groups to twist slightly [83]. In $[AgN(SiMe_3)_2]_4$, the macrocyclic Ag_4N_4 skeleton is coplanar, the four nitrogen atoms creating an outer square [81]. The gold(I) amide structure $[AuN(SiMe_3)_2]_4$ is similar to those of copper and silver,

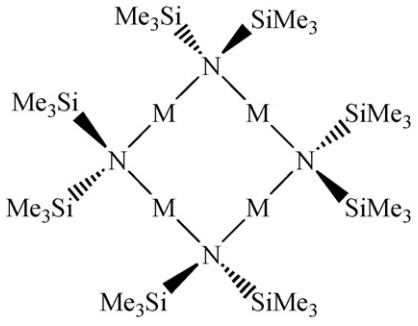

Fig. 9. Structure of $[MN(SiMe_3)_2]_4$, M = Cu, Ag, Au.

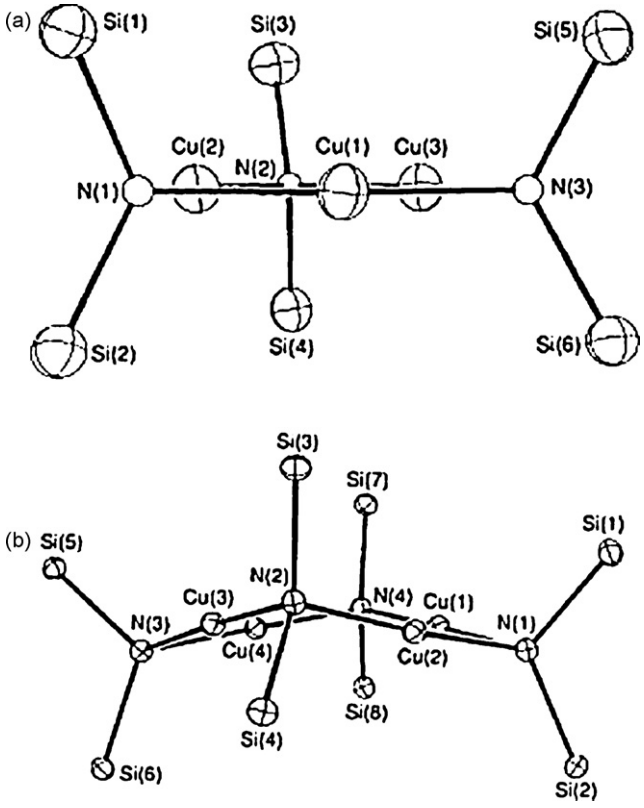

Fig. 10. (a) Cu_3N_3 arrangement in the trinuclear complex $[CuN(SiMePh_2)_2]_3$ and (b) Cu_4N_4 arrangement in the tetranuclear complex $[CuN(SiMe_2Ph)_2]_4$; from Ref. [85].

and it is the only tetranuclear gold amide structure reported so far [84].

A dramatic ligand effect was observed by using amido ligands with mixed substituents such as $[NRR']^-$. Amido ligands with methyl and phenyl substituents form complexes with trinuclear and tetranuclear copper centers. The reaction of the amido ligand $[N(SiMePh_2)_2]^-$ with copper(I) salt forms a trinuclear complex while $[N(SiMe_2Ph)_2]^-$ forms a tetranuclear copper complex (Fig. 10). In the trinuclear complex $[CuN(SiMePh_2)_2]_3$ the nitrogen atoms of the bridging amide ligands have almost negligible displacements from the copper plane. The structure is an equilateral triangle with nitrogen apices and the copper atoms at the midpoint in each side account for the slight outward deviation from a strict linear structure [85]. Using $[N(SiMe_2Ph)_2]^-$ ligand, the tetranuclear complex $[CuN(SiMe_2Ph)_2]_4$ crystallizes with four copper atoms, displaying only slight deviation. However, the nitrogen atoms display much greater deviation from the copper plane. The four nitrogen atoms describe a butterfly shape (fold angle 153.8°). The Cu···Cu distances in planar molecules are longer than those in the butterfly species [85].

The structures of copper and silver of cyclo amido ligands are reported such as $[Cu(tetrahydropyrrole)]_4$ [86] and [Ag(2,2′,6,6′-tetramethylpiperidine)]$_4$ [81]. The copper complex was synthesized in 38% yield and is thermally stable since it decomposes to metallic copper in boiling tetralin only. The structure has planar rather than butterfly Cu_4N_4 arrays. The nitrogen atoms in the silver complex are 0.57–0.58 Å out of the tetranuclear silver plane. Each piperidinato ligand is in a chair conformation (Fig. 11).

Power reported the first X-ray crystal structure of a late transition metal dialkylamide $[Cu(Et_2N)]_4$ [87]. The four copper atoms in $[Cu(R_2N)]_4$, R = Et, Me, define an almost perfect square. The four copper atoms are coplanar, and alternate nitrogen atoms are significantly above and below the copper plane [86,87]. The crystals

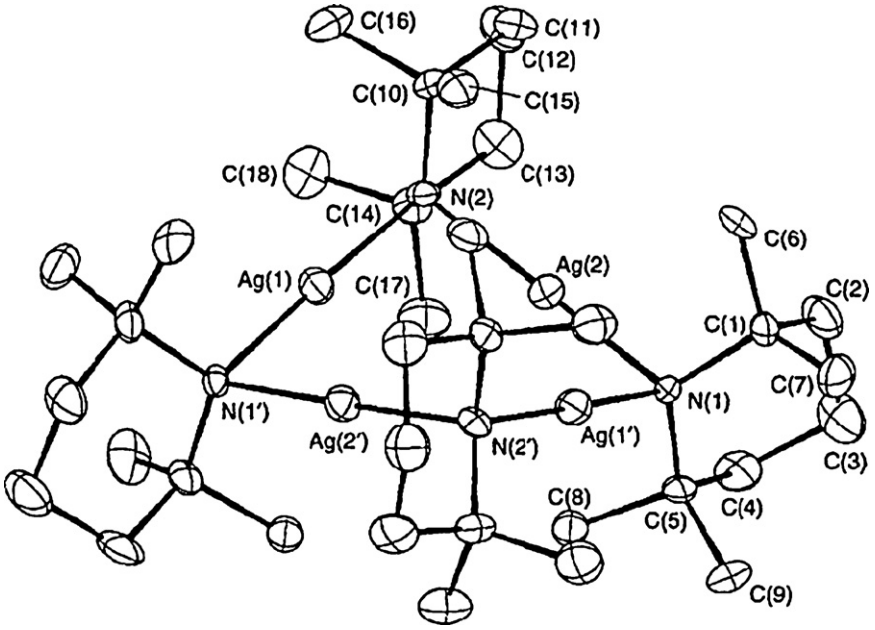

Fig. 11. Structure of [Ag(2,2′,6,6′-tetramethylpiperidine)]$_4$; from Ref. [81].

of [Cu(Et$_2$N)]$_4$ at 0 °C show a slight darkening after several weeks but solutions in n-hexane or ether undergo a rapid color change to blue or green [86]. Utilizing bulky substituents in amide synthesis formed the only example of a dimer of tetranuclear. A neutral dimer of tetranuclear complex [Cu(NHBu^t)]$_4$ is synthesized in 63% yield from the reaction of LiNHBu^t with both CuCl and CuSCN in dimethoxyethane solvent (Fig. 12). The copper complex contains two planar Cu$_4$N$_4$ rings with two intermolecular Cu···Cu interactions of 2.943(1) Å [88]. The amide ligands with mesitylene and phenyl substituents formed anionic multinuclear copper complexes such as [Cu$_6$(NMes)$_2$(NHMes)$_3$]$^-$, [Cu$_{12}$(NPh)$_8$]$^{4-}$ and [Cu$_{24}$(NPh)$_{14}$]$^{4-}$ [88].

Copper(I) chloride reacts with N(SnMe$_3$)$_3$ in dichloromethane at 40 °C to produce the donor–acceptor complex [ClCuN(SnMe$_3$)$_3$] which is transformed into the tetranuclear complex [{CuN(SnMe$_3$)$_2$}$_4$] by thermolysis at 140 °C in DME. [{CuN(SnMe$_3$)$_2$}$_4$] can also be obtained by the reaction of LiN(SnMe$_3$)$_2$ with Cu(SCN)$_2$ in DME at 80 °C [88].

Although Saegusa reported the synthesis of copper dialkylamides via amine exchange with copper mesitylene in THF at ambient temperature, Niemeyer successfully isolated a mixed-ligand tetranuclear copper complex [Cu$_4$(mesitylene)$_2$(amide)$_2$] in 42% yield [89]. The compound was prepared by mixing a solution of germanium amide Ge[N(SiMe$_3$)$_2$]$_2$ in hexane with copper mesitylene in toluene. There are additional peaks in the ^{1}H NMR spectrum which indicates the presence of other species in the solution [(Cu-amide)$_x$(Cu-mesitylene)$_y$] (Fig. 13). The structure is an almost planar eight-membered Cu$_4$C$_2$N$_2$ ring and slightly puckered with Cu–Cu distances range 2.4291(6)–2.6150(9) Å.

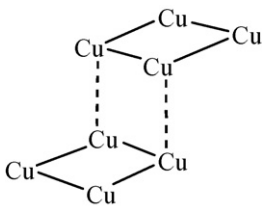

Fig. 12. Structure of the metallacycle in the dimer of the tetranuclear complex [Cu(NHBu^t)]$_4$.

Copper amides absorb carbon dioxide in benzene at ambient temperature in the presence of three equivalents of σ-donating bulky phosphine and isocyanide ligands to produce hexamethyldisiloxane (Me$_3$Si)$_2$O and a copper(I) isocyanate complex. Treatment of the resulting solution with alkyl iodide R′I gave R$_2$NCOOR′. In the absence of σ-donating ligand, copper diethylamide slowly absorbed CO$_2$ in benzene to produce Et$_2$NCOOCu [90].

There is strong motivation in chemical vapor deposition technology to understand the basic relationships between precursor properties and deposition parameters. Precursors could be designed on a more rational basis to allow selective deposition on particular surfaces or to produce pure films with bulk properties [91]. Despite its low volatility, the tetranuclear copper amide complex [CuN(SiMe$_3$)$_2$]$_4$ can be used as a precursor for chemical vapor deposition (CVD) of copper metal, under H$_2$ carrier gas, with both source and substrate at ca. 200 °C. To determine whether the photophysical properties of [CuN(SiMe$_3$)$_2$]$_4$ could be combined with the CVD behavior, the deposition experiments were carried out under Xe arc lamp irradiation, all under 1 atm H$_2$. Smaller amounts of Cu metal films are also deposited when the substrate temperature is as low as 145 °C (in the dark) or 136–138 °C (under Pyrex-filtered Xe arc lamp illumination) [83].

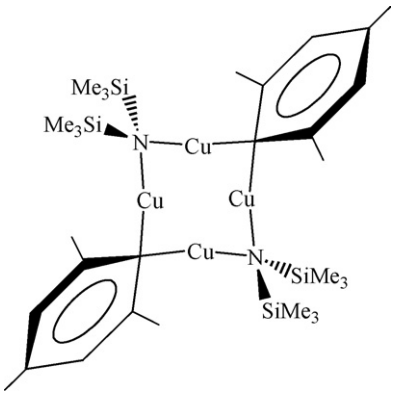

Fig. 13. Structure of [Cu$_4$(amide)$_2$(mesitylene)$_2$].

Table 4
Optimized geometries at MP2 level and selected experimental structural parameters for $[M(NH)_2CH]_2$ [95].

System	M···M (Å)
Optimized geometries at MP2 level	
$[Cu(NH)_2C(H)]_2$	2.528
$[Ag(NH)_2C(H)]_2$	2.712
$[Au(NH)_2C(H)]_2$	2.728
Experimental structural parameters	
$[Cu(4\text{-}MePh)_2N_2C(H)]_2$	2.497
$[Ag(4\text{-}MePh)_2N_2C(H)]_2$	2.705
$[Au(2,6\text{-}Me_2Ph)_2N_2C(H)]_2$	2.711

4. Amidinate complexes

The anionic amidinate ligands are known for their remarkable ability to bridge between the metal atoms, to facilitate the formation of short metal–metal distances, and to have flexible coordination modes. The use of amidinate ligands in the coordination chemistry of the transition metals has produced complexes with extraordinarily short metal–metal distances. Placing alkyl and aryl substituents on the amidinate NCN carbon influences the structural motifs of silver(I) complexes [92]. The structural arrangement of Group 11 amidinate complexes is determined by the substituents on the amidinate aryl groups as well as on the NCN carbon.

Amidinate ligands have been exploited for the synthesis of a variety of complexes spanning the transition elements [93]. Previous trials to synthesize $[M(ArN)_2C(H)]_2$ compounds, Ar = 4-MePh and M = Cu, Ag and Au, indicated that the stability series must be Cu ∼ Ag ≫ Au, since the trials to isolate a gold compound were unsuccessful [94]. Theoretical studies by Pyykkö for $[M(NH)_2C(H)]_2$ models, M = Cu, Ag and Au, predicted the M–M distances at the MP2 level (Table 4) [95]. Experimentally, systems containing amidinate ligands were known with copper and silver, but not with gold. The results for the models containing silver and copper are close to the X-ray structures of $[M(ArN)_2C(H)]_2$, Ar = 4-MePh and M = Cu, Ag. At the experimental and theoretical level, the Ag–Ag distances are 2.705 and 2.712 Å and the Cu–Cu distances are 2.497 and 2.528 Å, respectively. The hypothetical dinuclear gold(I) amidinate compound was calculated to have an Au···Au distance at the MP2 level of 2.728 Å. The dinuclear gold(I) amidinate complex now known proves the predicted Au–Au distance to be rather good at 2.711 Å.

4.1. Tetranuclear amidinate complexes

The X-ray structure of the tetranuclear copper(I) complex $[Cu(PhN)_2C(Ph)]_4$ features a pseudo-rhombic geometry, in which the Cu···Cu distances range is 2.5674(6)–2.6419(7) Å [96]. The Ag···Ag distances around the rhombus tetranuclear silver amidinate complexes with bulky substituents show a slight variation between structures within 2.90 Å for $[Ag(PhN)_2C(Et)]_4$ and $[Ag(4\text{-}Bu^n\text{-}PhN)_2C(Et)]_4$. These substituents appear to have little effect on the structure as the alkyl chains are pointing away from the Ag_4 plane and do not interact sterically with the core of the molecule. In $[Ag(4\text{-}OMe\text{-}PhN)_2C(Me)]_4$, the Ag···Ag distances are 2.8073(5)–2.9832(5) Å, and rhombic angles are irregular [92].

Tetranuclear gold(I) complexes were synthesized with substituents such as -C_6F_5, 3-CF_3-Ph, 3,5-Cl_2-Ph, 4-OMe-Ph, 4-Me-Ph and -Naph. Complexes of ligands with sterically bulky groups in the ortho positions such as 2,6-Me_2-Ph as well as on the NCN carbon, NC(Me)N and NC(Ph)N, were prepared. Tetranuclear gold(I) amidinate complexes are synthesized by the reaction of Au(THT)Cl with the potassium or sodium salt of the ligand in THF (Fig. 14). Syntheses involving various substituted amidinates resulted in tetranuclear gold(I) complexes, $[Au(ArN)_2C(H)]_4$ [97]. In the tetranuclear complexes, the four gold atoms are located at the corners of a rhomboid with the amidinate ligands bridged above and below the plane of the four gold(I) atoms with average Au···Au distances of ∼3.0 Å. The tetranuclear gold(I) complexes $[Au(ArN)_2C(H)]_4$, Ar = 4-MePh, 4-OMePh, 3-CF_3-Ph and 3,5-Cl_2Ph and $[Au(PhN)_2C(R)]_4$, R = Me, Ph, show a bright blue-green luminescence under UV light, in the solid state, at room temperature and 77 K. The different luminescence behavior of the tetranuclear amidinate complexes appears related to the substituents on the aromatic rings. There is a major contribution from the ligands to the emission process [97].

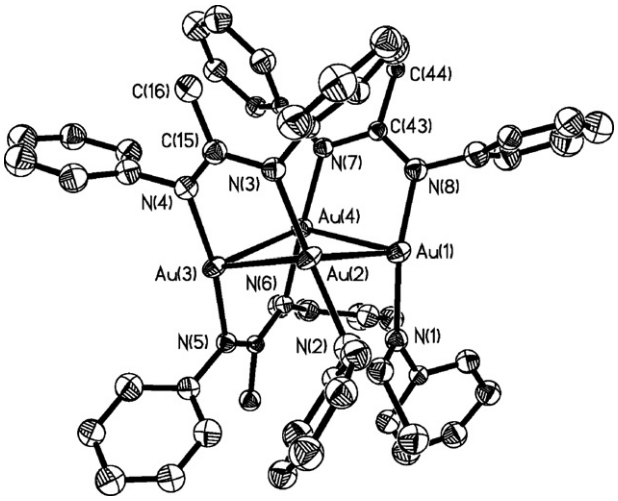

Fig. 14. Structure of $[Au(PhN)_2C(Me)]_4$; from Ref. [97].

4.2. Dinuclear and trinuclear amidinate complexes

A bulkier amidinate ligand $[(2,6\text{-}Me_2Ph)_2N_2C(Ph)]^-$ was used to prepare a dinuclear copper(I) complex $[Cu(2,6\text{-}Me_2Ph)_2N_2C(Ph)]_2$ (Table 5). Oxidation of the dinuclear copper complex resulted in one copper center oxidation (Fig. 15). The stability of Cu_2(I,II) species $[Cu(2,6\text{-}Me_2Ph)_2N_2C(Ph)(CH_3CN)]_2(SbF_6)$ could be enhanced by oxidation of the dinuclear copper complex with $AgSbF_6$ in the presence of coordinating solvents such as MeCN or THF at low temperatures. A short copper–copper separation of 2.4547(13) Å exists in the dinuclear cationic complex, each copper atom coordinated by an MeCN ligand. An analogous THF complex has comparable copper–copper distances of 2.4423(12) and 2.3974(11) Å, as determined for the two independent molecules in the unit cell [96].

Using sterically bulky groups in the ortho positions of the phenyl rings in ArNC(H)NHAr, Ar = 2,6-Me_2Ph, led to the formation of dinuclear and trinuclear metal complexes. This suggests

Table 5
The M···M distances (Å) for the dinuclear amidinate complexes.

Complex	M···M	Ref.
$[Cu(4\text{-}MePh)_2N_2C(H)]_2$	2.497(2)	[94]
$[Ag(4\text{-}MePh)_2N_2C(H)]_2$	2.705(1)	[94]
$[Cu(2,6\text{-}Me_2Ph)_2N_2C(Ph)]_2$	2.4571(2)	[96]
$[Au(2,6\text{-}Me_2Ph)_2N_2C(H)]_2$	2.711(3)	[98]
$[Cu(Bu^s)_2N_2C(Me)]_2$	2.4031(6)	[100]
$[Cu(Pr^i)_2N_2C(Me)]_2$	2.414(1)	[101]
$[Ag(Pr^i)_2N_2C(Me)]_2$[a]	2.645	[101]
$[Ag(2\text{-}OMePh)_2N_2C(H)]_2$	2.780	[102]
$[Ag(2\text{-}SMePh)_2N_2C(H)]_2$	2.805	[102]
$[Cu(Me_3SiN)_2C(Ph)]_2$	2.425	[104]
$[Ag(Me_3SiN)_2C(Ph)]_2$	2.655	[104]
$[Au(Me_3SiN)_2C(Ph)]_2$	2.644	[104]

[a] Exists as $[Ag(Pr^i)_2N_2C(Me)]_2[Ag(Pr^i)_2N_2C(Me)]_3$ (Ag···Ag distance in the trinuclear complex is 2.99(2) Å).

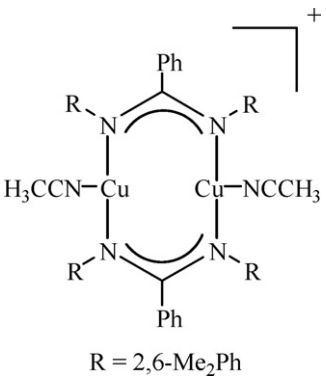

Fig. 15. Structure of $[Cu(2,6\text{-}Me_2Ph)_2N_2C(Ph)(CH_3CN)]_2^+$.

that steric factors can prevent the formation of tetranuclear amidinates [98,99]. The trinuclear $[Au_3(2,6\text{-}Me_2Ph\text{-form})_2(THT)Cl]$ and the dinuclear $[Au(2,6\text{-}Me_2Ph)_2N_2C(H)]_2$ complexes were isolated by the reaction of the potassium salt of the corresponding amidinate ligand with (THT)AuCl (Fig. 16). The Au···Au distance in the dinuclear complex $[Au(2,6\text{-}Me_2Ph)_2N_2C(H)]_2$ is 2.711(3) Å, close to the suggested distance by Pyykkö for $[Au(NH)_2C(H)]_2$ complex (2.728 Å) [95].

Melting point depression of *p*-xylene solutions and mass spectroscopy of $[Cu(Bu^s)_2N_2C(Me)]_2$ show that the copper amidinate complex exists as dinuclear units in the vapor phase and in solution [100]. While the dinuclear copper complex $[Cu(Pr^i)_2N_2C(Me)]_2$ is dimeric in both the solution and solid state, the corresponding silver complex $[Ag(Pr^i)_2N_2C(Me)]_2[Ag(Pr^i)_2N_2C(Me)]_3$ exists as a mixture of dinuclear and trinuclear complexes in a 1:1 (mol/mol) ratio in solution at room temperature and in a 1:2 (mol/mol) ratio in the solid state, as determined by ^1H NMR spectroscopy and X-ray crystallography (Fig. 17). Attempts to separate the dinuclear complex from the mixture by sublimation at 80 °C under 40 mTorr gave a 1:1 mixture of dinuclear and trinuclear complexes. This observation suggests that the sublimed dinuclear quickly equilibrated to a dinuclear/trinuclear mixture on the cold finger or in benzene solution during the NMR measurements [101].

$[Cu(4\text{-}MePh)_2N_2C(H)]_2$ $[Ag(4\text{-}MePh)_2N_2C(H)]_2$
$[Au(4\text{-}MePh)_2N_2C(H)]_4$

The structures of $[Ag(4\text{-}MePh)_2N_2C(H)]_2$ and $[Cu(4\text{-}MePh)_2N_2C(H)]_2$ complexes are infinite sheets of molecules in planes perpendicular to the crystallographic *c* axis. Within the sheets, there are van der Waals contacts between tolyl groups,

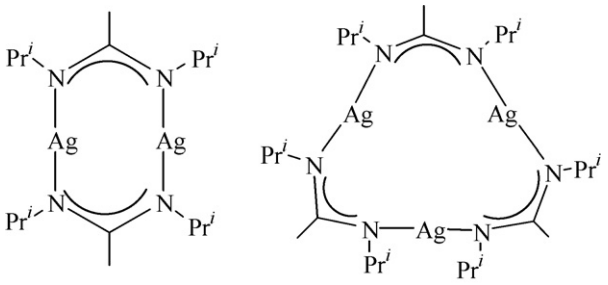

Fig. 17. Structure of $[Ag(Pr^i)_2N_2C(Me)]_2[Ag(Pr^i)_2N_2C(Me)]_3$.

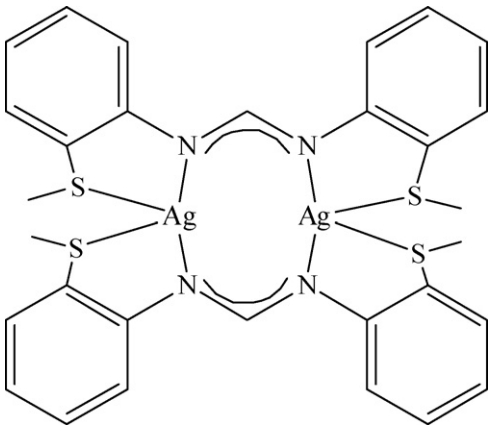

Fig. 18. Structure of $[Ag(2\text{-}SMePh)_2N_2C(H)]_2$.

while the sheets are separated by 3.570 Å in the copper complex and 3.520 Å in the silver complex. In both compounds, the metal–metal distances are unusually short. The Ag···Ag distance, though longer than the Cu···Cu distance (by 0.208 Å), is shorter in proportion to the sizes of the atoms [94].

The effect of increasing the coordination number of the silver(I) centers in silver amidinate complexes by ether oxygen $[Ag(2\text{-}OMePh)_2N_2C(H)]_2$ (Ag–O = 2.69–2.89 Å) and thioether sulfur $[Ag(2\text{-}SMePh)_2N_2C(H)]_2$ (Ag–S = 2.79–2.99 Å) donor substituents on the phenyl groups has been investigated by solution and solid state studies (Fig. 18). VT ^1H NMR (223–303 K) measurements show coupling on cooling between the proton attached to the amidinate carbon and the $^{107/109}Ag$ centers [102,103]. The Ag···Ag distance is increased relative to that in previously characterized amidinate dinuclears. One explanation for this increase (when external bonds

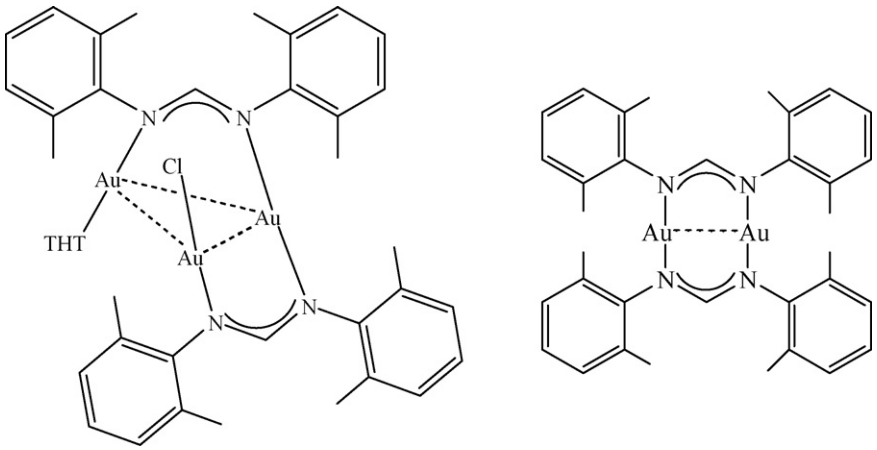

Fig. 16. Structure of the trinuclear and dinuclear gold(I) amidinate complexes.

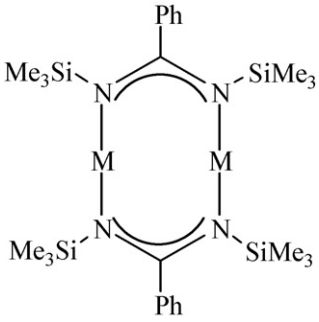

Fig. 19. Structure of $[M(Me_3SiN)_2C(Ph)]_2$, M = Cu, Ag, Au.

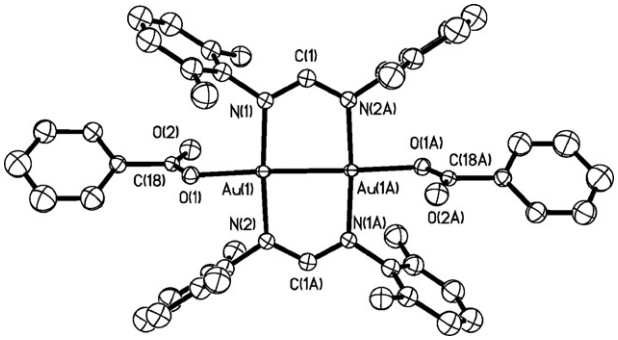

Fig. 21. Structure of $[Au_2(2,6\text{-}Me_2Ph\text{-}form)_2(PhCOO)_2]$; from Ref. [105].

to ether oxygen or thioether sulfur are formed) is that these ligand atoms are donating electron density into an anti-bonding Ag···Ag orbital, weakening a metallic bond between the two silver atoms.

Dinuclear benzamidinate complexes have been isolated with copper(I), silver(I) and gold(I), $[M(Me_3SiN)_2C(Ph)]_2$ (Fig. 19). The copper complex was prepared by the reaction of CuCl with the ligand in boiling acetonitrile, and the silver and gold complexes were prepared by the reaction of the ligand with silver acetate and Au(CO)Cl in acetonitrile suspensions. The complexes have approximate D_2 symmetry, although the eight-membered rings are not completely planar. All three complexes have short metal–metal distances (M···M 2.425 (Cu), 2.655 (Ag), 2.644 (Au) Å) [104].

4.3. Oxidative-addition reactions to the dinuclear gold amidinate complex

Oxidative-addition reactions to the dinuclear gold(I) amidinate complex $[Au(2,6\text{-}Me_2Ph)_2N_2C(H)]_2$ results in the formation of gold(II) complexes. The gold(II) amidinate complexes are the first gold(II) species isolated with nitrogen ligands. The complexes are stable at room temperature. Various reagents such as Cl_2, Br_2, I_2, benzoyl peroxide and CH_3I and halogenated solvents such as CH_2X_2, XCH_2CH_2X, CX_4 (X = Cl, Br, I) add to the dinuclear gold(I) amidinate complex to form oxidative-addition gold(II) products, $[Au_2XY(2,6\text{-}Me_2Ph\text{-}form)_2]$ (Au–Au ~ 2.5 Å) (Fig. 20) [98,105]. The methyl iodide addition product is the only organometallic gold(II) species formed to date with amidinate ligands. In the reaction of the haloalkyls CH_nX_m, the qualitative order of reactivity with the dinuclear gold complex (I > Br > Cl) inversely follows the order of carbon–halogen bond dissociation energy, C–Cl > C–Br > C–I.

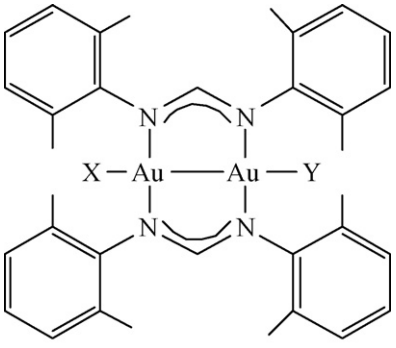

X = Y = Cl, Br, I, PhCOO

X = CH_3 and Y = I

Fig. 20. Gold(II) amidinate complexes prepared by oxidative-addition to the dinuclear gold(I) amidinate complex.

The oxidative-addition of benzoyl peroxide $(PhCOO)_2$ to a toluene solution of the dinuclear gold(I) amidinate complex leads to the isolation of the first stable dinuclear gold(II) nitrogen complex also possessing Au–O bonds, $[Au(2,6\text{-}Me_2Ph)_2N_2C(H)(PhCO_2)]_2$ (Au–Au 2.48 Å) (Fig. 21) [105]. The oxidative-addition of benzoyl peroxide to the dinuclear gold(I) ylide complex formed a gold(II) complex with the shortest Au···Au distance observed, 2.56–2.58 Å, for the dinuclear gold(II) ylide complexes [106]. The oxidative-addition of methyl iodide, CH_3I, to $[Au(2,6\text{-}Me_2Ph)_2N_2C(H)]_2$ in ether generates $[CH_3Au(2,6\text{-}Me_2Ph\text{-}form)_2AuI]$ in quantitative yield under nitrogen at 0 °C in the absence of light [107]. The Au–Au distance is 2.529(11) Å, while in the dinuclear gold(I) ylide, $[(CH_3)Au((CH_2)_2PMe_2)_2AuI]$, the gold(II)–gold(II) distance is 2.695(4) Å [108]. The reaction of the dinuclear gold(I) amidinate complex $[Au(2,6\text{-}Me_2Ph)_2N_2C(H)]_2$ with $Hg(CN)_2$ (1:2 stoichiometry) in THF forms a 2D coordination polymer, $[Au(2,6\text{-}Me_2Ph)_2N_2C(H)]_2{\cdot}2Hg(CN)_2{\cdot}2THF$, rather than the expected oxidative-addition product of the type formed with the ylides. In the case of the dinuclear gold(I) ylide, oxidation of the Au(I) to Au(II) resulted in the formation of a reduced mercury(0) product [109]. The adduct formation of $Hg(CN)_2$ to the $[Au(2,6\text{-}Me_2Ph)_2N_2C(H)]_2$ increases the Au···Au distance to ~2.9 Å [110,111].

The differences observed in the chemistry of these dinuclear gold(I) amidinate complexes compared with dinuclear gold(I) complexes with sulfur and carbon ligands may be understood by examining the respective HOMOs and LUMOs of the species. In the ylide complexes the HOMO is a metal–metal σ^* anti-bonding orbital, and the LUMO is a bonding σ orbital directed along the metal–metal axis. In the dinuclear gold(I) amidinates the HOMO is δ^* with regard to the pi orbitals of the nitrogen ligands. The LUMO is also largely ligand based [110].

4.4. Formation of mixed-ligand tetranuclear gold nitrogen complexes

Attempts to introduce less bulky anionic ligands to the dinuclear complex $[Au(2,6\text{-}Me_2Ph)_2N_2C(H)]_2$ cause the dinuclear gold(I) amidinate complex to rearrange and form tetranuclear gold(I) amidinate complexes [112]. The ligand exchange of the sterically bulky ligand $(2,6\text{-}Me_2Ph)_2N_2C(H)$ in the dinuclear gold(I) amidinate complex with less bulky anionic ligands such as $[3,5\text{-}Ph_2Pz]^-$ and $[(ArN)_2C(H)]^-$, Ar = 4-MePh, 4-OMePh, to form mixed-ligand species provides a facile procedure for the synthesis of mixed-ligand complexes along with the increased nuclearity (Fig. 22). Reacting the amidinate salt K[4-MePh-form] with the dinuclear gold(I) complex $[Au(2,6\text{-}Me_2Ph\text{-}form)]_2$ in a 1:1 stoichiometry in THF forms the dinuclear-tetranuclear complex $[Au_2(2,6\text{-}Me_2Ph\text{-}form)_2][Au_4(4\text{-}MePh\text{-}form)_4]{\cdot}2THF$. Adjusting the reaction ratio to 2:1 formed the tetranuclear complex $[Au(4\text{-}MePh\text{-}form)]_4$ [112].

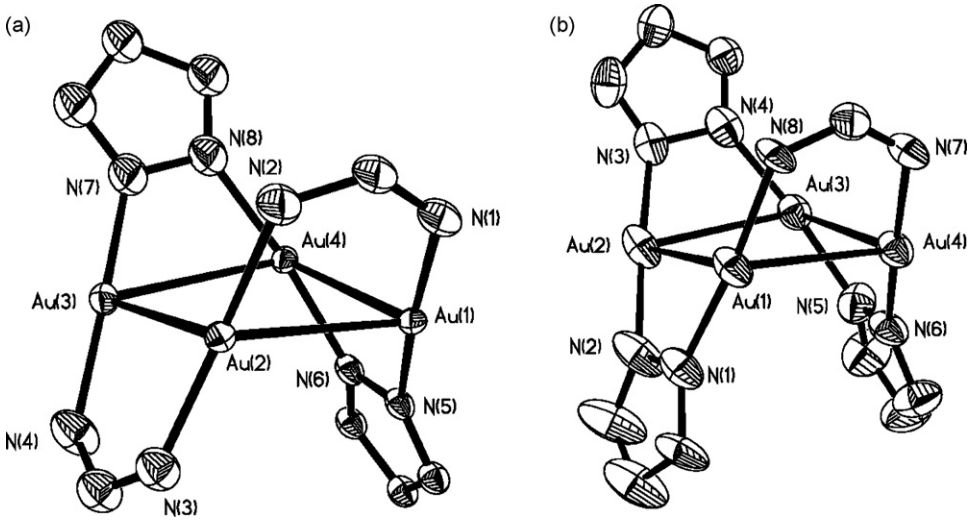

Fig. 22. Structure of (a) $[Au_4(3,5\text{-}Ph_2Pz)_2(2,6\text{-}Me_2Ph\text{-}form)_2]$ and (b) $[Au_4(3,5\text{-}Ph_2Pz)_3(2,6\text{-}Me_2Ph\text{-}form)]$; from Ref. [112]. Phenyl rings omitted for clarity.

The reaction of the diphenylpyrazolate salt Na[3,5-Ph_2Pz] with the dinuclear gold(I) complex $[Au(2,6\text{-}Me_2Ph\text{-}form)]_2$ in a 1:1 stoichiometric ratio resulted in the formation of two tetranuclear products, observed as blocks, $[Au_4(3,5\text{-}Ph_2Pz)_2(2,6\text{-}Me_2Ph\text{-}form)_2]\cdot 2THF$ and as needles, $[Au_4(3,5\text{-}Ph_2Pz)_3(2,6\text{-}Me_2Ph\text{-}form)]\cdot THF$. The Au···Au distances range in both complexes is 3.02–3.20 Å. Adjusting the reaction ratio to 1.5:1 resulted in the isolation of the tetranuclear mixed-ligand complex $[Au_4(3,5\text{-}Ph_2Pz)_3(2,6\text{-}Me_2Ph\text{-}form)]\cdot THF$. These results validate the calculations which indicate that the tetranuclear structure is favored over the dinuclear arrangement with amidinate ligands [112].

4.5. CO oxidation over Au/TiO_2 prepared from gold nitrogen complexes

Metal–organic and organometallic complexes have been widely used in the synthesis of catalysts, however, the use of metal–organic or organometallic gold complexes as catalyst precursors has been limited [113]. Gates and coworkers reported that a supported mononuclear gold complex is active for ethylene hydrogenation at 353 K [114]. A series of Au/TiO_2 catalysts have been prepared from precursors of various gold–nitrogen complexes (Au_n, $n = 2$–4) and their catalytic activity for CO oxidation studied [113]. The Au/TiO_2 catalyst synthesized from a tetranuclear gold amidinate complex shows the best performance for CO oxidation with the TEM image of this catalyst indicating an average gold particle size of 3.1 nm.

Several factors may contribute to the high activity of Au/TiO_2 catalysts [113]. First, the use of metal–organic complexes as precursors can avoid chloride. $HAuCl_4$ is widely used as a gold precursor in catalytic studies, invariably leaving a chloride residue in the catalyst after preparation. Recently, both experimental and theoretical studies have shown that chloride can poison the catalytic performance of gold catalysts for CO oxidation. Density functional calculations show that chloride can act as a poison by weakening the adsorption of O_2 and lowering the stability of the $CO{\cdot}O_2$ intermediate complex [115].

Clearly metal–organic precursors provide an attractive route for the preparation of chloride-free gold catalysts. Another explanation for the high activity of Au/TiO_2 catalysts also relates to the use of metal–organic precursor complexes. Upon deposition onto the oxide support, these complexes interact with the surface OH groups and become less mobile compared to gold atoms deposited using $HAuCl_4$. The catalyst particles appear to form at defect sites on the oxide as established by studies with MgO as the oxide surface. The defect sites may serve as calcination sites for the metal–organic catalyst precursors and perhaps inhibit agglomeration of gold particles during calcination. Factors preventing the sintering of gold lead to a narrow particle size distribution compared to the deposition–precipitation method of catalyst formation.

4.6. Amidinate complexes in atomic layer deposition

Atomic layer deposition (ALD) is a method currently used for manufacturing thin films in computer chips and displays [116]. Metal amidinates have been found to be suitable precursors for the ALD of transition metals and metal oxides [117]. Contrary to the success with metal amidinates [118,119], trials to utilize copper amides for ALD resulted in limited success. The copper(I) amidinates are sufficiently volatile, thermally stable, and highly reactive. The ALD copper films from copper amidinates show strong adhesion to the substrates, so that ALD copper seed layers are used to generate robust microelectronic interconnections. Complex $[Cu(Bu^s)_2N_2C(Me)]_2$ is especially attractive due to its thermal stability, low melting point, high volatility, and high reactivity to surfaces previously treated with molecular hydrogen (Scheme 1). It reacts readily with molecular hydrogen, which allowed the ALD

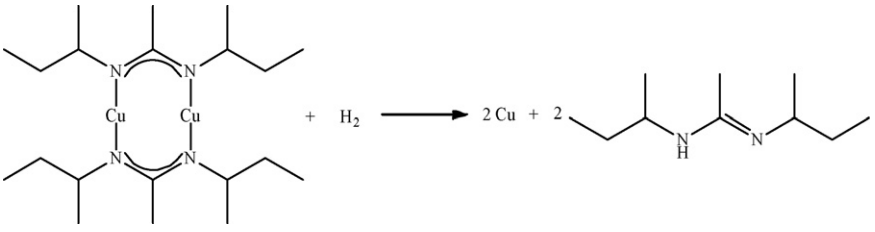

Scheme 1. Formation of copper metal in CVD process.

copper process at low temperatures. The advantage of another precursor $[Cu(Pr^i)_2N_2C(Me)]_2$ is that it has enough reactivity with molecular hydrogen to deposit pure copper metal films at a relatively low temperature of 200 °C. The disadvantage of this precursor is its high melting point of 147 °C, which causes it to sublime from its solid phase in the reservoir [120].

5. Guanidinate complexes

While amidinates are much more planar, Group 11 guanidinates have a large torsion in the dinuclear ring. The exocyclic amide moiety changes the coordination behavior of the ligand by permitting an additional resonance structure to exist (Fig. 23). When the ligand has an alkyl group in the exocyclic position, the π system is restricted to the dinuclear ring. When an amide is in the exocyclic position, the π system can extend to the exocyclic nitrogen, permitting the imide resonance structure [121,122].

5.1. Dinuclear, tetranuclear and hexanuclear guanidinate complexes

Guanidinate complexes are prepared in excellent yields by the metathesis of the alkali metal salts of the ligands with the corresponding coinage metal salt. The Cu···Cu distances in the colorless crystals of $[Cu\{Me_2NC(Pr^iN)_2\}]_2$ and $[Cu\{Pr^iN(H)C(Pr^iN)_2\}]_2$ complexes are 2.4233(10) and 2.4289(11) Å (Fig. 24). This ring twist (32.0–37.5°) can be attributed to the participation of the exocyclic amide of the guanidinates in the π system of the ring [121].

An interesting story is unfolding by Bunge et al. with respect to the chemistry and bonding in guanidinate complexes. Planar hexanuclear copper(I) guanidinate complexes $[Cu\{\mu\text{-}N{=}C(NEt_2)(NR_2)\}]_6$, $NR_2{=}NMe_2$ and cyclic $N(CH_2)_4$, are similar in structure (Scheme 2). The tetraalkylguanidinate ligands alternate above and below the plane of the Cu_6 ring with Cu–N–Cu bond angle 94.6° (av.) and Cu–Cu distance 2.72 (av.) Å (Fig. 25). The hexagonal Cu_6 core contains Cu–Cu–Cu bond angles ranging from 118.74(2)° to 120.978(19)°. A density functional theory (DFT) investigation was undertaken to provide insight into the bonding and potential cyclic conjugation responsible for the formation of the planar

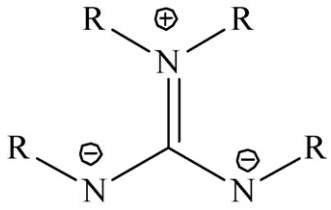

Fig. 23. Resonance structure of the guanidinate ligand.

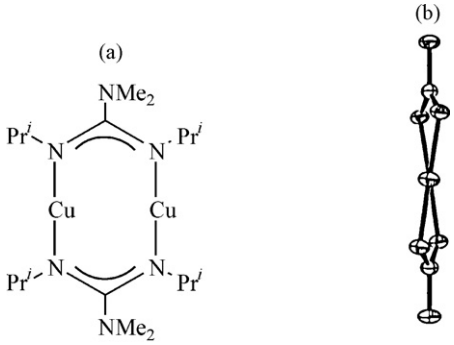

Fig. 24. (a) Structure of $[Cu\{Me_2NC(Pr^iN)_2\}]_2$ and (b) dinuclear core showing the twist (torsion angle is 32.0°).

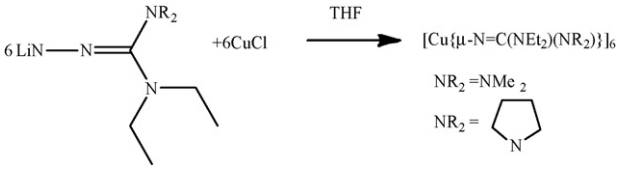

Scheme 2. Synthesis of $[Cu\{\mu\text{-}N{=}C(NEt_2)(NR_2)\}]_6$.

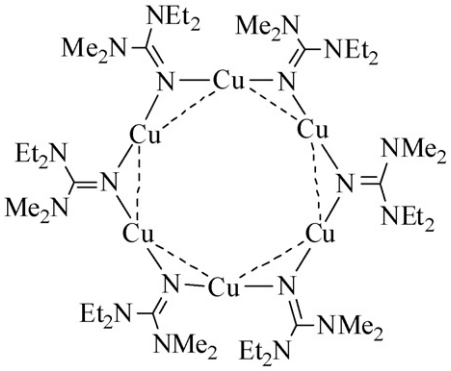

Fig. 25. Structure of $[Cu\{\mu\text{-}N{=}C(NEt_2)(NMe_2)\}]_6$.

hexanuclear copper guanidinate complexes. On the basis of the theoretical calculations, copper–copper interactions are weak and the factors controlling the stability of $[Cu(\mu\text{-TAG})]_6$ complexes are due to the strong Cu–N interactions [122].

5.2. Formation of mixed-ligand guanidinate complexes

The versatile coordination behavior of guanidinate ligands has been utilized in the synthesis of tetranuclear and trinuclear mixed-ligand complexes. A series of tetranuclear guanidinate-amide complexes were synthesized of the general formula $[M_2\{\mu\text{-}N{=}C(NEt_2)(NR_2)\}\{\mu\text{-}N(SiMe_3)_2\}]_2$, $NR_2{=}NMe_2$ and cyclic $N(CH_2)_4$ (Fig. 26). The structure of the complexes $[M_2(\mu\text{-TAG})\{\mu\text{-}N(SiMe_3)_2\}]_2$ exhibits only minor variation with alteration of the TAG ligand or the coinage metal. The tetranuclear complexes exist as a planar M_4N_4 ring with the metal atoms bridged by alternating TAG and $N(SiMe_3)_2$ ligands. The two silicon atoms on each $N(SiMe_3)_2$ ligand reside on opposite sides of the M_4N_4 plane. The M···M distances are 2.72 Å, Cu; 3.06 Å, Ag; 3.06 Å, Au [123]. An interesting trinuclear amide-guanidinate copper complex $[Cu_3(amide)(guanidinate)_2]$ (Fig. 27) was prepared by reacting $(CH_3)_2NCN$ and $LiN(SiMe_3)_2$ with CuCl. The colorless crystals show that the copper atoms are coplanar with a crystallographic 2-fold rotation axis and that Cu–Cu bonds bridged by the guanidinate ligands, 2.793(9) Å, are shorter than those bridged by the amide ligand, 2.6405(11) Å [124].

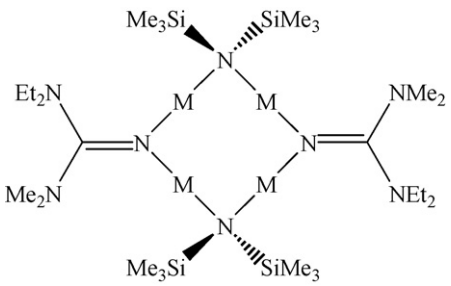

Fig. 26. Structure of $[M_2\{\mu\text{-}N{=}C(NEt_2)(NMe_2)\}\{\mu\text{-}N(SiMe_3)_2\}]_2$, M = Cu, Ag, Au.

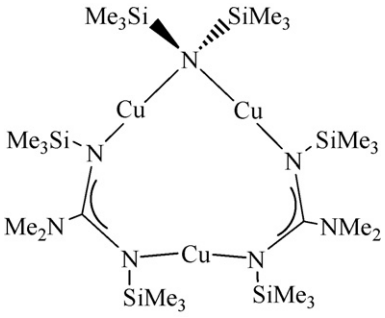

Fig. 27. Structure of $[Cu_3(amide)(guanidinate)_2]$.

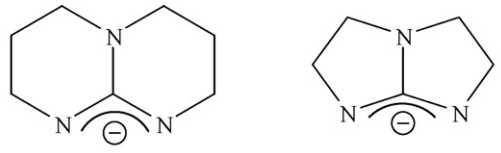

1,3,4,6,7,8-hexahydro-2H-pyramido[1,2-a]-pyramidinate **[hpp]⁻**

1,3,6-triazabicyclo [3.3.0]oct-4-ene **[tbo]⁻**

Fig. 28. Structure of the anionic, bidentate nitrogen ligands $[hpp]^-$ and $[tbo]^-$.

5.3. Bicyclic guanidinate complexes

Work with the Hhpp ligand was pioneered by Cotton and coworkers who showed that the dinuclear metal complexes with Cr(II), Mo(II), or W(II), ionize readily, the latter more readily than cesium (Fig. 28) [125]. The hpp ligand apparently shows a different behavior with different Group 11 elements, forming a tetranuclear complex with gold and silver but to date only a dinuclear complex of copper(I) has been reported.

$[Cu(hpp)]_2$ $[Ag(hpp)]_4$ $[Au(hpp)]_4$

The dinuclear $[Cu(hpp)]_2$, hpp = 1,3,4,6,7,8-hexahydro-2*H*-pyrimido[1,2-*a*]pyrimidine, was reported by Cotton (Fig. 29). The question of whether such a short Cu–Cu distance of 2.453(1) Å justifies the postulation of a metal–metal bond was addressed using the density functional theory (DFT). The density functional calculations show that the close approach of the copper atoms is predictable without involving significant amount of covalent bonding. The very short copper–copper distance can be attributed

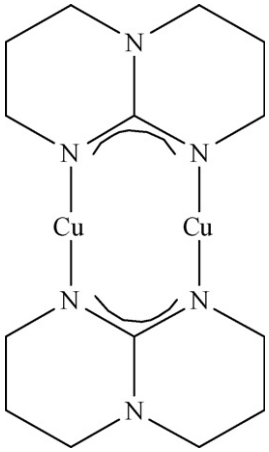

Fig. 29. Structure of $[Cu(hpp)]_2$.

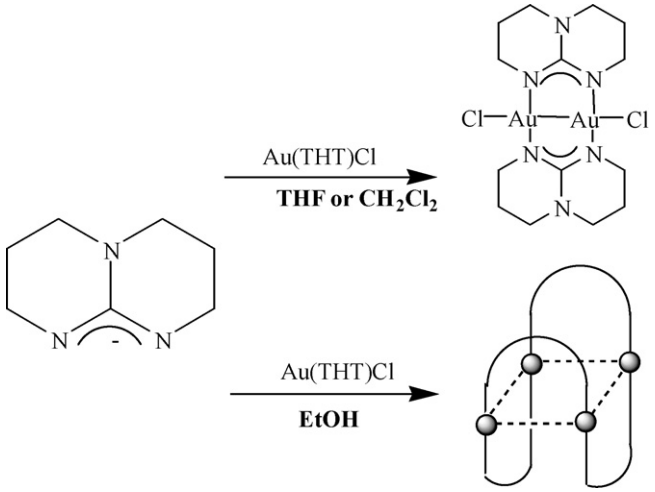

Scheme 3. Synthesis of $[Au_2(hpp)_2Cl_2]$ and $[Au_4(hpp)_4]$.

to a combination of strong Cu–N bonding and very short (ca. 2.2 Å) bite distances for the ligands [126]. The reaction of $AgNO_3$ with Na[hpp] forms a tetranuclear complex $[Ag_4(hpp)_4]$. The four silver atoms are located at the corners of a rhomboid with the hpp ligands bridged above and below the plane of the four silver atoms (Ag···Ag 2.8614(6) Å). The rhomboidal geometry of the Ag_4 complex seems to be the result of steric factors [127].

It appears that the nuclearity of the gold(I) hpp compound depends on factors such as the disproportionation rate of the gold(I) in a given solvent and the presence of oxidants (Scheme 3). The short ligand bite distance should promote tetranuclear product $[Au(hpp)]_4$ formation over dinuclear species but in the presence of oxidizing solvents and solvents supporting rapid disproportionation and in the presence of coordinating ligands like chloride, a gold(II) product $[Au_2(hpp)_2Cl_2]$ is isolated [128]. This solvent role regarding the formation of a dinuclear gold(II) or a tetranuclear gold(I) product is noted when Na[hpp] is reacted with (THT)AuCl. In THF the product is the dinuclear gold(II) species, $[Au_2(hpp)_2Cl_2]$, along with gold metal. In oxidizing solvents such as the chlorocarbon dichloromethane, $[Au_2(hpp)_2Cl_2]$ is produced in high yield without gold(0) formation. If ethanol is used as the solvent, the product is the tetranuclear gold(I) species, $[Au(hpp)]_4$. Using silver benzoate in a CH_3CN/THF solution to remove the chlorides formed a hexanuclear Au(II)-Ag(I) complex $[(PhCOO)_6Au_4(hpp)_4Ag_2]$ with a very short Au–Au distance, 2.4473(19) Å (Fig. 30) [129]. The X-ray crystal structure of $[Au_2(hpp)_2Cl_2]$ revealed a Au(II)–Au(II) distance of 2.4752(9) Å. The gold–gold distances in the tetranuclear $[Au_4(hpp)_4]$ complex are 2.8975(5)–2.9392(6) Å, similar to those found in the tetranuclear gold amidinate complexes. With the related smaller ring guanidinate $[Au_4(tbo)_4]$ the average Au···Au distance is 3.16 Å [128] (Fig. 31).

The ready oxidation of these complexes with the electron-rich bicyclic guanidinate ligand clearly shows that ligands which favor short metal–metal distances promote reduction of the electron

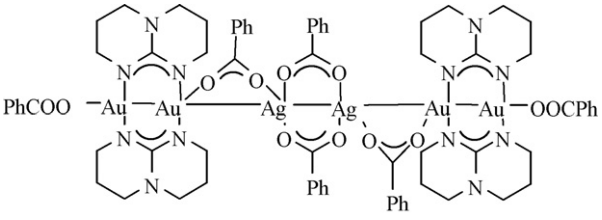

Fig. 30. Structure of $[(PhCOO)_6Au_4(hpp)_4Ag_2]$.

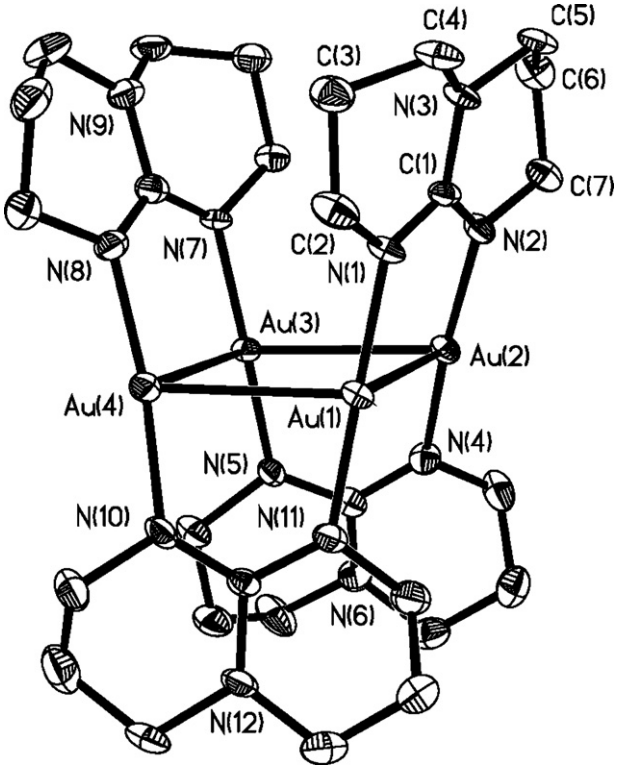

Fig. 31. Structure of $[Au_4(hpp)_4]$; from Ref. [128].

density between the metal atoms by electron loss. Density Functional Theory (DFT) and MP2 calculations on $[Au_2(hpp)_2Cl_2]$ show that the Highest Occupied Molecular Orbital (HOMO) is predominately hpp and chlorine-based with some Au–Au δ^* character and that the Lowest Unoccupied Molecular Orbital (LUMO) has metal-to-ligand (M–L) and metal-to-metal (M–M) σ^* character (approximately 50% hpp/chlorine, and 50% gold). DFT calculations on $[Au_4(hpp)_4]$ show that the HOMO and HOMO-1 are a mixture of metal–metal anti-bonding character and metal–ligand anti-bonding character and that the LUMO is predominately metal based σ character (85% Au and 15% hpp) [128].

6. Triazenide complexes

Triazenide anions are isoelectronic with carboxylate and amidinate, and act as bridging ligands with closed-shell Group 11 elements. Four structural motifs are reported so far as dinuclear, trinuclear, tetranuclear and polymeric units. Due to their limited scope of applications, the chemistry of Group 11 triazenide complexes has been comparatively neglected.

$[Cu(PhNNNPh)]_2$ $[Ag(PhNNNPh)]_2$ $[Au(PhNNNPh)]_4$

The crystal structure of the dinuclear copper(I) triazenide complex $[Cu(PhNNNPh)]_2$ was determined at room temperature [130a] and redetermined at 150 K [130b]. The Cu···Cu distances are 2.4405(10) Å at 150 K and ~2.45(8) Å at room temperature. The structure of the copper(II) complex $[Cu_2(PhNNNPh)_4]$ was determined which shows the *syn-syn* structure analogous to that of copper(II) acetate monohydrate. The copper–copper distance is 2.441(2) Å [131]. The yellow crystals of the silver complex $[Ag(PhNNNPh)]_2$ show that the triazenide ligands bridge the silver centers in an eight-membered ring (Table 6) [132]. The ligands in the tetranuclear gold(I) complex $[Au(PhNNNPh)]_4$·THF bridge pairs of gold atoms alternatively above and below the rhombus of the four gold atoms [133].

Table 6
The M···M distances for the triazenide complexes.

Complex	M···M	Ref.
$[Cu(PhNNNPh)]_2$[a]	2.4405(10)	[130]
$[Cu_2(PhNNNPh)_4]$[b]	2.441(2)	[131]
$[Ag(PhNNNPh)]_2$	2.669(1)	[132]
$[Au(PhNNNPh)]_4$	2.856(1)–2.842(1)	[133]
$[Cu(4\text{-}CF_3\text{-}Ph)_2NNN]_4$	2.578(11)	[135]
$[Ag(4\text{-}CF_3\text{-}Ph)_2NNN]_n$	2.835(2)	[135]
$[Cu(4\text{-}F\text{-}Ph)_2NNN]_4$	2.607(6), 2.738(6)	[134]
$[Ag(4\text{-}F\text{-}Ph)_2NNN]_4$	2.8064(4), 2.8337(4)	[134]
$[Ag(4\text{-}OMe\text{-}Ph)_2NNN]_2$	2.680(1)	[137]
$[Ag(2\text{-}OMe\text{-}Ph)_2NNN]_4$	2.7633(16)–2.8174(15)	[138]
$[Cu(2\text{-}OOCCH_3\text{-}Ph)_2NNN]_2$	2.4289(12)	[140]
$[Ag(2\text{-}OOCCH_3\text{-}Ph)_2NNN]_2$	2.704(2)	[140]
$[Cu(2,6\text{-}Pr^i_2\text{-}Ph)_2NNN]_2$	2.4458(4)	[141]
$[Ag(2,6\text{-}Pr^i_2\text{-}Ph)_2NNN]_3$	3.01184(17)–2.92745(16)	[141]
$[Au(2,6\text{-}Pr^i_2\text{-}Ph)_2NNN]_2$	2.6762(4)	[141]

[a] Copper(I) complex.
[b] Copper(II) complex.

Electron-withdrawing substituents such as –F and $–CF_3$ form tetranuclear silver and copper triazenide complexes except the $–CF_3$ substituent which forms polymer with silver(I). The four metal atoms in $[Cu(4\text{-}F\text{-}Ph)_2NNN]_4$ and $[Ag(4\text{-}F\text{-}Ph)_2NNN]_4$ complexes form a planar rhombus [134]. The copper complex is slowly oxidized in methanol to form $[Cu(4\text{-}F\text{-}Ph)_2NNN(OCH_3)]_4$. The cubane-like Cu_4O_4 unit is formed by two parallel Cu_2O_2 rings [134]. The air-stable orange crystals of $[Cu(4\text{-}CF_3\text{-}Ph)_2NNN]_4$ display tetranuclear units of S4 symmetry with the four copper atoms forming a slightly folded rhombus. The zigzag chains of $[Ag(4\text{-}CF_3\text{-}Ph)_2NNN]_n$ polymer crystallize with short silver-silver distances and Ag–Ag–Ag bond angles of 113.7° and 114.1° (Fig. 32). The bridging triazenide ligands alternate above and below the Ag–Ag chain [135]. The tetranuclear copper(I) complex $[Cu(MeNNNMe)]_4$ is isolated with the four copper atoms are arranged as a diamond-shaped [136].

$[Ag(4\text{-}OMe\text{-}Ph)_2NNN]_2$ $[Ag(2\text{-}OMe\text{-}Ph)_2NNN]_4$

Complex $[Ag(4\text{-}MeO\text{-}Ph)_2NNN]_2 \cdot 2/3py$ crystallizes from pyridine as orange-yellow, air-stable crystals. The triazenide ligands form planar Ag_2N_6 heterocycles [137]. A tetranuclear silver complex $[Ag(2\text{-}MeO\text{-}Ph)_2NNN]_4$·THF is isolated if the methoxy groups are in the ortho position. Each silver atom is bonded to two oxygen atoms from the methoxy groups with silver–oxygen bond distances range of 2.499(8)–2.543(10) Å [138]. The dinuclear silver triazenide complex forms yellow pyridine adduct $[Ag(4\text{-}EtO\text{-}Ph)_2NNN]_2 \cdot 2py$ (Fig. 33). Pyridine ligand is weakly coordinated to each silver atom with a $Ag–N_{pyridine}$ bond distance of 2.455 Å [139]. The structures of $[M(2\text{-}OOCCH_3\text{-}Ph)_2NNN]_2$, M = Cu, Ag, show a single ester carbonyl group coordinated to each metal center, with one ester of each ligand remaining unbound (Fig. 34). The carbonyl oxygen atoms of $[M(2\text{-}OOCCH_3\text{-}Ph)_2NNN]_2$ lie above and below the planar core [140].

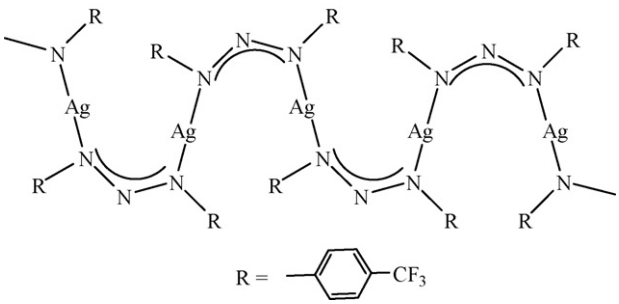

Fig. 32. Structure of $[Ag(4\text{-}CF_3\text{-}Ph)_2NNN]_n$.

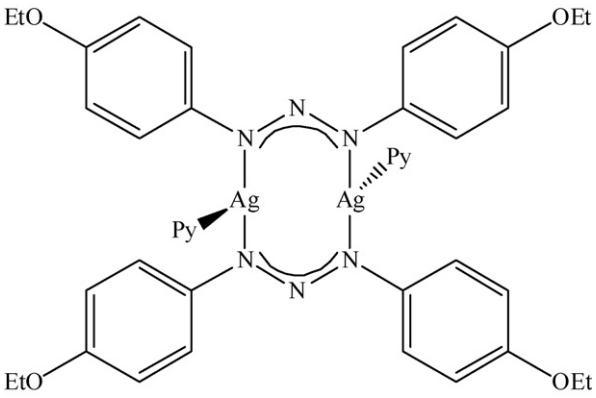

Fig. 33. Structure of $[Ag(4\text{-}EtO\text{-}Ph)_2NNN]_2$.

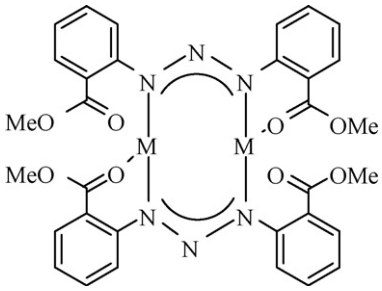

Fig. 34. Structure of $[M(2\text{-}OOCCH_3\text{-}Ph)_2NNN]_2$, M = Ag, Cu.

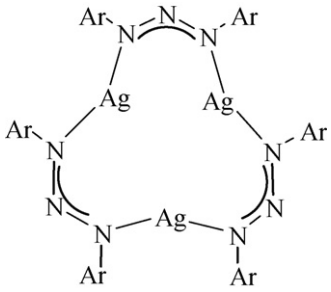

Fig. 35. Structure of $[Ag(2,6\text{-di-isopropylphenyl})N_3]_3$.

Johnson and coworkers reported the first trinuclear silver triazenide complex [141]. A homologous and homoleptic series of stable coinage metal complexes of the bulky ligand N,N′-bis(2,6-diisopropylphenyl)triazene have been synthesized with the general formula $[M(triazenide)]_n$ (M = Cu (dinuclear)), Au (dinuclear), Ag (trinuclear) (Fig. 35). Both the gold and copper complexes are essentially planar.

7. Pentaazadienide complexes

Pentaazadienide ligand coordinates with either the outer two nitrogen atoms, one outer and one inner nitrogen atom or all the three nitrogen atoms (Fig. 36) [142]. The pentaazadienide anion

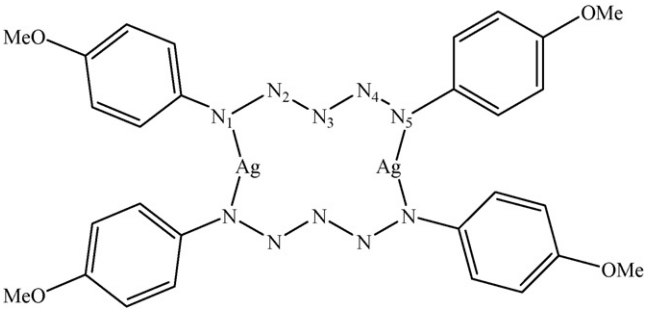

Fig. 37. Structure of $[Ag(4\text{-}OMe\text{-}Ph)_2N_5]_2$ with (N1)-η1 and (N5)-η1 bridging.

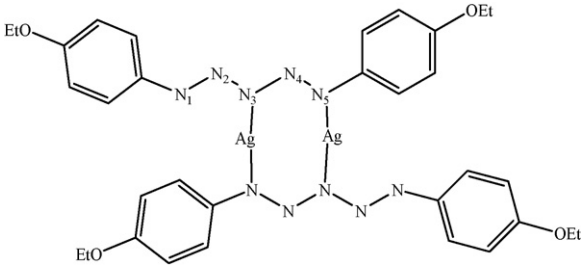

Fig. 38. Structure of $[Ag(4\text{-}EtO\text{-}Ph)_2N_5]_2$ with (N1)-η1 and (N3)-η1 bridging.

demonstrated its surprising versatility as a ligand and its ability to promote short metal–metal contacts in complexes with coinage metal ions.

The reaction of 1,5-ditolylpentaazadiene with $[Ag(NH_3)_2]^+$ in a concentrated ammonia solution yields an orange-red dinuclear silver(I) complex $[Ag(4\text{-}R\text{-}Ph)_2N_5]_2$, R = Me (Ag–Ag 3.5417(5) Å), R = OMe (Ag–Ag 3.762(2) Å). In the centrosymmetric and approximately planar complex, the silver centers are coordinated by the outer nitrogen atoms of the pentaazadienide chain forming a 12-membered Ag_2N_{10} ring, N–Ag–N 160° (Fig. 37) [132,137]. The treatment of $[Ag(4\text{-}Me\text{-}Ph)_2N_5]_2$ with iodine formed the azo compound [4-Me-Ph-N=N-4-Me-Ph] and nitrogen. The cationic complex $[Et_4N][Ag_2\{(4\text{-}R\text{-}Ph)_2N_5\}_3]$ is obtained by the reaction with $[Et_4N]Br$ in THF. The coordination of pentaazadienide in the dinuclear silver(I) complex $[Ag(4\text{-}EtO\text{-}Ph)_2N_5]_2$ is (N1)-η1 and (N3)-η1 bridging. This results in a short Ag···Ag contact of 2.8344(8) Å (Fig. 38) [137].

A unique copper complex of pentaazadienide $[Cu(4\text{-}R\text{-}Ph)_2N_5]_3$, R = 4-Me, 4-OEt, is prepared from excess copper(II) ammine $[Cu(NH_3)_4]^{2+}$ and 1,5-di(*p*-tolyl)pentaaza-1,4-dienide in an aqueous ammonia solution [143]. Initially a dark brown $Cu(II)L_2$ (L = 1,5-bis(4-R-phenyl)pentaazadienide) is obtained. Upon heating in pyridine the mononuclear copper(II)L_2 complex is reduced to trinuclear complex $[Cu(I)L]_3$ (Fig. 39). In $[Cu(I)L]_3$ a linear $[Cu–Cu–Cu]^{3+}$ chain is coordinated by the three nitrogen atoms of three pentaazadienide ligands, such that each Cu atom maintains a trigonal planar coordination. The three copper atoms are in a linear chain, Cu–Cu–Cu bond angle is 180°. In R = 4-Me, 4-OEt, the Cu–N bond distances to the outer nitrogen atoms are somewhat longer than the distances to the inner nitrogen atom. The Cu···Cu distances of ∼2.35 Å in the linear

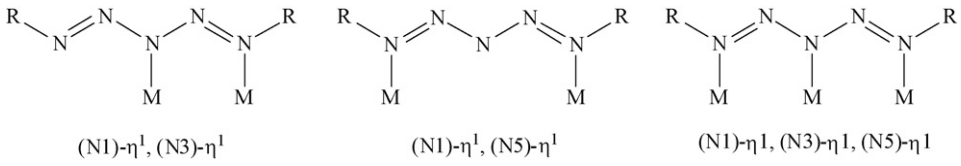

(N1)-η^1, (N3)-η^1 (N1)-η^1, (N5)-η^1 (N1)-η1, (N3)-η1, (N5)-η1

Fig. 36. Coordination modes of the pentaazadienide ligand.

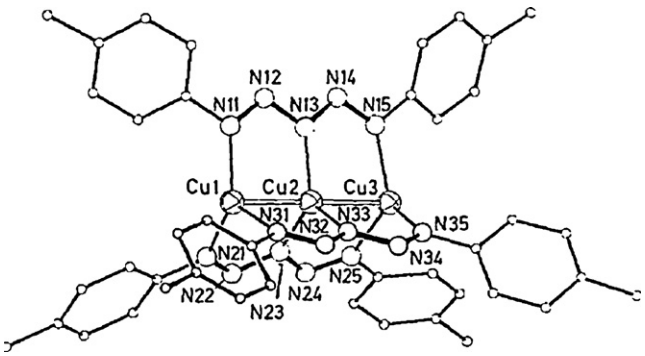

Fig. 39. Structure of $[Cu(4\text{-}Me\text{-}Ph)_2N_5]_3$ with (N1)-η1, (N3)-η1 and (N5)-η1 bridging; from Ref. [143].

Table 7
The M···M and M–N distances (Å) for the complexes $\{M[HC\{(H)C(Dipp)N\}_2]\}_2$ [146–148].

Complex	M···M	M–N
$\{Cu[HC\{(H)C(Dipp)N\}_2]\}_2$	4.99	1.870(8)
$\{Ag[HC\{(H)C(Dipp)N\}_2]\}_2$	5.0	2.111(8)
$\{Au[HC\{(H)C(Dipp)N\}_2]\}_2$	4.96	2.026(3)

Cu–Cu–Cu chain are extraordinary short in copper(I) chemistry [144].

8. β-Diketiminate

In numerous complexes, β-diketiminate ligands adopt the closed conformation (type A) to form a six membered chelate ring [145]. The structures in the rare open conformation (type B) (Fig. 40) category are dinuclear and tetranuclear. The reaction of Group 11 salts with 2,6-diisopropylphenyl β-diketiminate ligand $[HC\{(H)C(Dipp)N\}_2]$ without substituents on the carbon framework forms dinuclear 12-membered macrocyclic complexes $\{M[HC\{(H)C(Dipp)N\}_2]\}_2$, M = Cu, Ag and Au [146–148]. The metal(I) atoms exhibit nearly linear N–M–N bond angles. The ring is perfectly flat and the aromatic rings are almost perpendicular to the macrocyclic plane (Table 7). Generally, the basic structures of $\{M[HC\{(H)C(Dipp)N\}_2]\}_2$ are very similar. The M–N bond distances vary according to the covalent radii of Ag > Au > Cu. The transannular ligand separation follows the same trend, and the silver complex has the longest distance between the two β-diketiminate ligands [148].

The β-diketiminate ligands with strong electron-withdrawing groups such as cyanide and nitro form a macrocyclic tetranuclear silver(I) complex with the open conformation (type B) and the linear polymer silver(I) complex with a trigonal planar geometry supported by the ligand with the closed conformation (type A). The reaction of cyano 2,6-diisopropylphenyl β-diketiminate with $AgPF_6$ formed a macrocyclic tetranuclear 24-membered ring silver(I) complex, $\{Ag[CNC\{(H)C(Dipp)N\}_2]\}_4$. The molecule displays a saddle-shape structure in which one molecule of CH_2Cl_2 solvent is entrapped in the cavity. The distance between the carbon atom of CH_2Cl_2 and the nitrogen atom of the cyano group is 4.97 Å [147]. Similarly, the tetranuclear copper(I) complex $\{Cu[MeC\{(H)C(Dipp)N\}_2]\}_4$ is obtained from the reaction of the lithium salt of the methyl β-diketiminate $[MeC\{(H)C(Dipp)N\}_2]$ and $[Cu(MeCN)_4]PF_6$ in THF (Fig. 41). The structure of the copper complex was confirmed by high-resolution FAB-MS, elemental analysis, and ^1H NMR measurements. The quality of the crystallographic data is not satisfactory due to the solvent molecule disorder [146].

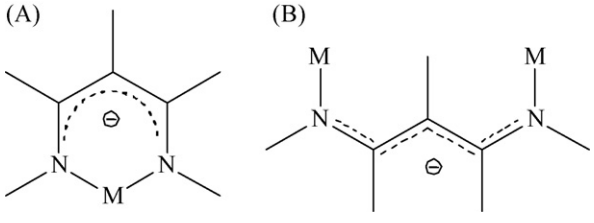

Fig. 40. Structures of the β-diketiminate ligand in A and B coordination types.

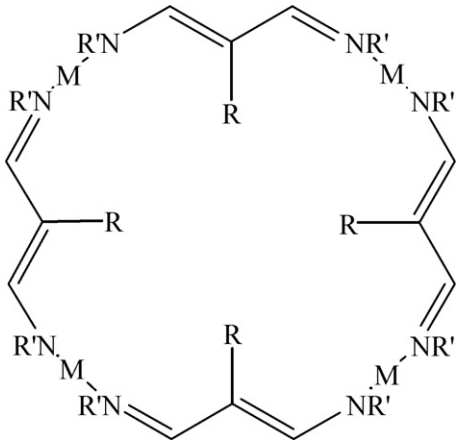

Fig. 41. Structure of $\{M[(R)C\{(H)C(Dipp)N\}_2]\}_4$, R = CN (M = Ag), R = Me (M = Cu), R′ = 2,6-diisopropylphenyl.

The structure–function relationship of various copper–nitrogen complexes including diketiminate ligands is critical in understanding the nature of reactive intermediates that form upon reaction of O_2 with copper(I) centers in proteins. The binding and activation of dioxygen by copper ions is central to the function of numerous biological and synthetically useful catalytic systems [149]. Volatile copper(I) β-diketiminate complexes are suitable precursors for the deposition of copper films in a pulsed CVD process that meets the industry requirements for vapor phase precursors by lacking halogen and oxygen atoms, while maintaining reasonable volatility at a suitably low temperature [150].

9. Pyrazolate complexes

The chemistry of pyrazolate metal complexes is quite extensive [19–24]. Monovalent Group 11 metal pyrazolate complexes exist in various forms: infinite chain, planar trinuclear, saddle-shaped tetranuclear, and figure-8-shaped hexanuclear units. While the trinuclear and infinite chain are by far the most common complexes, the hexanuclear and tetranuclear complexes are relatively rare.

9.1. Infinite chain complexes

Silver(I) pyrazolate infinite chain complex $[Ag(Pz)]_n$ is prepared in 50% yield by the reaction of $AgNO_3$ and pyrazole in 20% NH_4OH [151a]. Another report on the synthesis of $[Ag(Pz)]_n$ in >98% yield involves adding 25% NH_3 (water solution) to a solution of $AgNO_3$ in H_2O until the initially formed Ag_2O is completely dissolved. A water solution of pyrazole is then added dropwise to form a white precipitate [151b]. X-ray crystal structure of $[Ag(Pz)]_n$ displays infinite helical chains in which each pyrazolate ligand bridges two silver(I) atoms (Fig. 42). Furthermore, such chains are linked by interchain Ag···Ag interactions to form a 2D layer (Table 8) [151a,152].

The structures of two copper pyrazolate phases α-$[Cu(Pz)]_n$ and β-$[Cu(Pz)]_n$ were determined by *ab-initio* X-ray powder diffrac-

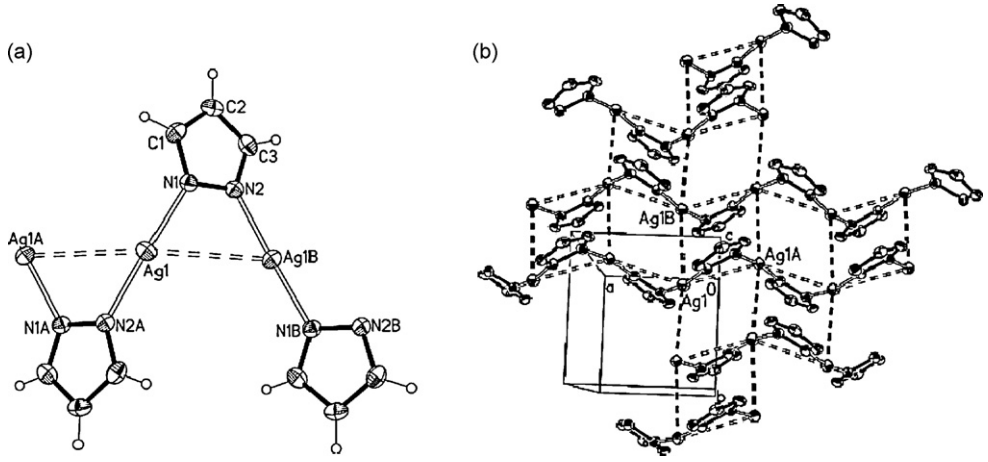

Fig. 42. (a) Structure of $[Ag(Pz)]_n$. (b) Two-dimensional network in $[Ag(Pz)]_n$ linked by Ag···Ag interactions; from Ref. [151a].

Table 8
Crystallographic data for the infinite chain silver(I) and copper(I) pyrazolates.

Complex	M···M$_{intrachain}$	M···M$_{interchain}$	M–M–M$_{intrachain}$	Ref.
$[Ag(Pz)]_n$[a]	3.4034(4)	3.2731(2)	143.7(1)	[152]
$[Ag(Pz)]_n$[b]	3.3718(7)	3.2547(6)	143.72(3)	[151]
α-$[Cu(Pz)]_n$[a]	3.1653(6)	3.3373(2)	148.0(1)	[152]
β-$[Cu(Pz)]_n$[a]	3.1453(2)	2.972(6)	142.3(2)	[152]

[a] Determined by X-ray powder diffraction.
[b] Determined by X-ray crystallography.

tion structural characterization. Polymer α-$[Cu(Pz)]_n$ consists of infinite chains with the pyrazolate anions bridging symmetry-related metal atoms. Each copper atom is linearly coordinated by two bridging pyrazolate ligands. The copper atoms within each chain are not linear, but rather show a folded ribbon arrangement. The polymeric chains stack with Cu···Cu intermolecular contacts between metal atoms of different chains [152]. The β-$[Cu(Pz)]_n$ phase also contains folded polymeric ribbons, similar to those found in the α-phase. The packing of the β-phase contains dimers of polymeric chains with Cu···Cu contact much shorter than within each chain. The α-$[Cu(Pz)]_n$ and β-$[Cu(Pz)]_n$ phases differ mainly in the interchain copper–copper contacts and in the crystal packing of the polymeric chains [152].

9.2. Saddle-like tetranuclear complexes

Large substituents in the 3-, 4- and 5-positions of the pyrazolate ring lead to tetranuclear structures. Table 9 lists the M···M distances of the tetranuclear pyrazolate complexes. The trend of the M···M distances follows the order of the M(I) covalent radii, Ag > Au > Cu [153]. The four copper atoms display a square geometry in $[Cu\{3\text{-}(Bu^t)\text{-}5\text{-}(Pr^i)Pz\}]_4$ [154], a diamond geometry in $[Cu\{3,5\text{-}(Bu^t)_2Pz\}]_4$ [155] and a slightly bent square in $[Cu\{3,5\text{-}(csb)_2Pz\}]_4$, csb = 3,5-(carbo-*sec*-butoxy) [155]. There are two kinds of crystallographically independent but structurally similar tetranuclears units in the crystal structure of $[Ag\{3,5\text{-}(Bu^t)_2Pz\}]_4 \bullet CH_2Cl_2$, defining a parallelogram and ideal rhombic geometry [156]. Two quite similar structures were determined for the tetranuclear gold pyrazolate complex as $[Au\{3,5\text{-}(Bu^t)_2Pz\}]_4$ and $[Au\{3,5\text{-}(Bu^t)_2Pz\}]_4 \cdot CH_2Cl_2$ [157].

Recrystallization of the trinuclear complex [Cu{(py)(2-(3(5)-Pz),6-(Me)py)$_3$}]$_3$·0.5py from toluene affords yellow plates of the dimer of tetranuclear complex [Cu{(2-(3(5)-Pz),6-(Me)py)$_4$}]$_4$·3tol. The structure is a molecular pair composed of two tetranuclear copper units with Cu···Cu interaction of 3.0045(13) Å (Fig. 43). The tetranuclear core structure folds into a trapezoidal or saddle-type conformation [158]. The coordination sphere of the copper centers is highly variable, with two copper atoms being three-coordinate and the other two being four- and two-coordinate. Bubbling carbon monoxide through a toluene solution of the trinuclear complex leads to the formation of $[Cu(CO)(2\text{-}(3(5)\text{-}pz),6\text{-}Mepy)]_3$, featuring coordination of one CO molecule per copper on the same face of a nine-membered Cu_3N_6 ring framework. This compound can also be obtained from solutions of the tetranuclear complex in toluene upon admittance of CO. This result indicates that the tetranuclear complex rearranges in the presence of CO to afford a presumably more stable trinuclear species [158].

Table 9
The M···M distances (Å) for the tetranuclear pyrazolate complexes.

Complex	M···M	Ref.
$[Cu\{3\text{-}(Bu^t)\text{-}5\text{-}(Pr^i)Pz\}]_4$	3.07	[154]
$[Cu\{3,5\text{-}(csb)_2Pz\}]_4$[a]	3.400(2)–3.535(2)	[155]
$[Cu\{3,5\text{-}(Bu^t)_2Pz\}]_4$	3.088(2)–3.119(2)	[155]
$[Ag\{3,5\text{-}(Bu^t)_2Pz\}]_4$	3.136(1)–3.216(1)	[156]
$[Au\{3,5\text{-}(Bu^t)_2Pz\}]_4$	3.118(1)–3.189(1)	[157]
[Cu{2-(3(5)-Pz,6-(Me)py)}]$_4$	3.58(12)	[158]
$[Cu\{3,5\text{-}(Ph)_2Pz\}]_4$	3.09–3.13	[159]

[a] csb = carbo-*sec*-butoxy.

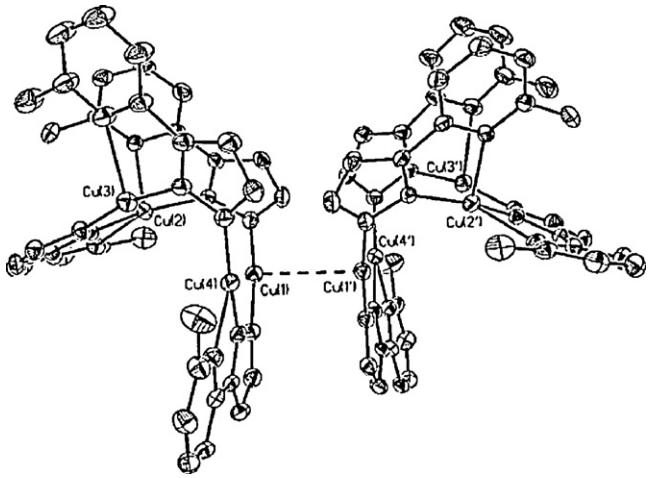

Fig. 43. Structure of the molecular pair of [Cu{(2-(3(5)-Pz),6-(Me)py$_4$}]$_4$; from Ref. [158].

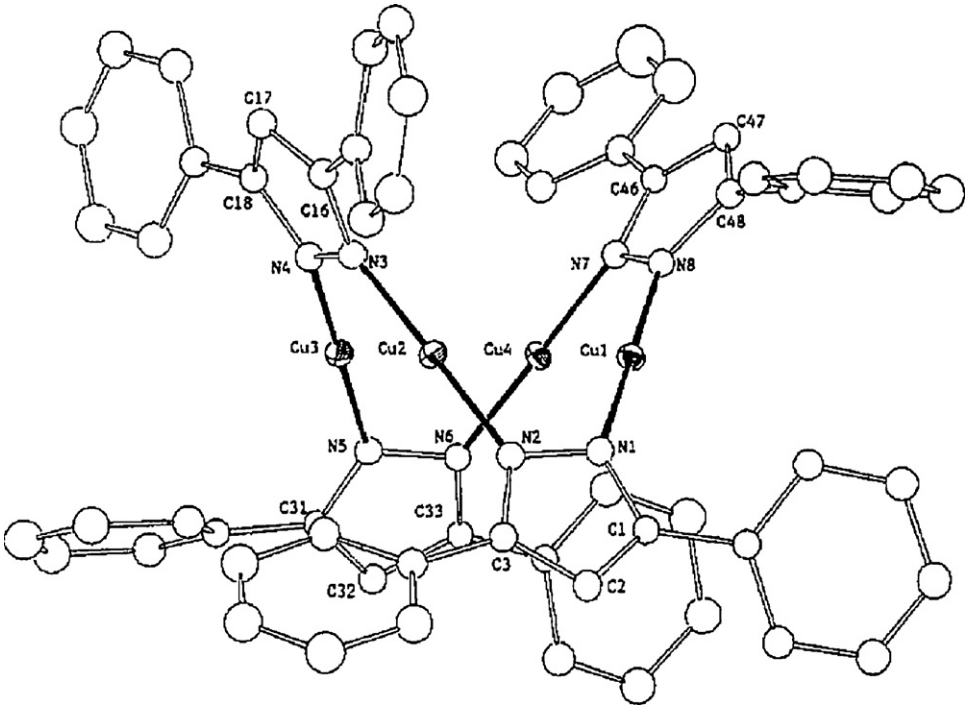

Fig. 44. Structure of $[Cu\{3,5\text{-}(Ph)_2Pz\}]_4$; from Ref. [159].

The paradoxical coordination behavior of the diphenylpyrazolate ligand $[3,5\text{-}(Ph)_2Pz]^-$ deserves some comments. The work from two different laboratories demonstrated that this ligand forms two different complexes with copper(I), based on the synthetic method utilized. Trinuclear and tetranuclear pyrazolate complexes have been isolated so far with copper. The tetranuclear complex $[Cu\{3,5\text{-}(Ph)_2Pz\}]_4$ (Fig. 44) is synthesized in 98% yield by the reaction of an acetone solution of 3,5-diphenylpyrazole with $[Cu(CH_3CN)_4]^+$ in acetone under nitrogen in the presence of Et_3N. The identity of the powder and single-crystal phases was confirmed by X-ray powder diffraction [159]. The trinuclear copper pyrazolate complex $[Cu\{3,5\text{-}(Ph)_2Pz\}]_3$ is synthesized from the reaction of CuCl with $Na[3,5\text{-}(Ph)_2Pz]$ by initiating the reaction with the addition of $AgNO_3$ to precipitate the $C1^-$ ion. A colorless product formed consisting of $[\{3,5\text{-}(Ph)_2Pz\}Ag]_3$ (>80%), lesser amounts of $[Ag_xCu_y\{(3,5\text{-}(Ph)_2Pz)_3\}]$ ($x+y=3$ by mass spectroscopy and elemental analysis), and $[Cu\{3,5\text{-}(Ph)_2Pz\}]_3$ as a minor product [160].

9.3. Propeller hexanuclear complexes

Another story is revealed, covering the coordination chemistry of diphenylpyrazolate ligand. The ligand forms trinuclear and tetranuclear complexes with copper, trinuclear complexes with silver, and trinuclear and hexanuclear complexes with gold. The hexanuclear gold pyrazolate complex $[Au\{3,5\text{-}(Ph)_2Pz\}]_6$ with an 18-atom ring is synthesized when $Na[3,5\text{-}(Ph)_2Pz]$ (1.0 mmol) and AgO_2CPh are added to a THF solution of Ph_3PAuCl (0.66 mmol), although in a small yield. The pyrazolate rings form a two-blade propeller-like body (D_2 symmetry) (Fig. 45). The geometry of the six gold centers is best described as an edge-sharing bitetrahedron. The Au···Au distances range from 3.085(2) to 6.010(1) Å [160,161].

9.4. Planar trinuclear complexes

9.4.1. Fluorinated trinuclear pyrazolates

In the absence of adverse steric interactions, the intramolecular M···M contacts are shorter in the non-fluorinated pyrazolate substituents. The fluorinated substituents form chains of trinuclear metal units. Electron-withdrawing groups weaken the intermolecular metal–metal contacts and favor long-range interactions in infinite chains of trinuclear units instead of dimers of trimers [162].

The efforts by Dias on the synthesis and structure of fluorinated metal pyrazolate complexes provided scrupulous information on the overlooked long-range interactions in the unit cell. The X-ray structure of $[Cu\{3\text{-}(CF_3)Pz\}]_3$ exhibits unsymmetrical arrangement of pyrazolate ligands with two CF_3 groups in the "head-to-head" arrangement. There is long intermolecular Cu···Cu contacts forming extended chains [162]. The fluorinated copper pyrazolate complex $[Cu\{3,5\text{-}(CF_3)_2Pz\}]_3$ forms chains of trinuclear copper units between copper atoms of neighboring trinuclear complexes. The structure shows that the Cu_3N_6 ring skeleton is planar [162,163]. The silver complex $[Ag\{3,5\text{-}(CF_3)_2Pz\}]_3$ features discrete trinuclear silver units as well as pairs of trinuclear silver units coupled via two Ag···Ag interactions. The trinuclear complexes and pairs of trinuclear units alternate in the crystal lattice [164]. The complex $[Au\{3,5\text{-}(CF_3)_2Pz\}]_3$ exists as discrete trinuclear complexes (Fig. 46). Among the three coinage metal complexes,

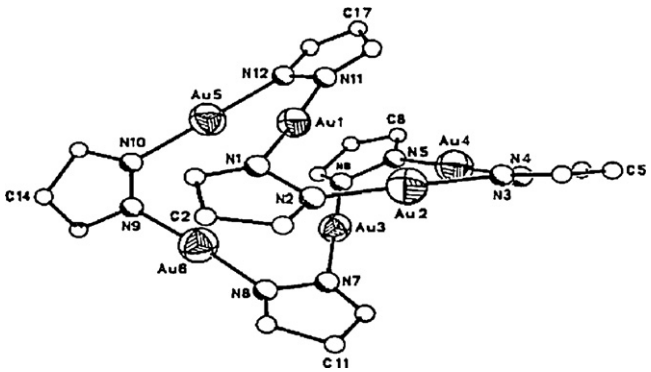

Fig. 45. Structure of the six gold pyrazolates in $[Au\{3,5\text{-}(Ph)_2Pz\}]_6$, from Ref. [160]. Phenyl rings omitted for clarity.

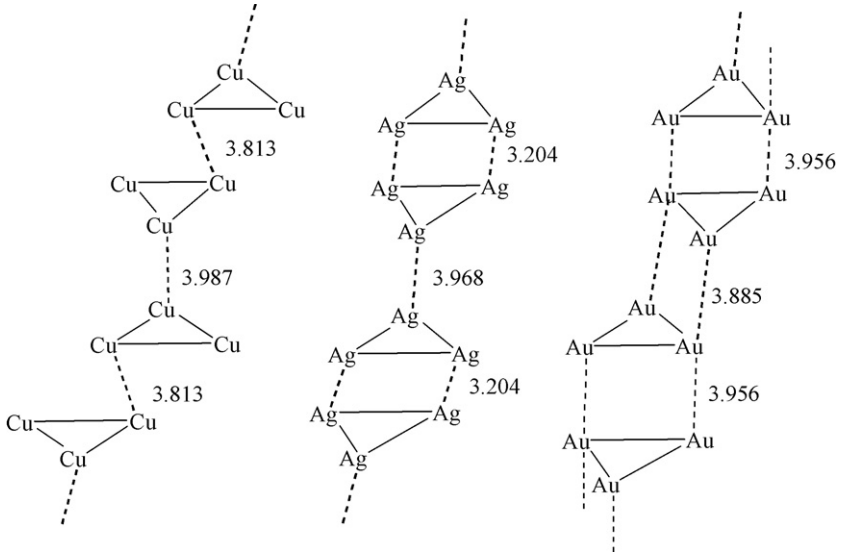

Fig. 46. Structure of $[M\{3,5\text{-}(CF_3)_2Pz\}]_3$ (M = Cu, Ag, Au) showing the packing of the M_3 metallacycles; reproduced from Ref. [162].

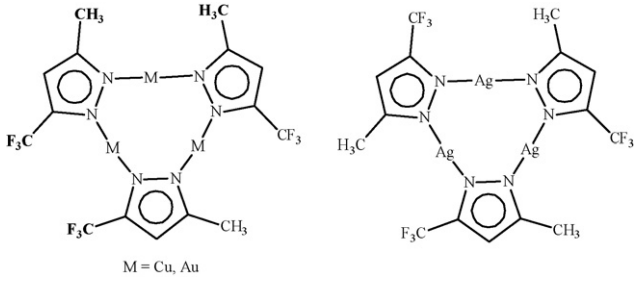

Fig. 47. Structure of $[M\{3\text{-}(CF_3),5\text{-}(Me)Pz\}]_3$.

metal–nitrogen distances are longest in the silver and shortest in the copper system. These M–N bond length values agree with the trend expected based on covalent radii of the coinage metals [165,166].

Structure of the planar copper complex $[Cu\{3\text{-}(CF_3),5\text{-}(Me)Pz\}]_3$ exhibits unsymmetrical CF_3 groups, and two groups exist in "head-to-head" arrangement [162]. The trinuclear copper units form extended chains (Fig. 47). X-ray structure of the silver complex $[Ag\{3\text{-}(CF_3),5\text{-}(Me)Pz\}]_3$ shows that the neighboring pairs of the trinuclear units are linked by two equal and relatively short Ag···Ag contacts across a crystallographic inversion center [164]. The dimer of trinuclear units interacts further via additional Ag···Ag links, forming extended stepladder-shaped columns. The gold complex $[Au\{3\text{-}(CF_3),5\text{-}(Me)Pz\}]_3$ exists as discrete planar gold triangles (Table 10). The structure consists of sheets of $[Au\{3\text{-}(CF_3),5\text{-}(Me)Pz\}]_3$ units stacked in an "offset" fashion along the *c* axis such that one gold atom in each trinuclear unit lies approximately over the midpoint of one of the edges of the triangle in the layer below it. The intermolecular Au···Au distances are long to suggest any bonding interaction. The supramolecular organization may be due to hydrogen–fluorine and fluorine–fluorine interactions between the molecules. The complex exhibits unsymmetrical arrangement of the pyrazolate ligands with two of them in the "head-to-head" arrangement [167].

Table 10
The M···M distances (Å) observed for the trinuclear fluorinated pyrazolates.

Complex	$M\cdots M_{intramolecular}$	$M\cdots M_{intermolecular}$	Ref.
$[Cu\{3\text{-}(CF_3)Pz\}]_3$	3.214–3.264	3.100–3.482	[162]
$[Cu\{3,5\text{-}(CF_3)_2Pz\}]_3$	3.218–3.247	3.813–3.987	[162]
$[Ag\{3,5\text{-}(CF_3)_2Pz\}]_3$	3.441–3.541	3.3073(13)	[164]
$[Au\{3,5\text{-}(CF_3)_2Pz\}]_3$	3.44–3.55	3.998(2)	[162]
$[Cu\{3\text{-}(CF_3),5\text{-}(Me)Pz\}]_3$	3.201–3.245	3.704–3.915	[162]
$[Ag\{3\text{-}(CF_3),5\text{-}(Me)Pz\}]_3$	3.392–3.493	3.3553(4)	[165]
$[Au\{3\text{-}(CF_3),5\text{-}(Me)Pz\}]_3$	3.3455(8)	3.880(1)–4.023(1)	[167]
$[Cu\{3\text{-}(CF_3),5\text{-}(Ph)Pz\}]_3$	3.147–3.258	3.848–4.636	[162]
$[Ag\{3\text{-}(CF_3),5\text{-}(Bu^t)\text{-}Pz\}]_3$	3.413–3.489	3.4804(7)	[165]
$[Ag\{3\text{-}(C_3F_7),5\text{-}(Bu^t)Pz\}]_3$	3.394–3.448	5.376	[165]

The arrangement of the pyrazolate ligands in $[Cu\{3\text{-}(CF_3),5\text{-}(Ph)Pz\}]_3$ is unsymmetrical with two CF_3 groups in "head-to-head" arrangement [162]. The nine-membered Cu_3N_6 metallacycle shows significant deviation from planarity, perhaps because of the adverse steric effects of having the -CF_3 and -Ph substituents on the neighboring pyrazolate ligands. The intertriangle contacts between the copper atoms are rather long (alternating with one another in the infinite zigzag chains of trinuclear units). The extended packing of the trinuclear copper units of $[Cu\{3\text{-}(CF_3),5\text{-}(Ph)Pz\}]_3$ is similar to that observed in $[Cu\{3,5\text{-}(CF_3)_2Pz\}]_3$. However, $[Cu\{3,5\text{-}(CF_3)_2Pz\}]_3$ features a planar nine-membered metallacycle and somewhat shorter intertrinuclear Cu···Cu separations based on the data collected at 100 K [162].

Complex $[Ag\{3\text{-}(CF_3),5\text{-}(Bu^t)Pz\}]_3$ features a slightly concave shape. These trinuclear units crystallize as dimers of trinuclear units [164]. The six silver atoms of the two trinuclear units adopt a chair conformation. The concave shape appears to be primarily a result of the intertrinuclear steric interactions between the pyrazolate ligand substituents [164]. The nine-membered Ag_3N_6 metallacycle in $[Ag\{3\text{-}(C_3F_7),5\text{-}(Bu^t)Pz\}]_3$ shows a significant deviation from planarity. The C_3F_7 groups point above and below the Ag_3N_6 plane to avoid the *t*-butyl substituents on the adjacent pyrazolate ligands. There are also close intertrinuclear Ag···F (3.096 Å) contacts, probably a result of crystal packing [164]. Vapor-Pressure Osmometry (VPO) measurements of silver pyrazolate complexes such as $[Ag\{3,5\text{-}(CF_3)_2Pz\}]_3$, $[Ag\{3\text{-}(C_3F_7),5\text{-}(Bu^t)Pz\}]_3$ and $[Ag\{3,5\text{-}(Pr^i)_2Pz\}]_3$ show that at higher concentrations, these silver pyrazolates adopt solution structures similar to those in the solid state [165].

9.4.2. Non-fluorinated trinuclear pyrazolates

Complex $[Cu\{3,5\text{-}(Ph)_2Pz\}]_3$ shows significant deviation from planarity, resembling the silver trinuclear complex and contrasting the rigorously planar gold trinuclear complex(vide infra). One pyrazolate ring is below the three copper atoms plane, the second

Table 11
The M···M distances (Å) for the trinuclear non-fluorinated pyrazolates.

Complex	$M\cdots M_{intramolecular}$	$M\cdots M_{intermolecular}$	Ref.
$[Cu\{3,5\text{-}(Ph)_2Pz\}]_3$	3.280(1)–3.406(1)		[168]
$[Ag\{3,5\text{-}(Ph)_2Pz\}]_3$ (from THF)	3.280–3.406		[160]
$[Ag\{3,5\text{-}(Ph)_2Pz\}]_3$ (from CH_2Cl_2)	3.35	2.9712(14)	[169]
$[Au\{3,5\text{-}(Ph)_2Pz\}]_3$	3.368(1)		[160]
$[Ag(Pz)]_3$	3.414(5)–3.431(4)	3.43	[152]
$[Au\{3,5\text{-}(4'\text{-}MeOPh)_2Pz\}]_3$	3.2560(16)–3.3970(15)		[172]
$[Au\{3,5\text{-}(4'\text{-}PhOPh)_2Pz\}]_3$	3.224(1)–3.358(1)		[173]
$[Au\{3,5\text{-}(Me)_2\text{-}4\text{-}(octyl)\text{-}Pz\}]_3$	3.335(1)–3.3566(1)	3.255(2)	[174]
$[Cu\{3,5\text{-}(Me)_2Pz\}]_3$	3.195–3.257	2.946	[175]
$[Ag\{3,5\text{-}(Me)_2Pz\}]_3$	3.318(9)–3.388(11)	3.230(13), 3.328(13)	[176]
$[Cu\{3,4,5\text{-}(Me)_3Pz\}]_3$	3.212	3.069	[177]
$[Au\{3,4,5\text{-}(Me)_3Pz\}]_3$	3.350(1)–3.376(1)		[178]
$[Cu\{3,5\text{-}(Pr^i)_2Pz\}]_3$	3.195–3.235	2.989	[154]
$[Ag\{3,5\text{-}(Pr^i)_2Pz\}]_3$	3.324–3.489	2.9870(4)	[179]

one is above, and the third one is rotated and bisected by this plane to accommodate the twist of the Cu_3N_6 ring. The Cu–N bond lengths are unusually long with an average of 2.081(7) Å [168].

Solvents used in crystallization affect the intertrinuclear contacts. Complex $[Ag\{3,5\text{-}(Ph)_2Pz\}]_3$ synthesized in CH_2Cl_2 solvent exists as dimer of trimers and displays one short Ag···Ag contact (Fig. 48 and Table 11) [169]. $[Ag\{3,5\text{-}(Ph)_2Pz\}]_3$ crystallizes from THF/Et_2O as isolated trinuclear units. The dimer of trinuclear of $[Ag\{3,5\text{-}(Ph)_2Pz\}]_3$ crystallizes as needles in the monoclinic space group C2/c. However, the trinuclear complex $[Ag\{3,5\text{-}(Ph)_2Pz\}]_3{\cdot}2THF$ crystallizes as blocks from THF/ether in the monoclinic space group $P2_1/n$ [160]. The intramolecular Ag···Ag interactions in $[Ag\{3,5\text{-}(Ph)_2Pz\}]_3{\cdot}2THF$ are shorter than those in the dimer of trinuclear complex $[Ag\{3,5\text{-}(Ph)_2Pz\}]_3$.

Single point energy (SPE) calculations on the crystal structure geometries of the trinuclear silver models and the dimer of trimers model found a binding energy of 13.6 kcal/mol $[Ag\{3,5\text{-}(Ph)_2Pz\}]_3$, which is larger than expected. The SPE calculations showed a stabilization of the trinuclear unit in the dimer of trimer structure by 6.8 kcal/mol. This indicates that there is a significant amount of intermolecular phenyl ring interaction or other packing forces in the trinuclear unit crystal, which compensates for the destabilizing effect of the metallacycle distortion [169]. The models for the silver trinuclear complexes and the dimer of trimers were then geometry optimized and the binding energy of dimer of trinuclear complex $[Ag\{3,5\text{-}(Ph)_2Pz\}]_3$ was calculated to be 3.49 kcal/mol, significantly lower than the binding energy calculated from the crystal structures. DFT calculations indicate that the silver–silver interaction in the dimer of trinuclear complex $[Ag\{3,5\text{-}(Ph)_2Pz\}]_3$ is due to dispersion forces and that the distortion of the metallacycle in $[Ag\{3,5\text{-}(Ph)_2Pz\}]_3$ is due to intermolecular phenyl ring interaction or other packing forces [169].

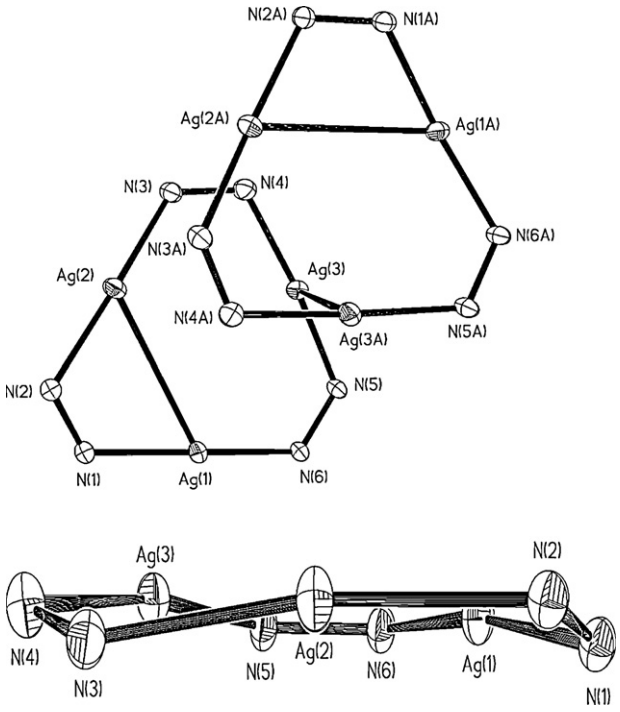

Fig. 48. Structure of the Ag_3N_6 metallacycle in $[Ag\{3,5\text{-}(Ph)_2Pz\}]_3$; from Ref. [169].

The gold centers in $[Au\{3,5\text{-}(Ph)_2Pz\}]_3$ are 3.368(1) Å apart, and form an equilateral triangle. The planes of the phenyl rings are 45° to the plane of the Au_3N_6 ring. In the unit cell, the discrete pyrazolate gold trinuclear molecules are coplanar and parallel to each other in the unit cell along the *c* axis [160].

The coordination chemistry of the pyrazolate ligand without substituents is reminiscent of diphenylpyrazolate, but less controversial. The ligand forms α- and β-polymers with copper [152], polymer [151,152] and trinuclear [152] with silver and supramolecular with gold [170]. The planar trinuclear silver pyrazolate complex $[Ag(Pz)]_3$ is prepared by adding 35% hydrogen peroxide dropwise to a stirred CH_2Cl_2 solution of $[(PPh_3)Ag(Pz)]_2$. A polymer $[Ag(Pz)]_\infty$ is obtained using a different preparation (*vide supra*) [151]. X-ray powder diffraction studies of $[Ag(Pz)]_3$ show comparable intramolecular and intermolecular metal–metal contacts [152].

Raptis provided two examples of supramolecular architecture, reasoning that pyrazolates with no substituents or with one methyl group makes the supramolecular architecture formation facile. The two structures provide a definitive picture of fine-tuning the metallophilic interactions. In $[Au(Pz)]_3$ complex, there are intramolecular gold–gold interactions of 3.372(1)–3.401(1) Å. The gold complex forms a 2D network through intermolecular aurophilic interactions. Each trinuclear forms a dimer with two gold–gold interactions of 3.313(1) Å. Moreover, each dimer interacts with four other dimers through a single Au···Au contact of 3.160(1) Å to form a two-dimensional net [170]. In $[Au\{4\text{-}(Me)Pz\}]_3$ complex, the intramolecular Au···Au distances range from 3.314(2) to 3.426(2) Å. With an intermolecular Au···Au distance of 3.6 Å five gold trinuclear units exist as independent units, and two more as a dimer of trinuclear units, while the remaining eight trinuclear units, along with their symmetry-related counterparts, constitute a 16-membered aggregate of trinuclear units. In the dimer of trinuclear units, the two, almost eclipsed, trinuclear units form a slightly twisted, trigonal prismatic hexanuclear array. The intermolecular Au···Au distances, prism edges, are 3.318(2), 3.600(2) and 3.707(2) Å [170].

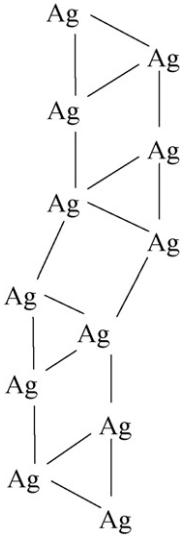

Fig. 49. Folded ribbon of silver–silver contacts in $[Ag\{3,5\text{-}(Me)_2Pz\}]_3$.

Trinuclear gold pyrazolate complexes with long chain substituents produce room-temperature columnar mesophases [171]. X-ray powder diffraction measurements demonstrated that the supramolecular columnar arrangement is present in the crystalline solids and in the mesomorphic phase. The X-ray crystal structure of $[Au\{3,5\text{-}(4'\text{-}MeOPh)_2Pz\}]_3$ yields a unit cell which contains two independent trinuclear units. The mean stacking separation between two consecutive trinuclear units is 4.54 Å [172]. The molecular packing of the trinuclear complex $[Au\{3,5\text{-}(4'\text{-}PhOPh)_2Pz\}]_3$ corresponds to a columnar distribution. The distance between the centroids of the Au_3 planes of consecutive trinuclear units in the column is ca. 6.7 Å [173]. The X-ray crystal structure of $[Au\{3,5\text{-}(Me)_2\text{-}4\text{-}(octyl)Pz\}]_3$ at room temperature consists of planar trinuclear molecules. The three gold atoms form an almost perfect equilateral triangle. The dimers of trinuclear units form a tilted columnar stack along the *b* axis with an average distance of 4.64 Å [174].

The structure of $[Cu\{3,5\text{-}(Me)_2Pz\}]_3$ complex displays intermolecular M···M separation shorter than the intramolecular distance. The trinuclear units are arranged in pairs about crystallographic inversion centers with two copper atoms from one metallacycle being positioned close to two copper atoms from the second unit through two intertrinuclear Cu···Cu interactions. The third copper atom is positioned above the center of a dimethylpyrazolate ring at the opposite end of the inversion-related trinuclear unit [175]. Based on the X-ray powder diffraction studies the packing contacts and intermolecular interactions in $[Ag\{3,5\text{-}(Me)_2Pz\}]_3$ are similar to the copper analogue. The Ag···Ag interactions of 3.358 and 3.279 Å extend over the whole crystal giving a folded ribbon of silver–silver contacts (Fig. 49) [176].

The structure of $[Cu\{3,4,5\text{-}(Me)_3Pz\}]_3$ consists of trinuclear molecules linked by weak Cu···Cu interactions. The copper atom not involved in the weak interactions is at 3.281 Å from the mean plane of the trimethylpyrazolate ring at the opposite end of the inversion-related trinuclear unit [177]. The gold complex $[Au\{3,4,5\text{-}(Me)_3Pz\}]_3$ is synthesized by reductive transformation of $[Au^{III}_2Cl_4\{3,4,5\text{-}(Me)_3Pz\}_2]$ in the presence of Et_3N to trinuclear mixed-valence complexes $Au^IAu^{III}_2$, $Au^I_2Au^{III}$ and finally the homovalent gold(I) complex $[Au\{3,4,5\text{-}(Me)_3Pz\}]_3$ as colorless prismatic crystals [178].

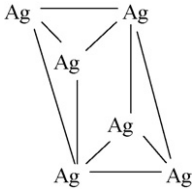

Fig. 50. Structure of the metallacycle in the dimer of $[Ag(PzIN)]_3$.

The nine-membered ring in $[Cu\{3,5\text{-}(Pr^i)_2Pz\}]_3$ is planar with short intermolecular distance [154]. The trinuclear units exist in pairs in $[Ag\{3,5\text{-}(Pr^i)_2Pz\}]_3$ resulting in Ag···Ag bonded dimers of trinuclear units. The hexanuclear silver units adopt a chair conformation with a short Ag···Ag intermolecular distance [179].

9.4.3. Trinuclear pyrazolates with side arms

The silver(I) atoms in the dimer of trinuclear unit $[Ag(PzIN)]_3$ (IN = iminonitroxide) are T-shaped three-coordinate but are linear two-coordinate with pyrazolate nitrogen atoms (Fig. 50). The Ag–N_{IN} bondings are weaker than the Ag–N_{Pz} bonds. This trinuclear unit involves the five-membered chelate structures. Considerably short Ag···Ag distances are found between neighboring triangles related with the inversion symmetry. Only two silver centers in each trinuclear unit are involved in the Ag···Ag interactions. There are two distorted Ag_4 tetrahedral skeletons with the interatomic distances of 3.69–3.85 Å. The two tetrahedrons are fused with the silver–silver edge. The molecule can be regarded also as Ag_6 complex surrounded by six PzIN radical anions [180].

The molecular structure of $[Ag\{3,5\text{-}(Pr^iSCH_2)_2\text{-}Pz\}]_3$ shows the presence of a trinuclear cyclic array of three linearly coordinated silver atoms (Table 12). The Ag_3N_6 ring skeleton is planar. The Ag–S distances of 3.094 and 3.111 Å are longer than the maximum bond length generally accepted for Ag–S bonds. There are two unsupported intermolecular Ag···Ag separations resulting in the arrangement of each two trinuclear units in pairs [181]. The molecular weight determination using Vapor-Pressure Osmometry (VPO) found the structure to be hexanuclear in toluene.

It is entirely conceivable that a slight distortion in the metallacycle could result from the pyridine side arm pyrazolate interaction with the metal centers. There is a slight distortion in the structures of Group 11 pyrazolate complexes with pyridine side arm. Solvothermal reactions of 4-(pyrid-4′-yl)-3,5-$(Me)_2$PzH with CuBr in $NH_3{\cdot}H_2O$/EtOH affords the trinuclear copper(I) complex $[Cu\{4\text{-}(pyrid\text{-}4'\text{-}yl)\text{-}3,5\text{-}(Me)_2Pz\}]_3$. The central Cu_3N_6 ring is nearly coplanar with a mean deviation of 0.0393 Å. The molecules are

Table 12
The M···M distances (Å) for the trinuclear side arm pyrazolates.

Complex	$M\cdots M_{intramolecular}$	$M\cdots M_{intermolecular}$	Ref.
$[Ag\{3,5\text{-}(Pr^iSCH_2)_2Pz\}]_3$	3.453–3.700	3.041(1)	[181]
$[Cu\{4\text{-}(pyrid\text{-}4'\text{-}yl)\text{-}3,5\text{-}(Me)_2Pz\}]_3$	3.172–3.230	3.439	[182]
$[Cu\{2\text{-}(3(5)\text{-}Pz)Py\}]_3{\cdot}2py$	3.52(5)	2.905(3)	[183]
$[Ag\{2\text{-}(3(5)\text{-}Pz)Py\}]_3{\cdot}2py$	3.227(3)		[183]
$[Ag\{2\text{-}(3(5)\text{-}Pz)Py\}]_3$	3.127(2)		[184]
$[Ag\{3,5\text{-}(Pr^i)_2,4\text{-}(Br)Pz\}]_3$	3.413–3.489	3.0438(5)	[179]
$[Ag\{3,5\text{-}(Pr^i)_2,4\text{-}(NO_2)Pz\}]_3$	3.296–3.529		[179]
$[Cu\{3,5\text{-}(Me)_2,4\text{-}(NO_2)Pz\}]_3$	3.185(11), 3.255(13)	3.329(7)	[185]

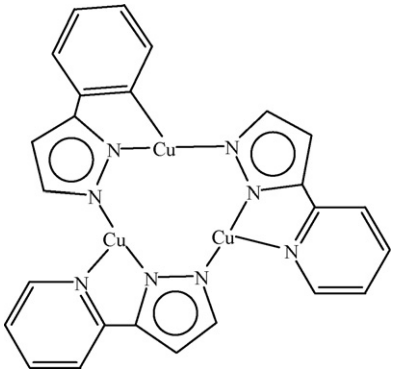

Fig. 51. Structure of $[Cu\{2\text{-}(3(5)\text{-}Pz)Py\}]_3$.

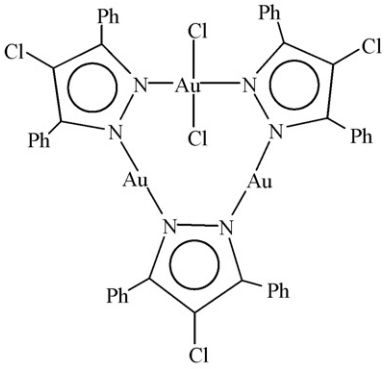

Fig. 53. Structure of $[Au^{III}Au^{I}{}_2Cl_2\{(3,5\text{-}(Ph)_2\text{-}4\text{-}Cl\text{-}Pz)_3\}]$.

stacked in pairs via a long intermolecular Cu···Cu interaction. The long Cu···Cu distance suggests repulsion among the pyridyls on the paired trinuclear units [182]. The structure of $[Cu\{2\text{-}(3(5)\text{-}Pz)Py\}]_3$ reveals two virtually planar triangular copper units coupled via two Cu···Cu interactions (Fig. 51). Within the trinuclear copper unit, the pyrazolate-bridged copper atoms are almost linearly coordinated to two pyrazolate rings. Compound $[Ag\{2\text{-}(3(5)\text{-}Pz)py\}]_3{\cdot}2py$ is isomorphous to $[Cu\{2\text{-}(3(5)\text{-}Pz)py\}]_3{\cdot}2py$, although its structure is slightly more distorted. The inversion-related triangular silver units are coupled along the longer Ag···Ag side by a pair of contacts, the orientation of which is more slanted with respect to the planes of the trinuclear units by comparison to $[Cu\{2\text{-}(3(5)\text{-}Pz)py\}]_3{\cdot}2py$ [183]. The non-solvated silver complex exhibits an almost planar conformation (mean deviation 0.1483 Å) and silver–silver interactions of 3.127(2) Å [184].

The structure of $[Cu\{(py)(2\text{-}(3(5)\text{-}Pz),6\text{-}(Me)py)_3\}]_3{\cdot}0.5py$ reveals a trinuclear copper complex composed of two three-coordinate sites and one four-coordinate copper site (Fig. 52). The Cu_3N_6 ring substantially deviates from planarity. This deviation is most likely due to the methyl substituent that forces the three ligands to assume a propeller type arrangement. Only one copper atom in $[Cu\{(py)(2\text{-}(3(5)\text{-}Pz),6\text{-}(Me)py)_3\}]_3{\cdot}0.5py$ is tetrahedrally coordinated. The N_{Pz}-Cu-N_{Pz} bond angles for the two three-coordinate copper sites are consistent with an in-plane distortion from a T-shaped geometry. For these copper sites, the average Cu–N_{Pz} bond distance is shorter than the one observed for the four-coordinate site [158].

The trinuclear complexes with electron-withdrawing groups $[Ag\{3,5\text{-}(Pr^i)_2,4\text{-}(X)Pz\}]_3$, X = Br, form dimers of trinuclear units leading to a pseudo octahedral Ag_6 unit. All three silver atoms of $[Ag\{3,5\text{-}(Pr^i)_2,4\text{-}(Br)Pz\}]_3$ complex show close intertrinuclear Ag···Ag interactions. The trinuclear units deviate from planarity and adopt bowl shaped structures facilitating these Ag···Ag contacts. The packing diagram of the silver complex shows the presence of several intertrinuclear Ag–Br distances of ~3.5 Å [179]. The $[Ag\{3,5\text{-}(Pr^i)_2,4\text{-}(X)Pz\}]_3$, X = NO_2, units exist as isolated trinuclear units. However, there are close intramolecular Ag–O contacts between the silver and the oxygen atoms of the nitro groups. This may be a reason for the absence of intertrinuclear Ag···Ag interactions [179]. The XRPD of $[Cu\{3,5\text{-}(Me)_2,4\text{-}(NO_2)Pz\}]_3$ exhibits a stepped-ribbon secondary structure of triangular complexes. These data indicate that electron-withdrawing groups weaken the intramolecular Cu···Cu contacts and favor long-range interactions in infinite chains of trinuclear units instead of dimers of trimers. $[Cu\{3,5\text{-}(Me)_2,4\text{-}(NO_2)Pz\}]_3$ packs as chains of trinuclear copper units with intertrinuclear Cu···Cu separations of 3.261 Å [185].

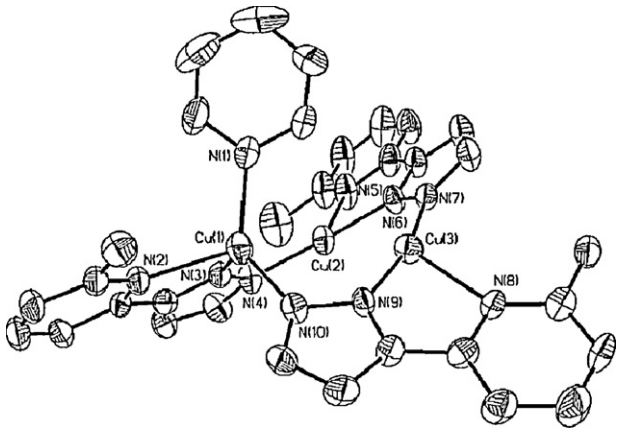

Fig. 52. Structure of $[Cu\{(py)(2\text{-}(3(5)\text{-}Pz),6\text{-}(Me)py)_3\}]_3{\cdot}0.5py$; from Ref. [158].

9.4.4. Oxidative-addition reactions to the trinuclear gold pyrazolates

Trinuclear gold pyrazolate complexes undergo oxidative-addition reactions of halogens at the metal centers. There is evidence that electronic factors, more than steric ones, may influence the reactivities of the gold atoms shown in these compounds. Oxidative-addition trials of $[Au\{3,5\text{-}(Ph)_2Pz\}]_3$ by chlorinating reagents resulted in a limited success (Fig. 53). The syntheses of red crystals of trinuclear gold(III) pyrazolate complexes is achieved by two procedures: oxidation of a trinuclear gold(I) pyrazolate complex using chlorine carrier such as aqua regia (50% yield) and the reaction of $AuCl_3(py)$ with Na[3,5-Ph_2Pz] (yield 89%). Surprisingly, both procedures have a common type of product, the mixed-valence $Au^{I}{}_2/Au^{III}$ pyrazolate complexes. This observation suggests an unusual stability for the $d^{10}d^{10}d^8$ configuration of the pyrazolate metallacycle [186]. The result of the reaction of $[Au\{3,5\text{-}(Ph)_2Pz\}]_3$ complex with aqua regia is most surprising. It can be argued that the oxidation of the first gold atom improves the π-acceptor ability of the two pyrazolate ligands coordinated to it, so that they remove sufficient electron density from the remaining two gold(I) atoms to prevent their oxidation. Halogens also fail to oxidize $[Au\{3,5\text{-}(Ph)_2Pz\}]_3$ complex beyond the $Au^{I}{}_2/Au^{III}$ state. The halogenation of the 4-position of the pyrazolate rings of the trinuclear gold pyrazolate complex caused the formation of $[Au^{I}{}_2Au^{III}Cl_2\{3,5\text{-}(Ph)_2\text{-}4\text{-}Cl\text{-}Pz\}_3]$. The small deviations of the nine-membered metallacycle from perfect planarity cause the intramolecular Au–Au distances to be unequal, 3.3352(7), 3.3677(6) and 3.4011(7) Å [186]. Similar results are obtained by aqua regia oxidation of $[Au\{4\text{-}(Me)Pz\}]_3$. The Au–Au distances are 3.368(1), 3.389(1), and 3.363(1) Å [178].

Addition of aqua regia to solid $[Au\{3,5\text{-}(Me)_2Pz\}]_3$ yields an orange-red solid product shown by X-ray structural characterization to be a mixture of the trinuclear complexes $[Au^{III}{}_3Cl_6$

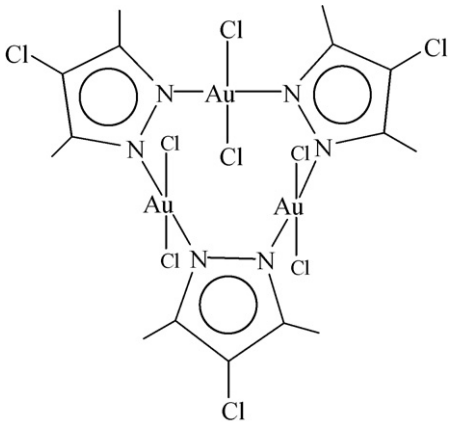

Fig. 54. Structure of $[Au^{III}{}_3Cl_6\{(4\text{-Cl-}3,5\text{-}(Me)_2Pz)_3\}]$.

$\{(4\text{-Cl-}3,5\text{-}(Me)_2Pz)_3\}]$, $[Au^{I}Au^{III}{}_2Cl_4\{(4\text{-Cl-}3,5\text{-}(Me)_2Pz)_3\}]$ and $[Au^{I}{}_2Au^{III}Cl_2\{(4\text{-Cl-}3,5\text{-}(Me)_2Pz)_3\}]$ (Fig. 54). Along with the oxidation of the gold centers, aqua regia chlorinated the 4-position of the pyrazolate rings, similar to chlorination of 4-position in diphenylpyrazolate rings. The composition of the mixture of the three complexes is difficult to control and varies with solution concentration and sample age. Dichloromethane solutions of the crude reaction product are initially red, but slowly become pale orange and eventually yellow, as $[Au^{III}{}_3Cl_6\{(4\text{-Cl-}3,5\text{-}(Me)_2Pz)_3\}]$ decomposes to $[Au^{I}Au^{III}{}_2Cl_4\{(4\text{-Cl-}3,5\text{-}(Me)_2Pz)_3\}]$ and eventually to stable $[Au^{I}{}_2Au^{III}Cl_2\{(4\text{-Cl-}3,5\text{-}(Me)_2Pz)_3\}]$ complex [187].

9.5. Pyrazolate complexes in light emitting diodes

The electronic and optoelectronic properties of coinage metal pyrazolate complexes are critical in developing optical devices of industrial applications [188]. Aida et al. demonstrated that medium-sized Group 11 dendritic metallacycles form luminescent superhelical fibers. The dendritic fiber of copper(I) is particularly interesting, since it involves a long-range interaction. The use of metal–metal interactions as driving forces for self-organization of dendritic macromolecules provides a novel strategy for the fabrication of mesoscopic functional materials [189]. The first phosphorescent organogels, using a trinuclear gold(I) pyrazolate complex carrying long C_{18} alkyl chains, were reported (Fig. 55).

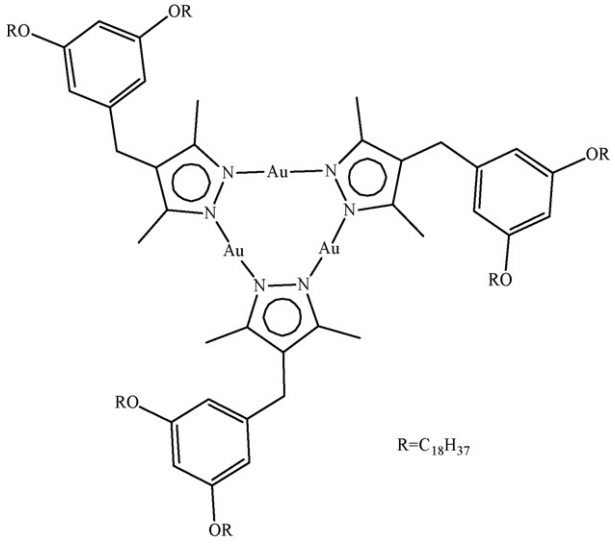

Fig. 55. Structure of the trinuclear gold pyrazolate complex with C_{18} alkyl chains.

The strong self-assembling nature of the paraffinic side chains promotes the metallophilic interaction even at room temperature in hexane. Doping organogel with a small amount of silver(I) results in a blue luminescence without disruption of the gel, while removal of doped silver(I) with chloride anion results in complete recovery of the original red-luminescent gel. Upon heating, these organogels undergo gel-to-sol transition due to the destabilization of the metallophilic interactions, where the red luminescence of the nondoped system becomes hardly visible, while the blue luminescence of the silver(I) doped system turns green. On cooling, these solutions undergo gelation and synchronously recover their original luminescence. The observed RGB (red–green–blue) emissions are all long-lived and assigned to electronic transitions from triplet-excited states. The sol–gel transition, coupled with silver(I) doping/dedoping, allows reversible switching of the RGB luminescence color [190].

Omary et al. described the photophysical properties of a series of fluorinated trinuclear copper(I) pyrazolate complexes and related non-fluorinated analogues [162]. This study illustrates the significant impact of packing via Cu···Cu intertrimer interactions on the photophysical properties of trinuclear copper pyrazolate complexes. Despite the inherent weakness of such closed-shell metal–metal interactions in the electronic ground state, their strong enhancement in the emissive excited states is responsible for the bright luminescence bands that can be tuned across the visible region. Because of their bright phosphorescence at room temperature, the multinuclear coinage metal pyrazolate complexes are efficient materials for MOLEDs [162].

10. Triazolate complexes

1,2,4-Triazoles combine the coordination geometry of both pyrazoles and imidazoles, and in addition act as bridging ligands between two metal centers. They show a great coordination diversity, especially when the triazole ring is substituted with additional donor groups. A variety of coordination modes have been identified in the transition metal chemistry of 1,2,4-triazolates $[Tz]^-$, attracting considerable attention in recent years [27,28].

The number of reports on metal compounds with triazoles in the literature is rapidly growing. Several triazolate coordination polymers with interesting structures have been synthesized under hydrothermal conditions. The self-assembly of these nets is presumably controlled by steric hindrance, which is subsequently applied to the rational design of the close-packed 2D networks and the porous 3D network. A few structurally characterized copper(I) triazolate complexes are reported such as $[Cu(Tz)]_n$ [191], $[Cu\{3,5\text{-}(Me)_2Tz\}]_n$ [192] $[Cu\{3,5\text{-}(C_3H_7)_2Tz\}]_n$ [192] and $[Cu_2(\mu_3\text{-}Tz)(\mu_3\text{-}Cl)_2]_n$ [193]. Also, polymeric silver(I) triazolate complexes are reported such as $[Ag(Tz)]_n$ [191], $[Ag_2\{[3,5\text{-}(CF_3)_2Tz]_6Ag_4\}]_n$ [194] and $[Ag_3\{[3,5\text{-}(Ph)_2Tz]_6Ag_5\}(BF_4)_2]_n$ [195]. The third triazolyl nitrogen atom plays a major role in the formation of network structures in metal ion coordination. The discrete trinuclear Group 11 triazolate complexes are scarce in the literature.

Copper(I) and silver(I) triazolate derivatives of $[3,5\text{-}(C_3F_7)_2Tz]^-$ are readily synthesized by the reaction of 3,5-bis(heptafluoropropyl)triazole with their metal(I) oxides in toluene and a small amount of acetonitrile. X-ray structures of $[M\{3,5\text{-}(C_3F_7)_2Tz\}]_3$, M = Cu, Ag, show the presence of two molecules of toluene for each trinuclear unit forming sandwiched molecules of the type [Toluene][Trinuclear][Toluene] [196]. The closest M···C(tol) distances to the toluene molecules on the opposite faces of the trinuclear units are at 2.87 and 2.91 Å for the copper complex and 2.84 and 2.92 Å for the silver complex. The Cu···Cu distances are 3.215, 3.264 and 3.263 Å and the Ag···Ag distances are 3.501, 3.474 and 3.319 Å [196].

The X-ray structure of the trinuclear gold(I) triazolate complex $[Au\{(3,5\text{-}(Pr^i)_2Tz)\}]_3$ at 95 K and at room temperature was determined. The trinuclear molecule dimerizes into a fully overlapping dimer of trinuclear prismatic unit via three Au···Au aurophilic interactions. The conformation of the dimer of trinuclear unit is remarkably different although the crystal packing is similar at both room temperature and 95 K. The Au···Au intertrinuclear distances of 3.19, 3.55 and 3.55 Å at 95 K and 3.46, 3.42 and 3.42 Å at room temperature suggest C_2 and D_3 effective symmetries [197].

11. Poly(azolyl)borate complexes

Tris(azolyl)borates or scorpionates are anionic, 6 e^- donor, face-capping ligands similar to cyclopentadienyl ligands. They are hard σ-donor nitrogen ligands. Conventional face-capping four-coordinate complexes coordinated to solvents, phosphine ligands, isocyanides and other coordinating molecules have been discussed thoroughly in several reviews. In this review, multinuclear complexes will be discussed. The coordination numbers, geometries, metal–metal and Cu–N distances within the tris(azolyl)borates set vary with the size of the ligand substituents. Denoting these ligands will follow Curtis abbreviations for $HB(pz)_3$ as Tp [198]. The 3-substituent is denoted by a superscript over Tp; thus Tp^{Me} is $HB(3\text{-}Mepz)_3$ and 5-substituent follows the 3-substituent, separated by comma; thus, $Tp^{Me,Me}$ is $HB(3,5\text{-}Me_2pz)_3$. The 4-substituent is denoted by a superscript 4Me; thus, Tp^{4Me} is $HB(4\text{-}Mepz)_3$.

11.1. Dinuclear and trinuclear hydrotris(pyrazolyl)borate complexes

A detailed study was provided by Ibers et al. on the structural properties for $[TpCu]_2$ and $[Tp^{Me,Me}Cu]_2$ complexes (Table 13) [199]. The compound $[TpCu]_2$ was prepared in 57% yield via the carbonyl compound [TpCu(CO)] by evaporation of the solvent to yield the decarbonylated product (Eq. (5)). When the reaction was carried out with $K[Tp^{Me,Me}]$, the product was the less labile carbonyl complex $[Tp^{Me,Me}Cu(CO)]$, which on prolonged heating and pumping yields $[Tp^{Me,Me}Cu]_2$.

$$K[Tp] + CuCl + CO \rightarrow [TpCu(CO)] \rightarrow [TpCu]_2 \quad (5)$$

In $[TpCu]_2$, each $HBpz_3$ moiety presents two terminal pyrazolyl ligands (one to each copper) and one crosswise bridging pyrazolyl ligand. The coordination geometry about each copper atom is a distorted tetrahedron. The Cu–Cu distance in the dinuclear complex is 2.660(1) Å. The copper complex of the $Tp^{Me,Me}$ lacks symmetrically bridging pyrazolyl rings, so that the coordination number of each copper atom has decreased from four to three. The coordination geometry is best described as distorted trigonal planar. The molecular weight of $[TpCu]_2$, determined by osmometry in $CHCl_3$, was reported to be that of a dimer [199].

A series of copper(I) complexes of sterically hindered tris(pyrazolyl)hydroborates $[Tp^{RR'}Cu]_2$ (R = t-Bu, R′ = H or R = R′ = Ph) were isolated [200]. In the copper complex $[Tp^{Ph,Ph}Cu]_2$, the $Tp^{Ph,Ph}$ ligands bridge between three-coordinate copper centers (Fig. 56). In $[Tp^{t\text{-}Bu}Cu]_2{\cdot}Et_2O$, each $Tp^{t\text{-}Bu}$ ligand bridges between the copper(I) centers by binding via one pyrazolyl group to each metal. The third pyrazolyl ring in each ligand is directed away from the dicopper(I) core. Both free pyrazolyl rings in the dimer are disposed on the same side of the molecule. The copper atoms are two-coordinate with close to linear geometries. The dimeric structure of $[Tp^{Ph,Ph}Cu]_2$ is almost identical to that of $[Tp^{Me,Me}Cu]_2$ [200]. In the structure of the sterically encumbered compound $[Tp^{t\text{-}Bu,i\text{-}Pr}Cu]$ each copper site is coordinated exclusively by two pyrazolyl moieties, belonging to two independent $Tp^{t\text{-}Bu,i\text{-}Pr}$ ligands, in an essentially linear fashion [201]. The short copper–nitrogen distances reflect the low copper coordination number.

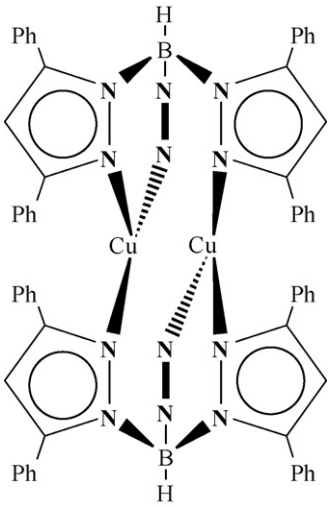

Fig. 56. Structure of $[Tp^{Ph,Ph}Cu]_2$.

The crystal structure of the 1:1 complex of silver(I) with hydrotris(3,5-dimethylpyrazolyl)borate $[Tp^{Me,Me}Ag]_2$ has been shown to be an unsymmetrical dimer, in which each $Tp^{Me,Me}$ ligand bridges both metals by coordinating two pyrazolyl donors to one silver center and one to the other silver, such that one silver is four-coordinate and the other is two-coordinate (Fig. 57) [202]. However two of the pyrazolyl donors around the

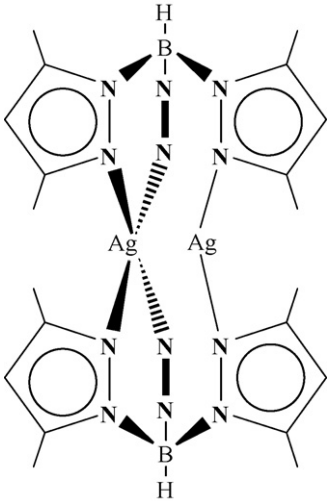

Fig. 57. Structure of $[Tp^{Me,Me}Ag]_2$.

Table 13
The M···M distances (Å) for the dinuclear poly(azolyl)borate complexes.

Complex	M–M	Ref.
$[TpCu]_2$	2.660(1)	[199]
$[Tp^{Me,Me}Cu]_2$	2.506(1)	[199]
$[Tp^{Me,Me}Ag]_2$	2.7956(4)	[202]
$[Tp^{Ph,Ph}Cu]_2$	2.544(2)	[200]
$[Tp^{t\text{-}Bu}Cu]_2$	3.284	[200]
$[Tp^{t\text{-}Bu,i\text{-}Pr}Cu]_2$	3.456	[201]

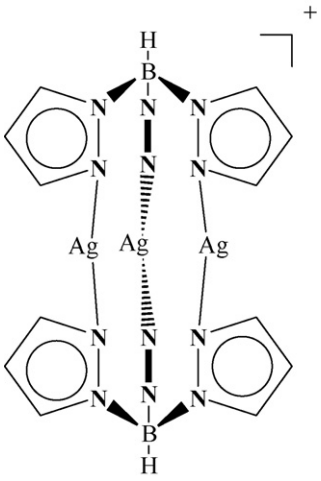

Fig. 58. Structure of $[Ag_3(Tp^{An})_2][ClO_4]$, An = anisyl substituent. Anisyl groups omitted for clarity.

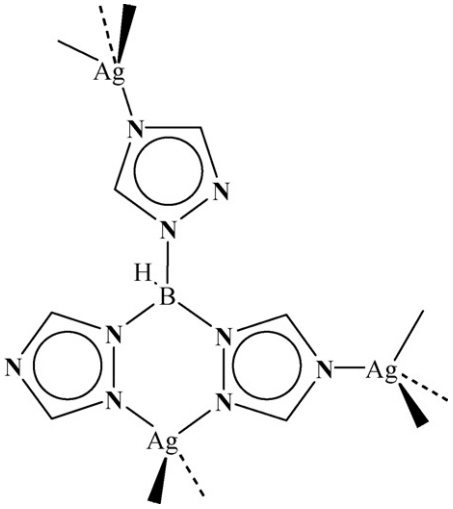

Fig. 59. Structure of [hydrotris(1,2,4-triazolyl)borato]silver(I) polymer.

'four-coordinate' metal centers are also involved in weak, unsymmetrical bridging interactions with the 'two-coordinate' metal centers.

An interesting trinuclear silver complex $[Ag_3L_2]ClO_4$, L = tris[3-(2-pyridyl)-pyrazolyl]borate, is obtained which contains a triangle $[Ag_3]^{3+}$ core [203]. The core comprises an equilateral triangle of silver centers (Ag–Ag separations 2.977 Å and Ag–Ag–Ag angle 60°). Each silver atom is coordinated by a bidentate arm from each of the two ligands in addition to the two silver-silver interactions. The silver centers are in highly distorted six-coordinate geometries, which may be considered as 'octahedral' in which the silver–nitrogen bond lengths are Ag–N_{py} 2.43 Å (av.) and Ag–N_{pz} 2.27 Å (av.) [203]. The crystal structure of another interesting trinuclear silver(I) complex of the ligand tris[3-(2-methoxyphenyl)pyrazol-1-yl]hydroborate (Tp^{An}, where the suffix 'An' denotes the anisyl substituent), $[Ag_3(Tp^{An})_2][ClO_4]$, shows the complex contains a triangle of silver(I) atoms, with Ag···Ag separations of 3.927(2) Å. Each face of the triangle is capped by a single Tp^{An} ligand which donates one pyrazolyl nitrogen atom to each silver ion (Fig. 58) [204]. Each silver atom is therefore in an approximately linear two-coordinate environment.

11.2. Infinite chain hydrotris(pyrazolyl)borate complexes

The replacement of the pyrazole rings in poly(pyrazolyl)borate ligands by 1,2,4-triazole leads to novel [hydrotris(1,2,4-triazolyl)borato]silver(I) complex, which can bridge between metal centers, thereby creating coordination polymers [205]. In the 2D coordination mode, the hydrotris(triazolyl)borate ligand bis-chelates one silver center with two endodentate nitrogen centers and also bridges to two other silver atoms through two of the three exodentate nitrogen donors (Fig. 59). Hence, in one triazolyl ring both nitrogen centers become utilized as donor atoms. The coordination sphere of silver is a strongly distorted tetrahedron.

Eichhorn et al. reported the first crystallographically characterized examples of cyanoscorpionate coordination polymers $[Tp^{Ph,4CN}Cu]_n$ and $[Tp^{t\text{-}Bu,4CN}Cu]_n$ [206]. The pseudotetrahedral coordination environment of the copper(I) ion includes the three pyrazole nitrogen atoms of a $Tp^{R,4CN}$ ligand and is completed by a cyano nitrogen atom of another $Tp^{R,4CN}$ ligand. A one-dimensional polymer is thus formed in which only one cyano group from a given ligand is coordinated to a neighboring copper (Fig. 60). The polymers display a zigzag motif, with approximately 90° corners defined by the angle between the coordinated cyano group and its symmetry-related partner [206].

11.3. Formation of mixed-ligand hydrotris(azolyl)borate complexes

The reaction of $Cu(OAc)_2{\cdot}2H_2O$ with $K[Tp^{Me,Me}]$ or K[Tp] and pyrazole in methanol gave the dimeric complexes $[Cu(\mu\text{-}pz)(Tp^{Me,Me})]_2$ (Cu–Cu 3.875 Å) [207] and $[Cu(\mu\text{-}pz)(Tp)]_2$ (Cu–Cu 3.584 Å) [208]. The coordination geometry of the copper ions is distorted square pyramidal (Fig. 61). The Tp ligands in the centrosymmetric $[Cu_2(Tp)_2(N_3)_2]$ dinuclear complex are linked by two end-on bridging azide groups. The two copper(II) centers exhibit distorted square-pyramidal coordination geometry (Fig. 61) and are separated by 3.136(2) Å [209].

A neutral trinuclear azide bridged copper(II) complex, $[LCu(\mu\text{-}N_3)_2Cu(\mu\text{-}N_3)_2CuL]$ (L = hydridotris(3,5-dimethylpyrazolyl)borate), is produced from the reaction between $[Cu_3L_2]Cl$ and an excess of trimethylsilyl azide in acetone or methanol. The structure contains a square-planar central copper and two distorted square-pyramidal terminal copper atoms. The three copper atoms are bridged by four azide ligands with a Cu–N_{azide} average distance of 1.99 Å. The average Cu–N_{azide}–Cu angle is 101.4° and the average Cu···Cu distance is 3.05 Å [210].

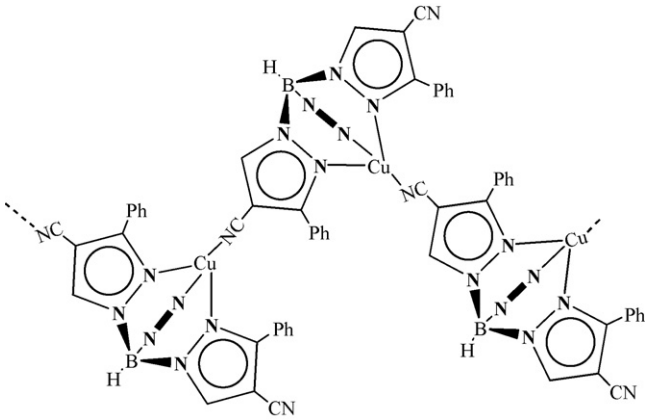

Fig. 60. Structure of $[Tp^{Ph,4CN}Cu]_n$ polymer.

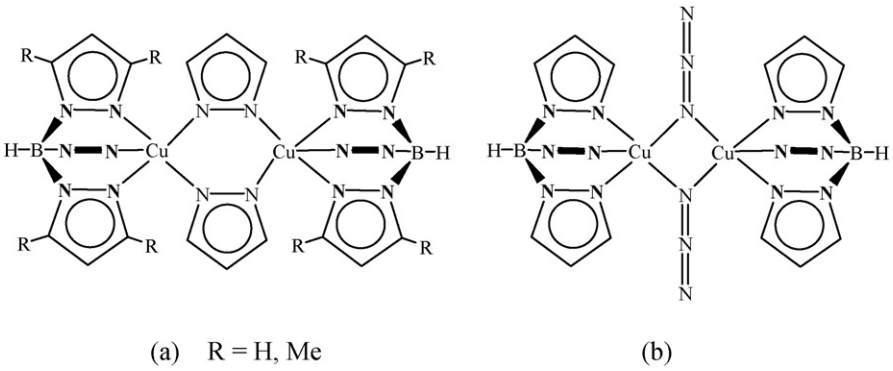

Fig. 61. Structure of mixed Tp ligand with (a) pyrazolate and (b) azide.

12. Future directions

The details of the excited states remain hidden despite the preparation of a growing number of nitrogen ligand complexes of coinage metals as well as high-level calculations, in contrast to the sulfur compounds. Nitrogen ligands are notoriously labile relative to sulfur and ylide ligands and thus there is some motivation to determine if this chemistry will serve the need for homogenous catalysts. Further investigations will likely reveal new gold–nitrogen reactivities related to homogenous catalysis.

Although metal centers are usually electrophilic, it has been shown based on reactivity, X-ray crystallography, electronic absorption and luminescence spectroscopy, and quantum mechanical calculations that the trinuclear gold(I) complexes are strong π bases. Their nucleophilic nature allows them to form acid–base adducts with a variety of organic and inorganic electrophiles. The fascinating photophysical properties promise a great potential for the utilization of such supramolecular acid–base stacks in a variety of optoelectronic applications that include molecular LEDs, selective optical sensing of hazardous small molecules and heavy metals, optical telecommunication devices, and solar cell dyes.

The investigation of gold for the treatment of rheumatoid arthritis and cancer helped the developing field of inorganic biochemistry. One of the recent discoveries is the biological role of nitric oxide in the cardiovascular and nervous systems. This simple diatomic molecule is an attractive therapeutic target to the inorganic medicinal chemists. There are opportunities for therapeutic studies. The role of coinage metal nitrogen complexes as donors of NO, and as scavengers for NO is an open area of study, and an example to inorganic medicinal drug design.

References

[1] (a) For example, see; C. Corti, R. Holliday, Gold: Science and Applications, CRC Press, 2010;
(b) L. Messori, G. Marcon, in: A. Sigel, H. Sigel (Eds.), Metal Ions in Biological Systems, vol. 42, Marcel Dekker Inc., New York, 2004;
(c) S. Patai, Z. Rappoport, The Chemistry of Organic Derivatives of Gold and Silver, John Wiley, 1999;
(d) C.F. Shaw, Chem. Rev. 99 (1999) 2589;
(e) I. Ott, Coord. Chem. Rev. 253 (2009) 1670;
(f) P.J. Barnard, S.J. Berners-Price, Coord. Chem. Rev. 251 (2007) 1889;
(g) A. Bindolia, M.P. Rigobello, G. Scutari, C. Gabbiani, A. Casini, L. Messori, Coord. Chem. Rev. 253 (2009) 1692;
(h) P.C. Bruijnincx, P.J. Sadler, Curr. Opin. Chem. Biol. 12 (2008) 197.
[2] (a) S.-C. Lo, P.L. Burn, Chem. Rev. 107 (2007) 1097;
(b) B.J. Coe, N.R.M. Curati, Comments Inorg. Chem. 25 (2004) 147.
[3] (a) L.R. Rudnick (Ed.), Lubricant Additives: Chemistry and Applications, CRC Press, 2009;
(b) D. Hutchison, US Patent 4,871,465 (1989).
[4] (a) A.S.K. Hashmi, D.F. Toste (Eds.), Modern Gold Catalyzed Synthesis, Wiley-VCH Verlag GmbH, 2009;
(b) G.C. Bond, C. Louis, D.T. Thompson, Catalysis by Gold (Catalytic Science Series), vol. 6, Imperial College Press, 2006;
(c) M.M. Diaz-Requejo, P.J. Perez, Chem. Rev. 108 (2008) 3379;
(d) P. Braunstein, L.A. Oro, P.R. Raithby (Eds.), Metal Clusters in Chemistry, Wiley-VCH, 1999;
(e) G.J. Hutchings, M. Brust, H. Schmidbaur, Chem. Soc. Rev. 37 (2008) 1759.
[5] T.T. Kodas, M.J. Hampden-Smith (Eds.), The Chemistry of Metal CVD, Wiley-VCH, 1994.
[6] (a) M. Bardaji, in: A. Laguna (Ed.), Modern Supramolecular Gold Chemistry: Gold–Metal Interactions and Applications, John Wiley & Sons, 2008, p. 403;
(b) J.A. Castellano, Liquid Gold: The Story of Liquid Crystal Displays and the Creation of an Industry, World Scientific Publishing Co., 2005;
(c) J.L. Serrano (Ed.), Metallomesogens: Synthesis, Properties and Applications, VCH, 1996.
[7] (a) P. Wasserscheid, T. Welton (Eds.), Ionic Liquid in Synthesis, Wiley-VCH Verlag GmbH and Co. KGaA, Weinheim, 2003;
(b) M. Hasan, I.V. Kozhevnikov, M.R.H. Siddiqui, A. Steiner, N. Winterton, Inorg. Chem. 38 (1999) 5637;
(c) M. Deetlefs, H.G. Raubenheimer, M.W. Esterhuysen, Catal. Today 72 (2002) 29.
[8] M. Noto, Y. Goto, M. Era, Chem. Lett. 32 (2003) 32.
[9] T.B. Gunnoe, Eur. J. Inorg. Chem. (2007) 1185.
[10] D.C. Bradley, M.H. Chishlom, Acc. Chem. Res. 9 (1976) 273.
[11] L.H. Gade, Acc. Chem. Res. 35 (2002) 575.
[12] T.R. Bailey, Sci. Synth. Product Class 12 (21) (2005) 811.
[13] M. Lappert, A. Protcheno, P. Power, A. Seeber, Metal Amide Chemistry, John Wiley & Sons Ltd., 2009.
[14] (a) G. La Monica, G.A. Ardizzoia, Prog. Inorg. Chem. 46 (1997) 151;
(b) A.A. Mohamed, A. Burini, R. Galassi, D. Paglialunga, J.R. Galan-Mascaros, K.R. Dunbar, J.P. Fackler Jr., Inorg. Chem. 46 (2007) 2348;
(c) G. Mezei, P. Baran, R. Raptis, Angew. Chem. Int. Ed. 43 (2004) 574;
(d) J.-M. Lehn, Science 295 (2002) 2400;
(e) K.D. Karlin, Y. Gultneh, in: J. Lippard (Ed.), Prog. Inorg. Chem., vol. 35, Wiley, New York, 1987, p. 219.
[15] (a) G. Mezei, P.A. Angaridis, P. Baran, R. Boča, F. Cervantes-Lee, W. Haase, R.G. Raptis, R. Werner, Inorg. Chem. 41 (2002) 2219;
(b) G. Mezei, R. Boča, L. Dlháň, T. Ortiz-Pérez, R.G. Raptis, J. Telser, Inorg. Chem. 42 (2003) 5801.
[16] (a) M. Shimizu, Y. Watanabe, H. Orita, T. Hayakawa, K. Takehira, Bull. Chem. Soc. Jpn. 66 (1993) 251;
(b) P. Gamez, P.G. Aubel, W.L. Driessen, J. Reedijk, Chem. Soc. Rev. 30 (2001) 376;
(c) E.I. Solomon, U.M. Sundaram, T.E. Machonkin, Acc. Chem. Res. 40 (2007) 445;
(d) E.I. Solomon, A.J. Augustine, J. Yoon, Dalton Trans. (2008) 3921.
[17] D.W. Bruce, in: D.W. Bruce, D. O'Hare (Eds.), Inorganic Materials, Wiley, Chichester, 1992.
[18] S. Coco, P. Espinet, in: F. Mohr (Ed.), Gold Chemistry: Highlights and Future Directions, Wiley & Sons, 2009, pp. 357–396 (Chapter 8).
[19] N. Masciocchi, S. Galli, A. Sironi, Comments Inorg. Chem. 26 (2005) 1.
[20] F. Mani, Coord. Chem. Rev. 120 (1992) 325.
[21] J.E. Cosgriff, G.B. Deacon, Angew. Chem. Int. Ed. 37 (1998) 286.
[22] G. La Monica, Ardizzoia, G. Attilio, Prog. Inorg. Chem. 46 (1997) 151.
[23] R. Mukherjee, Coord. Chem. Rev. 203 (2000) 151.
[24] M.A. Halcrow, Dalton Trans. (2009) 2059.
[25] (a) Y.I. Kuznetsov, L.P. Kazansky, Russ. Chem. Rev. 77 (2008) 219;
(b) A. Sugii, N. Ogawa, Y. Hgiwara, Talanta 31 (1984) 1079.
[26] (a) E. Buchner, M. Fritsch, Berichte 20 (1893) 256;
(b) O. Silberrad, Berichte 33 (1900) 85.
[27] D.S. More, S.D. Robinson, in: A.G. Sykes (Ed.), Advances in Inorganic Chemistry, vol. 32, AP, San Diego, 1988, p. 171.
[28] J.G. Haasnoot, Coord. Chem. Rev. 200–202 (2000) 131.
[29] K. Shibayama, S.W. Seidel, B.M. Novak, Macromolecules 30 (1997) 3159.
[30] C. Jones, Coord. Chem. Rev. (2009), doi:10.1016/j.ccr.2009.07.014.
[31] F.T. Edelmann, Coord. Chem. Rev. 137 (1994) 403.
[32] F.T. Edelmann, Adv. Organomet. Chem. 57 (2008) 183.
[33] J. Barker, M. Kilner, Coord. Chem. Rev. 133 (1994) 219.

[34] P.J. Bailey, S. Pace, Coord. Chem. Rev. 214 (2001) 91.
[35] M.P. Coles, Chem. Commun. (2009) 3659.
[36] (a) S. Trofimenko, Scorpionates: The Coordination Chemistry of Polypyrazolylborate Ligands, Imperial College Press, London, 1999;
(b) C. Pettinari, Scorpionates. II: Chelating Borate Ligands, Imperial College Press, 2008;
(c) S. Trofimenko, Polyhedron 23 (2004) 197;
(d) S. Trofimenko, Chem. Rev. 93 (1993) 943;
(e) K. Niedenzu, S. Trofimenko, Top. Curr. Chem. 131 (1986) 1;
(f) S. Trofimenko, Prog. Inorg. Chem. 34 (1986) 115;
(f) S. Trofimenko, Chem. Rev. 72 (1972) 497.
[37] (a) A. Bérces, Inorg. Chem. 36 (1997) 4831;
(b) M. Gennari, L. Marchio, Curr. Bioactive Compd. 5 (2009) 244.
[38] W. Kläui, M. Berghahn, G. Rheinwald, H. Lang, Angew. Chem. Int. Ed. 39 (2000) 2464.
[39] H.V.R. Dias, C.J. Lovely, Chem. Rev. 108 (2008) 3223.
[40] J.M. Smith, Comments Inorg. Chem. 29 (2008) 189.
[41] D. Rabinovich, Struct. Bond. 120 (2006) 143.
[42] A. Otero, J. Fernandez-Baeza, A. Antinolo, J. Tejeda, A. Lara-Sanchez, Dalton Trans. (2004) 1499.
[43] C. Pettinari, A. Cingolani, Lobbia, G. Gioia, F. Marchetti, D. Martini, M. Pellei, R. Pettinari, C. Santini, Polyhedron 23 (2004) 451.
[44] C. Pettinari, C. Santini, in: J.A. McCleverty, T.J. Meyer (Eds.), Comprehensive Coordination Chemistry II, vol. 1, 2004, p. 159.
[45] F.T. Edelmann, Angew. Chem. Int. Ed. 40 (2001) 1656.
[46] J. Beck, J. Strähle, Angew. Chem. Int. Ed. Engl. 27 (1988) 896.
[47] (a) Z. Dori, R. Ziolo, Chem. Rev. 73 (1973) 247;
(b) B.L. Evans, A.D. Yoffe, P. Gray, Chem. Rev. 59 (1959) 515;
(c) U. Muller, Struct. Bond. 13–16 (1973) 141.
[48] J. Strähle, Z. Anorg. Allg. Chem. 633 (2007) 1757.
[49] L. Bourget, M.F. Lappert, J.R. Severn, Chem. Rev. 102 (2002) 3031.
[50] (a) S. Patai (Ed.), Chemistry of Organic Derivatives of Gold and Silver, John Wiley & Sons, New York, 1999;
(b) H. Schmidbaur, Gold Bull. 23 (1990) 11;
(c) H. Schmidbaur, A. Schier, in: R. Crabtree, M. Mingos, K. Meyer (Eds.), Comprehensive Organometallic Chemistry III, vol. 2, Elsevier, New York, 2007, p. 251;
(d) P. Pyykkö, Angew. Chem. Int. Ed. Eng. 43 (2004) 4412;
(e) H. Schmidbaur, A. Schier, Chem. Soc. Rev. 37 (2008) 1931;
(f) P. Pyykkö, Chem. Soc. Rev. 37 (2008) 1967;
(g) F. Mendizabal, P. Pyykkö, Phys. Chem. Chem. Phys. (2004) 900;
(h) P. Pyykkö, M.O. Hakala, P.Z. Ejgierd, Phys. Chem. Chem. Phys. (2007) 3025.
[51] (a) D.M.P. Mingos, J. Yanu, S. Menzer, D.J. Williams, J. Chem. Soc. Dalton Trans. (1995) 319;
(b) R.B. Corey, K.Z. Pestrcov, Krystallografiya 89 (1934) 528.
[52] (a) P.C. Healy, N.K. Mills, A.H. White, J. Chem. Soc. Dalton Trans. (1985) 111;
(b) C.E. Housecroft, Coord. Chem. Rev. 152 (1996) 87;
(c) S.M. Cortez, R.G. Raptis, Coord. Chem. Rev. 162 (1997) 495;
(d) S.-L. Zheng, M.-L. Tong, X.-M. Chem, Coord. Chem. Rev. 246 (2003) 185.
[53] (a) H. Schmidbaur (Ed.), Gold Progress in Chemistry, Biochemistry, and Technology, Wiley, West Sussex, England, 1999;
(b) R. Puddephatt, The Chemistry of Gold, Elsevier, 1978;
(c) A. Granata, E. Monzani, L. Casella, J. Biol. Inorg. Chem. 9 (2004) 903.
[54] M.C. Gimeno, A. Laguna, in: J.A. McCleverty, T.J. Meyer, D.E. Fenton (Eds.), "Silver and Gold" in Comprehensive Coordination Chemistry II, vol. 6, Elsevier Pergamon, Oxford, UK, 2004.
[55] (a) J.J. Guy, P.G. Jones, M.J. Mays, G.M. Sheldrick, J. Chem. Soc. Dalton Trans. (1977) 8;
(b) H.-N. Adams, W. Hiller, J. Strähle, G.M. Sheldrick, Z. Anorg. Allg. Chem. 485 (1982) 81;
(c) W. Conzelmann, W. Hiller, J. Strähle, Z. Anorg. Allg. Chem. 512 (1984) 169.
[56] A. Burini, A.A. Mohamed, J.P. Fackler Jr., Comments Inorg. Chem. 24 (2003) 253.
[57] M.A. Cinellu, in: F. Mohr (Ed.), Gold Chemistry: Highlights and Future Directions, Wiley & Sons, 2009, pp. 47–78 (Chapter 2).
[58] H.E. Abdou, A.A. Mohamed, J.P. Fackler Jr., in: F. Mohr (Ed.), Gold Chemistry: Highlights and Future Directions, Wiley & Sons, 2009, pp. 1–45 (Chapter 1).
[59] J. Strähle, in: H. Schmidbaur (Ed.), Gold Progress in Chemistry, Biochemistry, and Technology, Wiley, West Sussex, England, 1999, pp. 311–348 (Chapter 11).
[60] G. Steinhauser, J. Evers, S. Jakob, T.M. Klapötke, G. Oehlinger, Gold Bull. 41 (2008) 305.
[61] L. Pauling, The Nature of the Chemical Bond, Cornell University Press, 1960.
[62] A.D. Yoffe, in: C.B. Colburn (Ed.), Developments in Inorganic Chemistry, vol. 1, Elsevier, New York, NY, 1966, p. 72.
[63] H. Wilsdorf, Acta Crystallogr. 1 (1948) 115.
[64] R. Soderquist, Acta Crystallogr. B24 (1968) 450.
[65] D. Fenske, K. Steiner, K. Dehnicke, Z. Anorg. Allg. Chem. 553 (1987) 57.
[66] W. Hiller, K. Hosler, K. Dehnicke, Z. Anorg. Allg. Chem. 574 (1989) 7.
[67] M.A.S. Goher, A.E.H. Abdou, M.A.M. Abu-Youssef, Trans. Metal Chem. 26 (2001) 39.
[68] F.A. Mautner, S. Hanna, R. Cortes, L. Lezama, M.G. Barandika, T. Rojo, Inorg. Chem. 38 (1999) 4647.
[69] T.M. Klapötke, B. Krumm, M. Scherr, J. Am. Chem. Soc. 131 (2009) 72.
[70] C.L. Schmidt, R. Dinnebier, U. Wedig, M. Jansen, Inorg. Chem. 46 (2007) 907.
[71] G.-C. Guo, Q.-M. Wang, T.C.W. Mak, J. Chem. Crystallogr. 29 (1999) 561.
[72] G.-C. Guo, T.C.W. Mak, Angew. Chem. Int. Ed. 37 (1998) 3268.
[73] T. Curtius, J. Rissom, J. Prakt. Chem. 58 (1898) 304.
[74] (a) W. Beck, E. Schuierer, K. Feldl, Angew. Chem. Int. Ed. Engl. 5 (1966) 249;
(b) W. Beck, W.P. Fehlhammer, P. Pollmann, E. Schuierer, K. Feldl, Chem. Ber. 100 (1967) 2335;
(c) W. Beck, H. Noth, Chem. Ber. 117 (1984) 419;
(d) H.H. Schmidtke, D. Garthoff, J. Am. Chem. Soc. 89 (1967) 1317;
(e) A. Vogler, C. Quett, H. Kunkely, Ber. Bunsen-Ges. Phys. Chem. 92 (1988) 1486.
[75] (a) T. Curtius, J. Rissom, J. Prakt. Chem. 58 (1898) 261;
(b) M. Wehlan, R. Thiel, J. Fuchs, W. Beck, W.P. Fehlhammer, J. Organomet. Chem. 613 (2000) 159.
[76] W. Beck, T.M. Klapötke, P. Klüfers, G. Kramer, C.M. Rienäcker, Z. Anorg. Allg. Chem. 627 (2001) 1669.
[77] T.M. Klapötke, B. Krumm, J.-C. Galvez-Ruiz, H. Noth, Inorg. Chem. 44 (2005) 9625.
[78] S. Afyon, P. Höhn, M. Armbrüster, A. Baranov, F.R. Wagner, M. Somer, R. Kniep, Z. Anorg. Allg. Chem. 632 (2006) 1671.
[79] (a) G. Beuter, J. Strähle, Angew. Chem. Int. Ed. Engl. 27 (1988) 1094;
(b) J. Mielcke, J. Strähle, Angew. Chem. Int. Ed. Engl. 31 (1992) 464;
(c) M. Laupp, J. Strähle, Angew. Chem. Int. Ed. Engl. 33 (1994) 207.
[80] H. Burger, U. Wannagat, Monatsh. Chem. 95 (1964) 1099.
[81] P.B. Hitchcock, M.F. Lappert, L.J.-M. Pierssens, Chem. Commun. (1996) 1189.
[82] T. Tsuda, K. Watanabe, K. Miyata, H. Yamamoto, T. Saegusa, Inorg. Chem. 20 (1981) 2728.
[83] (a) A.M. James, R.K. Laxman, F.R. Fronczek, A.W. Maverick, Inorg. Chem. 37 (1998) 3785;
(b) P. Miele, J.D. Foulon, N. Hovnanian, J. Durand, L. Cot, Eur. J. Solid State Inorg. Chem. 29 (1992) 573.
[84] S.D. Bunge, O. Just, W.S. Rees Jr., Angew. Chem. Int. Ed. Engl. 39 (2000) 3082.
[85] H. Chen, M.M. Olmstead, S.C. Shoner, P.P. Power, J. Chem. Soc. Dalton Trans. (1992) 451.
[86] S. Gambarotta, M. Bracci, A. Chiesi-Villa, C. Guastini, J. Chem. Soc. Dalton Trans. (1987) 1883.
[87] H. Hope, P.P. Power, Inorg. Chem. 23 (1984) 936.
[88] P. Reib, D. Fenske, Z. Anorg. Allg. Chem. 626 (2000) 1317.
[89] M. Niemeyer, Acta Crystallogr. E57 (2001) 491.
[90] (a) T. Tsuda, H. Washita, K. Watanabe, M.M. Wa, T. Saegusa, J. Chem. Soc. Chem. Commun. (1978) 815;
(b) T. Tsuda, H. Washita, T. Saegusa, J. Chem. Soc. Chem. Commun. (1977) 468.
[91] (a) T.T. Kodas, M.J. Hampden-Smith, in: T.T. Kodas, M.J. Hampden-Smith (Eds.), The Chemistry of Metal CVD, Wiley-VCH, 1994, p. 240 (Chapter 5);
(b) T.H. Baum, P.B. Comita, in: T.T. Kodas, M.J. Hampden-Smith (Eds.), The Chemistry of Metal CVD, Wiley-VCH, 1994, p. 305 (Chapter 6).
[92] S.J. Archibald, N.W. Alcock, D.H. Busch, D.R. Whitcomb, J. Clust. Sci. 11 (2000) 261.
[93] (a) F.A. Cotton, L.M. Daniels, C.A. Murillo, P. Schooler, J. Chem. Soc. Dalton Trans. (2007) 2000;
(b) F.A. Cotton, L.M. Daniels, C.A. Murillo, P. Schooler, J. Chem. Soc. Dalton Trans. (2001) 2000;
(c) F.A. Cotton, L.M. Daniels, J.H. Matonic, C.A. Murillo, Inorg. Chim. Acta 256 (1997) 277.
[94] F.A. Cotton, X. Feng, M. Matusz, R. Poli, J. Am. Chem. Soc. 110 (1988) 7077.
[95] P. Pyykkö, F. Mendizabal, Inorg. Chem. 37 (1998) 3018.
[96] X. Jiang, J.C. Bollinger, M.-H. Baik, D. Lee, Chem. Commun. (2005) 1043.
[97] (a) A.A. Mohamed, H.E. Abdou, M.D. Irwin, J.M. Lopez-de-Luzuriaga, J.P. Fackler Jr., J. Clust. Sci. 14 (2003) 253;
(b) H.E. Abdou, A.A. Mohamed, J.M. López-de-Luzuriaga, J.P. Fackler Jr., J. Clust. Sci. 15 (2004) 397;
(c) H.E. Abdou, A.A. Mohamed, J.P. Fackler Jr., J. Clust. Sci. 18 (2007) 630;
(d) H.E. Abdou, A.A. Mohamed, J.P. Fackler Jr., J. Chin. Chem. Soc. 54 (2007) 1107.
[98] H.E. Abdou, A.A. Mohamed, J.P. Fackler Jr., Inorg. Chem. 44 (2005) 166.
[99] H.E. Abdou, A.A. Mohamed, J.P. Fackler Jr., A. Burini, R. Galassi, J.M. López de Luzuriaga Fernández, M.E. Olmos, Coord. Chem. Rev. 253 (2009) 1161.
[100] Z. Li, S.T. Barry, R.G. Gordon, Inorg. Chem. 44 (2005) 1728.
[101] B.S. Lim, A. Rahtu, J.-S. Park, R.G. Gordon, Inorg. Chem. 42 (2003) 7951.
[102] S.J. Archibald, N.W. Alcock, D.H. Busch, D.R. Whitcomb, Inorg. Chem. 38 (1999) 5571.
[103] T. Ren, C. Lin, P. Amalberti, D. Macikenas, J.D. Protasiewicz, J.C. Baum, T.L. Gibson, Inorg. Chem. Commun. 1 (1998) 23.
[104] (a) S. Maier, W. Hiller, J. Strähle, C. Ergezinger, K. Dehnicke, Z. Naturforsch. B 43 (1988) 1628;
(b) D. Fenske, G. Baum, A. Zinn, K. Dehnicke, Z. Naturforsch. B 45 (1990) 1273.
[105] H.E. Abdou, A.A. Mohamed, J.P. Fackler Jr., Inorg. Chem. 46 (2007) 9692.
[106] (a) A. Grohman, H. Schmidbaur, in: E.W. Abel, F.G. Stone, G. Wilkinson (Eds.), Comprehensive Organometallic Chemistry II, vol. 3, Pergamon, Oxford, 1995, p. 1;
(b) L.C. Porter, J.P. Fackler Jr., Acta Crystallogr. 42 (1986) 1128.
[107] H.E. Abdou, A.A. Mohamed, J.P. Fackler Jr., Z. Naturforsch. B: Chem. Sci. 59B (2004) 1480.
[108] A. Laguna, M. Laguna, Coord. Chem. Rev. 193–195 (1999) 837.
[109] H.H. Murray, A.M. Mazany, J.P. Fackler Jr., Organometallics 4 (1985) 154.
[110] H.E. Abdou, Ph.D. Thesis, Texas A&M University, 2006.
[111] A.A. Mohamed, H.E. Abdou, J.P. Fackler Jr., Inorg. Chem. 45 (2006) 11.
[112] H.E. Abdou, A.A. Mohamed, J.P. Fackler Jr., Inorg. Chem. 46 (2007) 141.

[113] (a) Z. Yan, S. Chinta, A.A. Mohamed, J.P. Fackler Jr., D.W. Goodman, J. Am. Chem. Soc. 127 (2005) 1604;
(b) Z. Yan, S. Chinta, A.A. Mohamed, J.P. Fackler Jr., D.W. Goodman, Catal. Lett. 111 (2006) 15.
[114] J. Guzman, B.C. Gates, Angew. Chem. Int. Ed. 42 (2003) 690.
[115] P. Broqvist, L.M. Molina, H. Grönbecka, B. Hammer, J. Catal. 227 (2004) 217.
[116] (a) R. Rosenberg, D.C. Edelstein, C.-K. Hu, K.P. Rodbell, Annu. Rev. Mater. Sci. 30 (2000) 229;
(b) M. Ritala, M. Leskela, in: H.S. Nalwa (Ed.), Handbook of Thin Film Materials, vol. 1, Academic Press, New York, 2001, pp. 103–159.
[117] B.S. Lim, A. Rahtu, R.G. Gordon, Nat. Mater. 2 (2003) 749.
[118] (a) T. Chen, C. Xu, T.H. Baum, B.C. Hendrix, T.M. Cameron, J.F. Roeder, M. Stender, US Patent 0,162,550 A1 (2009);
(b) V.N. Vertoprakhov, S.A. Krupoder, Russ. Chem. Rev. 69 (2000) 1057.
[119] V. Krisyuk, L. Aloui, N. Prud'homme, B. Sarapata, F. Senocq, D. Samélor, C. Vahlas, ECS Trans. 25 (2009) 581.
[120] Z. Li, A. Rahtu, R.G. Gordon, J. Electrochem. Soc. 153 (2006) C787.
[121] J.P. Coyle, W.H. Monillas, G.P.A. Yap, S.T. Barry, Inorg. Chem. 47 (2008) 683.
[122] S.D. Bunge, J.A. Ocana, T.L. Cleland, J.L. Steele, Inorg. Chem. 48 (2009) 4619.
[123] S.D. Bunge, J.L. Steele, Inorg. Chem. 48 (2009) 2701.
[124] D. Guo, X. Qiao, H.-B. Tong, M. Zhou, Acta Crystallogr. E65 (2009) m405.
[125] (a) F.A. Cotton, N.E. Gruhn, J. Gu, P. Huang, D.L. Lichtenberger, C.A. Murillo, L.O. Van Dorn, C.C. Wilkinson, Science 298 (2002) 1971;
(b) C.C. Wilkinson, Ph.D. Thesis, Texas A&M University, 2005;
(c) D.B. Soria, J. Grundy, M.P. Coles, P.B. Hitchcock, J. Organomet. Chem. 690 (2005) 2278.
[126] F.A. Cotton, X. Feng, D.J. Timmons, Inorg. Chem. 37 (1998) 4066.
[127] M.D. Irwin, H.E. Abdou, A.A. Mohamed, J.P. Fackler Jr., Chem. Commun. (2003) 2882.
[128] A.A. Mohamed, A. Mayer, H.E. Abdou, M.D. Irwin, L. Perez, J.P. Fackler Jr., Inorg. Chem. 46 (2007) 11165.
[129] A.A. Mohamed, H.E. Abdou, A. Mayer, J.P. Fackler Jr., J. Clust. Sci. 19 (2008) 551.
[130] (a) I.D. Brown, J.D. Dunitz, Cryst. Struct. Commun. 14 (1961) 480;
(b) L.R. Falvello, E.P. Urriolabeitia, U. Mukhopadhyay, D. Ray, Acta Crystallogr. C55 (1999) 170.
[131] M. Corbett, B.F. Hoskins, N.J. McLeod, B.P. O'Day, Aust. J. Chem. 28 (1975) 2377.
[132] (a) J. Beck, J. Strähle, Z. Naturforsch. B: Anorg. Chem. Organ. Chem. 41B (1986) 4;
(b) C.F. Barboza de Silva, S. Schwarz, M.G. Mestres, J. Strähle, Z. Anorg. Allg. Chem. 630 (2004) 2231.
[133] J. Beck, J. Strähle, Angew. Chem. 98 (1986) 106.
[134] E. Hartmann, J. Strähle, Z. Anorg. Allg. Chem. 583 (1990) 31.
[135] E. Hartmann, J. Strähle, Z. Naturforsch. B: Chem. Sci. 43 (1988) 818.
[136] J.E. O'Connor, G.A. Janusonis, E.R. Corey, Chem. Commun. (1968) 445.
[137] E. Hartmann, R. Schmid, J. Strähle, Z. Naturforsch. B: Chem. Sci. 44 (1989) 778.
[138] M. Payehghadr, M.K. Rofouei, A. Morsali, M. Shamsipur, Inorg. Chim. Acta 360 (2007) 1792.
[139] E. Hartmann, J. Strähle, Z. Naturforsch. B: Chem. Sci. 43 (1988) 525.
[140] G. Rios-Moreno, G. Aguirre, M. Parra-Hake, P.J. Walsh, Polyhedron 22 (2003) 563.
[141] A.L. Johnson, A.M. Willcocks, S.P. Richards, Inorg. Chem. 48 (2009) 8613.
[142] J. Beck, J. Strähle, Angew. Chem. 100 (1988) 927.
[143] J. Beck, J. Strähle, Angew. Chem. 97 (1985) 419.
[144] R. Schmid, J. Strähle, Z. Naturforsch. B: Chem. Sci. 44 (1989) 105.
[145] L. Bourget-Merle, M.F. Lappert, J.R. Severn, Chem. Rev. 102 (2002) 3031.
[146] C. Shimokawa, Y. Tachi, N. Nishiwaki, M. Ariga, S. Itoh, Bull. Chem. Soc. Jpn. 79 (2006) 118.
[147] C. Shimokawa, S. Itoh, Inorg. Chem. 44 (2005) 3010.
[148] H.V.R. Dias, J.A. Flores, Inorg. Chem. 46 (2007) 5841.
[149] (a) For example, see; S. Hong, L.M.R. Hill, A.K. Gupta, B.D. Naab, J.B. Gilroy, R.G. Hicks, C.J. Cramer, W.B. Tolman, Inorg. Chem. 48 (2009) 4514;
(b) E. Solomon, R. Sarangi, J. Woertink, A. Augustine, J. Yoon, S. Ghosh, Acc. Chem. Res. 40 (2007) 581;
(c) J.P. Klinman, J. Biol. Chem. 281 (2006) 3013;
(d) G. Battaini, A. Granata, E. Monzani, M. Gullotti, L. Casella, Adv. Inorg. Chem. 58 (2006) 185;
(e) E.A. Lewis, W.B. Tolman, Chem. Rev 104 (2004) 1047;
(f) L.Q. Hatcher, K.D. Karlin, Adv. Inorg. Chem. 58 (2006) 131;
(g) S. Itoh, Curr. Opin. Chem. Biol. 10 (2006) 115.
[150] (a) J.S. Thompson, L. Zhang, J.P. Wyre, D.J. Brill, K.G. Lloyd, Thin Solid Films 517 (2009) 2845;
(b) A.Z. Bradley, J.S. Thompson, US Patent 0,247,905 A1 (2004);
(c) K.-H. Park, W.J. Marshall, J. Am. Chem. Soc. 127 (2005) 9330;
(d) J. Rickerby, J.H.G. Steinke, Chem. Rev. 102 (2002) 1525.
[151] (a) C.-Y. Zhang, J.-B. Feng, Q. Gao, Y.-B. Xie, Acta Crystallogr. E64 (2008) m352;
(b) E. Buchner, Berichte 22 (1889) 842.
[152] N. Masciocchi, M. Moret, P. Cairati, A. Sironi, G.A. Ardizzoia, G. La Monica, J. Am. Chem. Soc 116 (1994) 7668.
[153] A. Bayler, A. Schier, G.A. Bowmaker, H. Schmidbaur, J. Am. Chem. Soc. 18 (1996) 7006.
[154] K. Fujisawa, Y. Ishikawa, Y. Miyashita, K.-I. Okamoto, Chem. Lett. 33 (2004) 66.
[155] A. Maspero, S. Brenna, S. Galli, A. Penoni, J. Organomet. Chem. 672 (2003) 123.
[156] G. Yang, R.G. Raptis, Inorg. Chim. Acta 360 (2007) 2503.
[157] G. Yang, R.G. Raptis, Inorg. Chim. Acta 352 (2003) 98.
[158] K. Singh, J.R. Long, P. Stavropoulos, Inorg. Chem. 37 (1998) 1073.
[159] G.A. Ardizzoia, S. Cenini, G. La Monica, N. Masciocchi, M. Moret, Inorg. Chem. 33 (1994) 1458.
[160] H.H. Murray, R.G. Raptis, J.P. Fackler Jr., Inorg. Chem. 27 (1988) 26.
[161] R.G. Raptis, H.H. Murray, J.P. Fackler Jr., Chem. Commun. (1987) 737.
[162] H.V.R. Dias, H.V.K. Diyabalanage, M.G. Eldabaja, O. Elbjeirami, M.A. Rawashdeh-Omary, M.A. Omary, J. Am. Chem. Soc. 127 (2005) 7489.
[163] (a) H.V.R. Dias, S.A. Polach, Z. Wang, J. Fluorine Chem. 103 (2000) 163;
(b) M.A. Omary, M.A. Rawashdeh-Omary, M.A.W. Gonser, O. Elbjeirami, T. Grimes, T.R. Cundari, H.V.K. Diyabalanage, C.S.P. Gamage, H.V.R. Dias, Inorg. Chem 44 (2005) 8200;
(c) H.V.R. Dias, H.V.K. Diyabalanage, M.A. Rawashdeh-Omary, M.A. Franzman, M.A. Omary, J. Am. Chem. Soc. 125 (2003) 12072.
[164] H.V.R. Dias, C.S.P. Gamage, J. Keltner, H.V.K. Diyabalanage, I. Omari, Y. Eyobo, N.R. Dias, N. Roehr, L. McKinney, T. Poth, Inorg. Chem. 46 (2007) 2979.
[165] D.M.M. Krishantha, C.S.P. Gamage, Z.A. Schelly, H.V.R. Dias, Inorg. Chem. 47 (2008) 7065.
[166] B. Bovio, F. Bonati, G. Banditelli, Inorg. Chim. Acta 87 (1984) 25.
[167] M.W. Dodge, W.F. Wacholtz, J.T. Mague, J. Chem. Crystallogr. 35 (2005) 5.
[168] R.G. Raptis, J.P. Fackler Jr., Inorg. Chem. 27 (1988) 4179.
[169] A.A. Mohamed, L.M. Perez, J.P. Fackler Jr., Inorg. Chim. Acta 358 (2005) 1657.
[170] G. Yang, R.G. Raptis, Inorg. Chem. 42 (2003) 261.
[171] J. Barberà, A. Elduque, R. Gimenez, L.A. Oro, J.L. Serrano, Angew. Chem. Int. Ed. Engl. 35 (1996) 2832.
[172] J. Barberà, A. Elduque, R. Gimenez, F.J. Lahoz, L.A. Oro, J.L. Serrano, Inorg. Chem. 37 (1998) 2960.
[173] M.C. Torralba, P. Ovejero, M.J. Mayoral, M. Cano, J.A. Campo, J.V. Heras, E. Pinilla, M.R. Torres, Helv. Chim. Acta 87 (2004) 250.
[174] S.J. Kim, S.K. Kang, K.-M. Park, W.-C. Zin, M.-G. Choi, K. Kim, Chem. Mater. 10 (1998) 1889.
[175] M.K. Ehlert, S.J. Rettig, A. Storr, R.C. Thompson, J. Trotter, Can. J. Chem. 68 (1990) 1444.
[176] N. Masciocchi, P. Cairati, A. Sironi, Powder Diffract. 13 (1998) 35.
[177] M.K. Ehlert, S.J. Rettig, A. Storr, R.C. Thompson, J. Trotter, Can. J. Chem. 70 (1992) 2161.
[178] G. Yang, J.R. Martínez, R.G. Raptis, Inorg. Chim. Acta 362 (2009) 1546.
[179] H.V.R. Dias, V.K. Himashinie, Diyabalanage, Polyhedron 25 (2006) 1655.
[180] S. Yamada, T. Ishida, T. Nogami, Dalton Trans. (2004) 898.
[181] F. Meyer, A. Jacobi, L. Zsolnai, Chem. Ber. Recl. 130 (1997) 1441.
[182] J.-X. Zhang, J. He, Y. Yin, M.-H. Hu, D. Li, X.-C. Huang, Inorg. Chem. 47 (2008) 3471.
[183] K. Singh, J.R. Long, P. Stavropoulos, J. Am. Chem. Soc. 119 (1997) 2942.
[184] Z. An, R.-J. Zhou, Acta Crystallogr. E65 (2009) 1325.
[185] G.A. Ardizzoia, S. Cenini, G. La Monica, N. Masciocchi, A. Maspero, M. Moret, Inorg. Chem. 37 (1998) 4284.
[186] (a) R.G. Raptis, J.P. Fackler Jr., Inorg. Chem. 29 (1990) 5003;
(b) R.G. Raptis, H.H. Murray, J.P. Fackler Jr., Acta Crystallogr. C44 (1988) 970.
[187] G. Yang, R.G. Raptis, J. Chem. Soc. Dalton Trans. (2002) 3936.
[188] (a) M.A. Omary, O. Elbjeirami, C.S.P. Gamage, K. Sherman, H.V.R. Dias, Inorg. Chem. 48 (2009) 1784;
(b) S.M. Tekarli, T.R. Cundari, M.A. Omary, J. Am. Chem. Soc. 130 (2008) 1669;
(c) C. Yang, M. Messerschmidt, C. Coppens, M.A. Omary, Inorg. Chem. 45 (2006) 6592;
(d) T. Grimes, M.A. Omary, H.V.R. Dias, T.R. Cundari, J. Phys. Chem. A 110 (2006) 5823;
(e) P. Ovejero, M.J. Mayoral, M. Cano, M.C. Lagunas, J. Organomet. Chem. 692 (2007) 1690;
(f) E.M. Barranco, M.C. Gimeno, A. Laguna, M.D. Villacampa, Inorg. Chim. Acta 358 (2005) 4177;
(g) A.A. Mohamed, T. Grant, R.J. Staples, J.P. Fackler Jr., Inorg. Chim. Acta 357 (2004) 1761.
[189] M. Enomoto, A. Kishimura, T. Aida, J. Am. Chem. Soc. 123 (2001) 5608.
[190] A. Kishimura, T. Yamashita, T. Aida, J. Am. Chem. Soc. 127 (2005) 179.
[191] J.-P. Zhang, Y.-Y. Lin, X.-C. Huang, X.-M. Chen, J. Am. Chem. Soc. 127 (2005) 5495.
[192] J.-P. Zhang, S.-L. Zheng, X.-C. Huang, X.-M. Chen, Angew. Chem. Int. Ed. 43 (2003) 206.
[193] Q.-G. Zhai, C.-Z. Lu, S.-M. Chen, X.-J. Xu, W.-B. Yang, Cryst. Growth Des. 6 (2006) 1393.
[194] C. Yang, X. Wang, M.A. Omary, J. Am. Chem. Soc. 129 (2007) 15454.
[195] G. Yang, R.G. Raptis, Chem. Commun. (2004) 2058.
[196] H.V.R. Dias, S. Singh, C.F. Campana, Inorg. Chem. 47 (2008) 3943.
[197] C. Yang, M. Messerschmidt, P. Coppens, M.A. Omary, Inorg. Chem. 45 (2006) 6592.
[198] M.D. Curtis, K.-B. Shiu, W.M. Buttler, J. Am. Chem. Soc. 108 (1986) 1550.
[199] (a) C. Mealli, C.S. Arcus, J.L. Wilkinson, T.J. Marks, J.A. Ibers, J. Am. Chem. Soc. 98 (1976) 711;
(b) R.E. Davis, T.A. Dodds, T.-H. Hseu, J.C. Wagnon, T. Devon, J. Tancrede, J.S. McKennis, R. Pettit, J. Am. Chem. Soc. 96 (1974) 7564.
[200] S.M. Carrier, C.E. Ruggiero, R.P. Houser, W.B. Tolman, Inorg. Chem. 32 (1993) 4889.
[201] S. Kiani, J.R. Long, P. Stavropoulos, Inorg. Chim. Acta 263 (1997) 357.
[202] E.R. Humphrey, Z. Reeves, J.C. Jeffery, J.A. McCleverty, M.D. Ward, Polyhedron 18 (1999) 1335.

[203] A.J. Amoroso, J.C. Jeffery, P.L. Jones, J.A. McCleverty, E. Psillakis, M.D. Ward, J. Chem. Soc. Chem. Commun. (1995) 1175.
[204] E.R. Humphrey, N.C. Harden, L.H. Rees, J.C. Jeffery, J.A. McCleverty, M.D. Ward, J. Chem. Soc., Dalton Trans. (1998) 3353.
[205] C. Janiak, T.G. Scharmann, P. Albrecht, F. Marlow, R. Macdonald, J. Am. Chem. Soc. 118 (1996) 6307.
[206] N. Zhao, J.C. Bullinger, M.J. Van Stipdonk, C.L. Stern, D.M. Eichhorn, Inorg. Chem. 47 (2008) 5945.
[207] C.D. Nicola, F. Marchetti, M. Monari, L. Pandolfo, C. Pettinari, Inorg. Chem. Commun. 11 (2008) 665.
[208] Y.H. Xing, X.J. Zhang, Z. Sunb, J. Han, Y.H. Zhang, B.L. Zhang, M.F. Ge, S.Y. Niu, Spectrochim. Acta A 68 (2007) 1256.
[209] S. Wang, Y.Z. Li, J.L. Zuo, X.Z. You, Acta Crystallogr. E60 (2004) m376.
[210] M.H.W. Lam, Y.-Y. Tang, K.-M. Fung, X.-Z. You, W.-T. Wong, Chem. Commun. (1997) 957.